

Two eyes, one vision

Binocular motion perception in human visual cortex

Martijn Barendregt

ISBN/EAN: 978-94-6295-511-0

Copyright © 2016, Martijn Barendregt

Cover:	Bianca den Breejen
Lay out:	Martijn Barendregt
Printed by:	Proefschriftmaken.nl Uitgeverij BOXPress

Two eyes, one vision

Binocular motion perception in human visual cortex

Met twee ogen beweging zien in de visuele cortex van de mens

(met een samenvatting in het Nederlands)

Proefschrift

ter verkrijging van de graad van doctor aan de Universiteit Utrecht op gezag van de rector magnificus, prof.dr. G.J. van der Zwaan, ingevolge het besluit van het college voor promoties in het openbaar te verdedigen op vrijdag 2 september 2016 des ochtends te 10.30 uur

door

Martijn Barendregt

geboren op

1 maart 1987 te Rotterdam

Promotoren: Prof.dr. S.O. Dumoulin
Prof.dr. F.A.J. Verstraten
Copromotor: Dr. B. Rokers

Dit proefschrift werd (mede) mogelijk gemaakt met financiële steun van de
Nederlandse Wetenschaps Organisatie subsidie 406-11-197 aan F.A.J.
Verstraten & M. Barendregt

Somehow or other I had vaguely thought of myself as inhabiting this house which is my body, and looking out through its two round windows at the world. Now I find it isn't really like that at all. As I gaze into the distance, what is there at this moment to tell me how many eyes I have here – two, or three, or hundreds, or none? In fact, only one window appears on this side of my façade and that is wide open and frameless, with nobody looking out of it. It is always the other fellow who has eyes and a face to frame them; never this one.

D.E. Harding

Table of contents

GENERAL INTRODUCTION	9
THE CYCLOPEAN EYE IN HUMAN VISUAL CORTEX	15
STEREOMOTION SCOTOMAS OCCUR AFTER BINOCULAR COMBINATION	41
A NEURAL BASIS FOR MOTION AGNOSIA IN VISUAL CORTEX	71
MOTION AGNOSIA IS THE RESULT OF IMPAIRED VELOCITY PROCESSING	101
SUMMARY AND CONCLUSIONS	131
APPENDIX	
NEDERLANDSE SAMENVATTING	141
LIST OF REFERENCES	145
ACKNOWLEDGEMENTS	161
LIST OF PUBLICATIONS	165
CURRICULUM VITAE	167

Chapter 1

GENERAL INTRODUCTION

General introduction

Although we intuitively have the idea that our visual experience is an objective reality, it is in fact the result of a process of active inference performed by our brain. Our perception of the environment is constantly updated in an effort to integrate the incoming visual information with an internal model of how the physical world behaves. A clear example of this integration process is binocular perception. The two-dimensional retinal images from our two eyes each provide slightly different information about the position of objects in a visual scene due to the horizontal offset between the eyes, as illustrated in Figure 1.1, and the brain has to infer the actual three-dimensional position of those objects by integrating these two images. This happens, seemingly, without any effort and we therefore only experience a single image of the objects in a scene. However, because this inference is an active process and the brain not a perfect system, it can also very easily go wrong and result in misinterpretations.

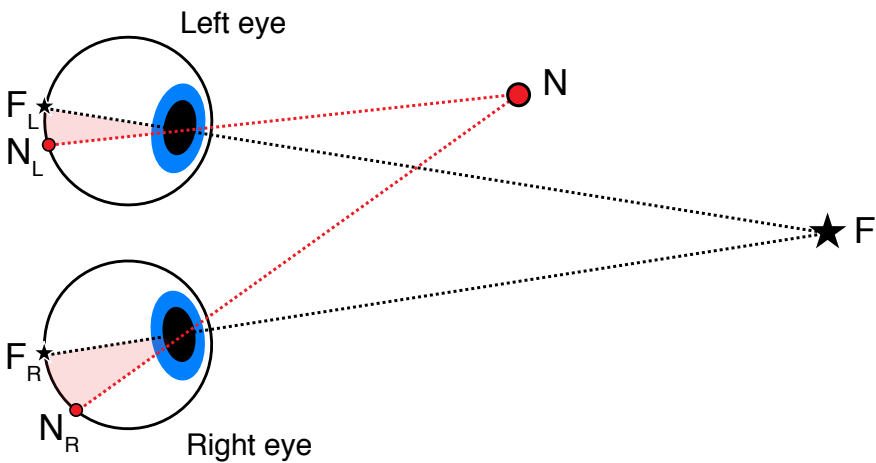


Figure 1.1 Because of the horizontal offset between the two eyes, much of the visual world projects onto different points in each eye. Here, the eyes are fixating the object at location F and therefore this object will fall on the same point in each retina (F_L and F_R). In contrast, objects that are not at the currently fixated distance (as most of the visual scene will be) projects onto different points in each eye. The object at location N projects onto different points (N_L and N_R) in the two eyes, illustrated by the highlighted red area in each eye.

Chapter 1

In this thesis we aim to further our understanding of the underlying neural mechanisms involved in the binocular perception of moving objects. To achieve this, we use two different approaches. In the first approach we use neuroimaging and normal functioning observers to study where in the human brain the two retinal images are integrated into a single visual representation of the world. In the second approach we investigate why a surprisingly large number of otherwise healthy people are unable to judge the direction in which objects are moving. The combination of these two approaches allows us to gain a better understanding of how the brain integrates binocular visual information and further our knowledge on how the visual system is able to determine the motion direction of moving objects.

A well-established feature of visual cortex is the idea that adjacent neurons will preferentially respond to stimulation at adjacent locations on the retina (Inouye, 1909). As a result, the visual cortex contains a fairly accurate map of the retina across the cortical surface, called a retinotopic map (Wandell, Brewer, & Dougherty, 2005), that we can study non-invasively using functional magnetic resonance imaging (MRI, Engel, Rumelhart, & Wandell, 1994; Sereno et al., 1995). There is not just one such map in the brain, over the years studies have identified increasing numbers of visual field maps across the brain (Wandell, Dumoulin, & Brewer, 2007; Wang, Mruczek, Arcaro, & Kastner, 2015). However, ultimately the brain needs to represent the position of objects in the three-dimensional world, not on our retina. A first step in the processing of the retinal visual input is to combine the information from the two retinas into a single representation of the current view an observer has of the environment. Most of what we now know about the way the brain performs this operation is based on electrophysiological measurements in animals. For most mammals visual input signals from the two eyes remain largely segregated up

General introduction

to primary visual cortex (Casagrande & Boyd, 1996). In addition to monocular neurons, the primary and secondary visual cortices contain a large number of binocular neurons that respond to input from both eyes simultaneously (Hubel, Wiesel, Yeagle, Lafer-Sousa, & Conway, 2013; Hubel & Wiesel, 1962). This transition from monocular to binocular neurons suggests that the combination of visual information from the two eyes occurs in the early visual cortical areas. Here, we aim to expand our model of how the visual system accomplishes the combination of binocular visual input by studying this process in the human brain. Specifically, we will investigate how the representation of visual input changes across different brain areas and different visual field maps.

Motion perception in general has been extensively studied and is well characterized in terms of the neural substrates, yet the neural mechanisms that underlie the perception of motion in depth are quite poorly understood by comparison. A possible reason for this gap in knowledge is the fact that it is easier to study frontoparallel motion (2D motion) because this type of motion (up-/down-/left-/rightward) can be readily presented on a 2-dimensional computer display. In contrast, to study motion in depth (3D motion) perception a more complicated setup is required in which the observer can be presented with a different image for each eye. Since 3D motion involves movement toward and away from the observer in depth, and it generally is not possible to move real-world objects in a sufficiently controllable manner in the lab, we make use of the fact that when an object moves in 3D the projection of this object on the two retinas moves in opposite directions. Using a setup in which we can present a different image to each eye separately, called a stereoscope (Wheatstone, 1838), allows us to simulate this type of movement in the lab.

Chapter 1

Here we aim to further the understanding of the neural mechanisms involved in motion in depth perception by investigating a particular visual deficit. Even though the ability to discriminate between approaching and receding motion seems quite critical for survival, there are studies that suggest that this ability can be impaired in otherwise normal, healthy individuals (Hong & Regan, 1989; Richards & Regan, 1973). An observer with such a visual field deficit is able to perceive motion in depth in most of their visual field but not in one specific region. Even though this visual deficit was first described over 40 years ago, there is currently very little known about the characteristics and potential underlying cause. In this thesis we will first make an effort to better characterize the inability to discriminate motion in depth and subsequently we will use neuroimaging methods to study where in the brain this deficit originates and what the possible underlying cause is.

When the inability to judge the direction of motion in depth was first described (Richards & Regan, 1973) it was termed a stereomotion scotoma. The term scotoma is typically used to describe a region in the visual field of an observer where visual acuity is severely reduced or entirely absent, i.e. a blind spot. This means that the term is generally used in the context of deficits that result in a lack of visual input from a specific region in the visual field. However, for the visual deficit that we investigate here there is no problem with visual input (as we will demonstrate) but the observer is unable to properly discriminate between different motion directions based on that visual input. Therefore we argue that the deficit can be described as a form of visual agnosia (Farah, 2004). Since this was a progressive insight, the terminology in this thesis incorporates both terms. In Chapter 3 we refer to stereomotion scotomas whereas in Chapters 4 and 5 we make the case that this should be considered a

General introduction

visual agnosia. This position will also be further discussed in the general conclusions at the end of the thesis.

Although magnetic resonance imaging (MRI) has been used to study in vivo brain function for years, recent advances in the strength of the magnetic field allow us to obtain very detailed measurements. These advances mean we can now study questions in a living, and functioning, human brain that were previously confined to the domain of invasive neural recordings in animals. Studying the properties of the brains' responses under various experimental conditions will be a central method in this thesis. In particular, we make use of the fact that the visual areas of the brain are organized into visual field maps and therefore we can predict which parts of the brain will respond to which portion of a visual display. This will be used in Chapters 2 and 4, where we use fMRI to measure the responses in these visual areas, but also strongly inform the behavioral methods used in the other chapters.

Chapter 2

THE CYCLOPEAN EYE IN HUMAN VISUAL CORTEX

Published as:

M Barendregt, BM Harvey, B Rokers & SO Dumoulin (2015) Transformation from a retinal to a cyclopean representation in human visual cortex. *Current Biology* **25** (15), 1982-1987

Acknowledgement of author contributions: MB, BH, BR and SOD designed the experiment and MB collected the data. MB performed data analysis under supervision of BR and SOD. MB wrote the manuscript and the other authors provided critical comments.

Abstract

We experience our visual world as seen from a single viewpoint, even though our two eyes receive slightly different images (Figure 2.1). One role of the visual system is to combine the two retinal images into a single representation of the visual field, sometimes called the cyclopean image (Julesz, 1971). Conventional terminology, i.e. retinotopy, implies that the topographic organization of visual areas is maintained throughout visual cortex (Inouye, 1909). However, following the hypothesis that a transformation occurs from a representation of the two retinal images (retinotopy) to a representation of a single cyclopean image (cyclopotopy), we set out to identify the stage in visual processing at which this transformation occurs in the human brain. Using binocular stimuli, population receptive field mapping (pRF), and ultra high-field (7 Tesla) functional magnetic resonance imaging (fMRI), we find that responses in striate cortex (V1) best reflect stimulus position in the two retinal images. In extrastriate cortex (from V2 to LO), on the other hand, responses better reflect stimulus position in the cyclopean image. These results pinpoint the location of the transformation from a retinal to a cyclopean representation and contribute to an understanding of the transition from sensory to perceptual stimulus space in the human brain.

Results

Observers viewed a contrast-defined bar stimulus with slight opposite horizontal offsets in each eye (binocular disparity), so that it was perceived behind the fixation plane (Figure 2.2, “Position in depth”). This stimulus moved across the visual field, producing systematic changes in fMRI response throughout early visual cortex (Engel et al., 1994; Sereno et al., 1995). Position in the retinal and cyclopean image of such a stimulus necessarily differ, such that the cyclopean position is always in between the positions in the two retinal images. We hypothesized that the neural response in visual cortex could either reflect the superimposed positions of the stimuli on both retinas (retinotopic representation Inouye, 1909) or the single position in the cyclopean image (cycloptopic representation).

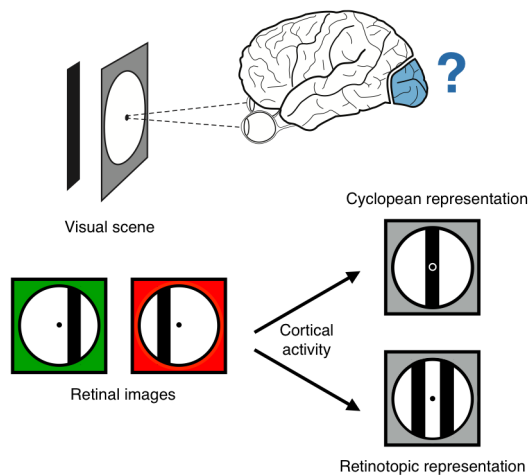


Figure 2.1 Does Cortical Representation of Binocular Stimuli Reflect the Retinal or the Cyclopean Image(s)? Elements of a 3D visual scene produce different retinal images in the two eyes. The visual system combines the retinal images into a single cyclopean image of the visual field. We investigated whether the cortical representation of such stimuli reflects their retinal or cyclopean image.

The cyclopean eye in human visual cortex

We used two control stimuli to generate two alternative models of the BOLD response, one based on stimulus positions in the two retinal images, and one based on stimulus position in the cyclopean image. The first control stimulus matched the position of the experimental stimulus in the cyclopean image: a contrast-defined bar was presented at identical locations in each retinal image without binocular disparity (Figure 2.2, “Single position”). The second control stimulus matched the position of the experimental stimulus in the two retinal images without being integrated into a cyclopean image: a contrast-defined bar temporally alternated between the left and right eye images of the experimental stimulus (Figure 2.2, “Offset positions”), so that it stimulated the same retinal locations, but due to the temporal alternation was not integrated into a single cyclopean image.

We used the BOLD response to the control stimulus to estimate the population receptive field (pRF), i.e. the region of visual space that optimally stimulated the neural population at each recording site (voxel) (Dumoulin & Wandell, 2008; Zuiderbaan, Harvey, & Dumoulin, 2012). In all experiments, we verified eye vergence by asking observers to perform a demanding task at fixation (on average 77% correct, Appendix Figure A2.1).

Representations can be discriminated in early visual cortex

We first verified that the two models predicted significantly different responses and that we could resolve differential activity between the two control stimuli using cross validation. Figure 2.3A compares how well predictions based on the “single position” and “offset positions” stimuli explained the measured fMRI responses in V1, V2 and V3 for the two control stimulus conditions. This analysis always included all responsive recording sites in each visual area. In V1 and V2, we could reliably discriminate responses elicited by the “single

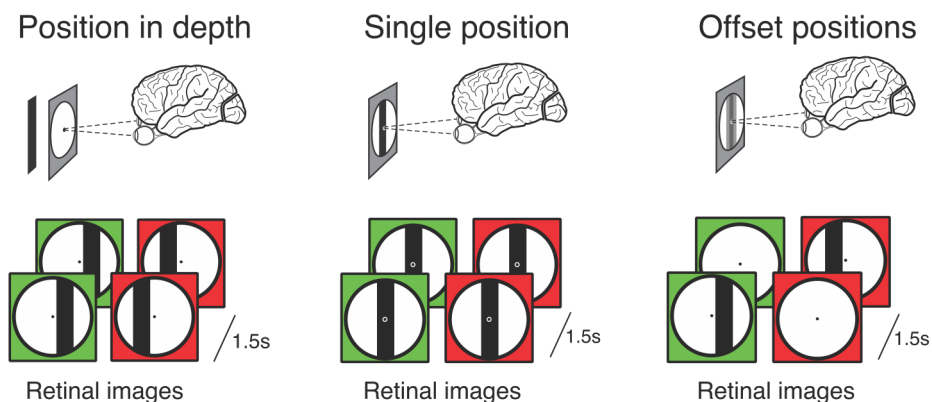


Figure 2.2 Stimuli used in the experiment. *Position in depth stimulus: two bars are presented simultaneously to both eyes with a horizontal offset. This results in the percept of a bar positioned in depth so that the stimulated retinal locations differ from the bar’s perceived location in the visual field. Single position stimulus: a bar is presented in the same position in both eyes, and repositioned every 1.5 seconds (1 TR) to estimate the population receptive field of each cortical location. Offset positions stimulus: presentation of the bar is alternated between the two eyes. Bars are presented in the same retinal locations as the ‘position in depth’ stimulus but alternate between the left and right eye to avoid the perception of a bar in depth.*

position” and “offset positions” stimuli. In V3, response predictions did not differ sufficiently to identify the stimulus representation when we include all responsive recording sites. Therefore, we limited our first analysis to V1 and V2.

V1 represents retinal stimulus location, while extrastriate cortex represents cyclopean stimulus location

To investigate the representation of the “position in depth” stimulus, we compared whether the responses elicited by viewing of the “position in depth” stimulus were better predicted by the pRF models based on either the retinal images or the cyclopean image (Figure 2.3B). The negative difference in V1 (*striped bar*, $t = -3.66$, $P = 2 \times 10^{-5}$, $n \geq 1135$ voxels/observer) indicates that a prediction based on the retinal model best describes V1’s responses. The positive difference in V2 (*black bar*, $t = 3.64$, $P = 2 \times 10^{-5}$, $n \geq 1010$ voxels/observer) indicates that a prediction based on the cyclopean model best

The cyclopean eye in human visual cortex

describes V2's responses. The difference between the results of V1 and V2 is also significant ($t = 11.47, P < 1 \times 10^{-7}$) further demonstrating that these areas have distinct representations of the visual input. Results for each individual observer can be found in Appendix Figure A2.4.

To investigate the representation of position in extrastriate cortex beyond V2, we repeated this analysis using only recording sites that could correctly discriminate between the control conditions (Figure 2.3B, right panel). By selecting recording sites based on control conditions, we avoid biases when evaluating the "position in depth" condition. We again find that the neural response is best predicted by the retinal model in V1 (*striped bar*, $t = -4.03, P = 8 \times 10^{-7}, n \geq 365 \text{ voxels/observer}$) and is best predicted by the cyclopean model in V2 (*first black bar*, $t = 3.24, P < 0.01, n \geq 293 \text{ voxels/observer}$).

Furthermore, the response to the stimulus in V3, V3A, LO1 and LO2 are also best predicted by the cyclopean model (*other black bars*, $t > 2.91, P < 0.005, n \geq 174 \text{ voxels/observer}$). As such, the BOLD response throughout extrastriate visual cortex is consistent with the representation of binocular stimuli according to their position in the cyclopean image rather than in the retinal images.

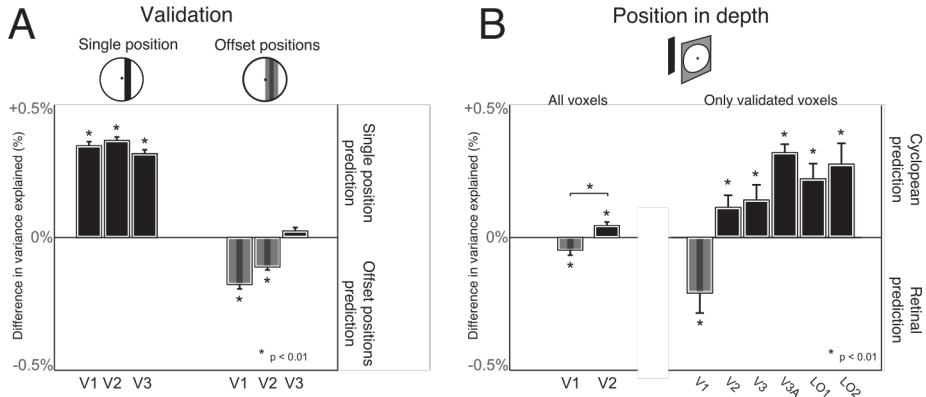


Figure 2.3 A: *In areas V1 and V2 our method successfully distinguishes between a stimulus presented at a single position in the visual field and a stimulus presented at two offset positions on the retina. Difference in variance explained between a model describing single versus offset positions for the two control conditions and early visual areas ($n=7$). Each bar represents the difference in variance explained between the two models when fitted to data collected using a particular stimulus (as indicated by the stimulus icon above the bars). We demonstrate that data from V1 and V2 correctly distinguish whether single position or offset position stimuli were shown. When we include all responsive voxels within each ROI we find that area V3 cannot correctly discriminate these two control stimuli for data obtained using the offset position stimulus. **B:** **Transformation from a representation of two distinct retinal images to a representation of the cyclopean image across cortical areas.** Difference in variance explained between a model describing cyclopean image versus two distinct retinal images for the “Position in depth” condition and early visual areas ($n=7$). The representation of the “Position in depth” stimulus in V1 is best explained by the retinal images of the stimulus (striped bar, $P < 0.01$) whereas the representation in V2 is best explained by the cyclopean image (black bar, $P < 0.01$). In the left panel all responsive voxels in areas V1 and V2 are included in the analysis. The right panel shows the same analysis limited to the voxels in visual areas V1 up to LO2 that are able to correctly discriminate between our two control stimuli. Both the left and right panel show the same transformation between area V1 and V2, going from a representation of the two retinal images in V1 to a representation of the cyclopean image in V2. Further, we see that the responses in subsequent extrastriate areas best reflect the cyclopean image as well. All errorbars represent mean \pm SEM.*

Responses reflect differences in position, not stimulus features

The temporal interleaving of the “offset positions” control stimulus used in the experiment results in a difference in temporal contrast energy. We therefore tested an additional stimulus condition in three observers to test whether the predictions made by our models accurately reflect the differences in representation of stimulus location rather than other stimulus features. We used a stimulus with a vertical, instead of horizontal, offset between the two eyes. Perceptually this stimulus is not fused into a single perceived position and therefore behaves similar to our “offset positions” stimulus. However, this stimulus is continuously presented to both eyes, rather than temporally interleaved, such that the stimulus energy is comparable to the “single position” and “position in depth” stimuli. Using the predictions generated by our control stimuli we test whether the responses to this “vertical offset” stimulus are best characterized as a response to two offset positions or a response to a single position. We found that the models consistent with a representation of the retinal images were significantly better at explaining the data obtained with this stimulus in both V1 ($t = -3.47$, $P = 5 \times 10^{-4}$, $n \geq 1260$ voxels/observer) and V2 ($t = -7.94$, $P = 2 \times 10^{-14}$, $n \geq 1010$ voxels/observer), suggesting that our results reflect a true difference in the representation of stimulus location (Figure 2.4).

Chapter 2

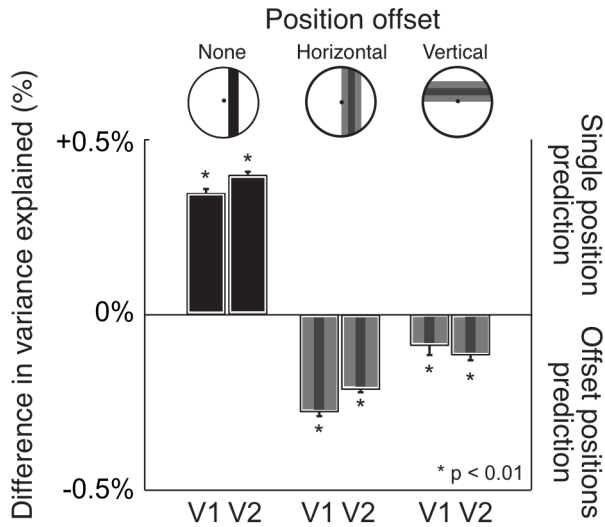


Figure 2.4 Responses reflect differences in stimulus position. To exclude the possibility that the differences in responses are due to differences in the stimulus energy of the control stimuli, we tested three observers using a stimulus containing vertical instead of horizontal disparity. The stimulus was presented continuously, so that it had the same stimulus energy as the “single position” stimulus, but unlike the horizontal disparity stimulus, the vertical disparity stimulus cannot be integrated into the representation of a single bar in the cyclopean image. We find that the responses to the “vertical offset” stimulus in both V1 and V2 are best described by the retinal position of the stimulus (V1: $P = 5 \times 10^{-4}$, V2: $P = 2 \times 10^{-4}$). All errorbars represent mean \pm SEM.

Discussion

We investigated the cortical responses to binocular stimuli in human visual cortex and found that the neural response best reflects a superimposed representation of the retinal position of visual stimuli in striate cortex (V1). We also found that responses in extrastriate cortex (V2 to LO) better reflect the position of visual stimuli in the cyclopean image. Taken together these results provide evidence for a transformation from two superimposed retinotopic maps to a single cyclopotopic map in early visual cortex.

Thus, the cortical responses in extrastriate cortex (starting in V2) are to some extent independent of stimulus position in the retinal images, and more closely reflect position in the cyclopean image. We would therefore predict that when retinal position of a stimulus is changed (but cyclopean position remains the same), the responses shift across the cortical surface in striate cortex but not extrastriate cortex. For example, two objects that are positioned directly behind each other with respect to an observer will result in responses in different locations in striate cortex but the same location in extrastriate cortex.

These results using fMRI in humans are consistent with previous work in other primates showing that in V1, neurons are commonly monocular, preferentially responding to input from one or the other eye, whereas from V2 onwards neurons are mostly binocular, responding to input from either eye (G. Chen, Lu, & Roe, 2008). We show here that this change in neural responsivity from V1 to V2 is accompanied by a change in the topographic organization of these visual areas.

We emphasize that our results are incompatible with the notion that the representation in extrastriate cortex reflects a simple summation of the two retinal images (Figure 2.5). If the representation in extrastriate areas were the result of a simple summation of V1's representation of the two retinal images, then the “offset positions” model, predicting a broader response, would be *better* at predicting the neural responses. This is indeed the case for stimuli with a vertical disparity, which the visual system does not integrate into a single cyclopean image. For stimuli with a horizontal disparity, which are integrated, we find that simple summation does not predict neural responses as well.

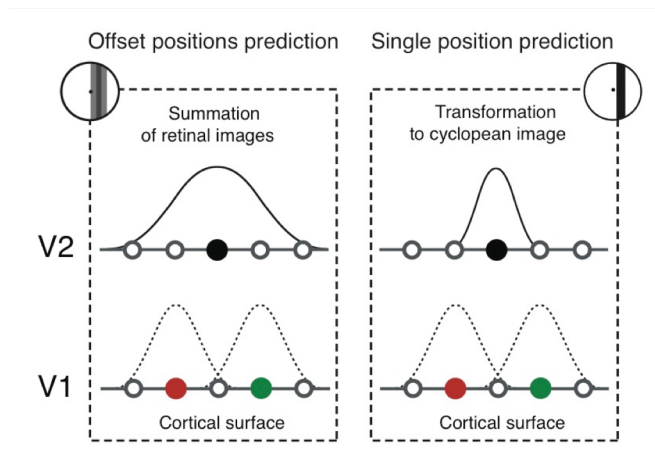


Figure 2.5 Responses in extrastriate cortex reflect the cyclopean image, independent of the position in the retinal images. Our results cannot be explained by assuming that the cortical responses in area V2 are based on the average of the stimulus positions in the two retinal images. Each panel illustrates a schematic view of the cortical surface in V1 and V2. The panel on the left depicts the prediction of a simple summation of the retinal images underlying the cortical responses in V2. The right panel shows the prediction of a response in V2 that is a transformation into a different position from the positions in the retinal images. Since our “single position” model provides a better prediction of the observed responses in V2, our data suggests that a transformation occurs between V1 and V2, such that responses in V1 reflect stimulus position in the two retinal images, whereas responses in V2 reflect stimulus position in the single cyclopean image.

Instead we suggest a transformation where the responses to the retinal images are combined with a corresponding binocular disparity. This means that two objects that are located exactly behind each other but at different distances from an observer elicit responses at different recording sites in V1 but not in V2 or subsequent extrastriate areas.

A well-known feature of the organization in visual cortex is the increase in population receptive field size between visual areas (Dumoulin & Wandell, 2008). While our data also show this increase between visual areas, we emphasize that this does not explain our results. If the difference in responses is solely due to larger population receptive fields in extrastriate cortex we should not have been able to dissociate between our two control stimuli (single versus offset bars). Given that we can dissociate between these stimuli we conclude that the increase in population receptive field size is not a sufficient explanation of our findings.

Further, the change in the proportion of neurons responding to monocular or binocular input between striate and extrastriate cortex is not sufficient to explain our results (Blasdel & Fitzpatrick, 1984; Hayhow, 1958; Talbot & Marshall, 1941), as binocular input alone does not a priori distinguish between a summed retinal and cyclopean visual field map representation (Figure 2.4). The goal of this study was not to identify where binocular combination occurs in visual cortex but rather to investigate how the human visual system infers the cyclopean representation from the two retinal images.

We would like to emphasize that our results do not provide evidence in favor of a spatiotopic representation of the visual field independent of fixation (d'Avossa et al., 2007; Gardner, Merriam, Movshon, & Heeger, 2008). Rather, our results

Chapter 2

are in line with the notion that the representation in extrastriate cortex reflects visual field location relative to fixation, i.e. a cyclopean representation (Julesz, 1971).

Our findings provide neurophysiological evidence of a representation of the cyclopean image in early visual cortex. Further research based on our results could investigate the role of monocular occluded objects in the cyclopean visual space, which has previously only been studied using psychophysical methods (Erkelens & Van Ee, 2002; Ono, Mapp, & Howard, 2002). Our results might shed light on psychophysical results showing that many low-level adaptation effects (assumed to be mediated in V1) do not transfer or only partially transfer interocularly, while some higher-level effects transfer almost completely.

The topographic organization of sensory and motor cortices is a central pillar of neuroscience, and has been instrumental to our understanding of cortical representation. Recently, we demonstrated a topographic organization that does not reflect the layout of sensory organs (Harvey, Klein, Petridou, & Dumoulin, 2013). In visual cortex the topographic maps are commonly thought to mirror the layout of the retina, and hence topographic regions of visual cortex are often referred to as retinotopic. Here, we demonstrate that early visual cortex deviates from the sensory organ layout, by representing the cyclopean image instead, which may be better suited to inform subsequent behavior.

In conclusion, our results show that the representation of position is systematically transformed between striate and extrastriate cortex. The transformation alters a retinotopic to a cyclopotopic representation. These results contribute to a growing body of work (Freeman, Ziemba, Heeger,

The cyclopean eye in human visual cortex

Simoncelli, & Movshon, 2013; Tong & Engel, 2001) dispelling the notion that V2 is simply a more complex version of V1.

Methods

Participants

fMRI data were collected in seven participants (three authors, one female, aged 27-38), all with normal or corrected-to-normal visual acuity. All were experienced psychophysical participants in both motion and depth experiments. We tested all participants on their stereovision (using the same fixation dot task as the experiment) prior to the experiment and found no abnormalities. Aside from the authors, all participants were naïve to the purpose of the experiment. Experiments were approved by the Medical Ethics committee of University Medical Center Utrecht, undertaken with the written consent of each participant and were carried out in accordance with the Code of Ethics of the World Medical Association (Declaration of Helsinki).

Stimuli

Visual stimuli were back-projected onto a screen (15x7.9 cm) located inside the MRI bore. The participant viewed the display through custom-built prisms that allowed separate presentation for each eye. The total viewing distance from the participant to the display screen was 41 cm.

Stimuli were generated in Matlab (Mathworks, USA) using the PsychToolbox version 3 (Brainard, 1997; Pelli, 1997). All stimuli were presented in a central, circular aperture with a diameter of 6 degrees. A small dot (0.1 degrees) presented in the center of the aperture was used to maintain fixation. Outside the stimulus aperture, the same pink noise (1/f) background was presented to both eyes, facilitating binocular fusion. See Figure 2.2 for illustrations of the different stimuli described here.

The cyclopean eye in human visual cortex

All stimuli consisted of a moving bar aperture (Figure 2.2) that moved through the visual field in 8 different directions. These bar apertures revealed a random $1/f$ noise (pink noise) pattern that was re-generated at 10Hz. The bar had a width of 0.75 degrees and moved through the aperture in 20 discrete steps of 0.3° , each lasting 1.5 seconds, the TR. As such, each bar pass lasted a total of 30 seconds.

In the main stimulus condition (“position in depth”), binocular disparity was introduced by displacing the bar stimulus by 0.25 degrees in opposite horizontal directions in the two eyes. Perceptually the stimulus simulated an uncrossed disparity, i.e. the bar is perceived as floating in depth behind the rest of the display.

For the first control stimulus (“single position”) the bars were presented in the same position in both eyes. Because there is no binocular disparity, this stimulus is perceived as a single bar at the same distance as the rest of the display. In the second control stimulus (“offset positions”), the bars were offset between the eyes by the same amount as the main stimulus, but were presented alternating between the two eyes, i.e. temporally interleaved, at 10 Hz. This stimulated the same retinal positions as the “position in depth” condition, but without the perceptual experience of a bar floating in depth.

Fixation task and monitoring binocular fusion

During the presentation of the stimuli the participant performed a simple task at fixation. At random intervals the fixation dot would move either slightly towards or slightly away from the participant in depth. The participant reported the direction of the change (i.e. towards or away) by pressing one of two response buttons. This task ensured fixation of gaze at the center of the display,

and ensured proper binocular fusion. The difficulty of the task, i.e. the amount of disparity, was adjusted so that most participants would be correct around 75% of the time. The behavioral results for this task (Appendix Figure A2.1) show that participants performed this discrimination task correctly on an average of 77% of trials.

Magnetic resonance imaging

All MRI data was collected at the University Medical Centre Utrecht using a Philips 7 Tesla MRI scanner.

T1-weighted anatomical MRI data were acquired using a 32-channel head coil at a resolution of 0.5x0.5x0.8 mm. These were subsequently resampled to 1 mm isotropic resolution. Repetition time (TR) was 7 ms, echo time (TE) was 2.84 ms, and flip angle was 8 degrees.

For four participants functional T2*-weighted 2D echo planar images were acquired using a 16 channel head coil. For the other three participants functional images were acquired using a 32 channel head coil. In all cases the resolution was 1.98x1.98x2 mm, field of view was 190x190x52 mm, TR was 1500 ms, TE was 25 ms, and flip angle was 80 degrees. The acquired volume was always oriented perpendicular to the Calcarine sulcus providing coverage of the occipital lobe and posterior parts of the parietal and temporal lobes.

Functional runs were each 248 time frames (372 seconds) in duration, of which the first eight time frames (12 seconds) were discarded to ensure the signal was at steady state. Data for all conditions was collected during 2-3 sessions per participant, for a total of 7-9 repetitions per condition.

Processing of functional imaging scans

Functional scans were first compensated for head movement and motion artifacts (Nestares & Heeger, 2000). Subsequently, the functional images were averaged and aligned to the whole-brain anatomical scan. The alignment was done automatically (Nestares & Heeger, 2000) and afterwards checked and refined manually if needed.

Model-based fMRI analysis

The population receptive field (pRF) is defined as the region of visual space that optimally stimulates a recording site (Dumoulin & Wandell, 2008). Using a previously described method, we estimated pRF properties (position and size) as well as the haemodynamic response function (HRF) from the fMRI data (Dumoulin & Wandell, 2008; Zuiderbaan et al., 2012).

Briefly, the pRF method is based on a forward model that estimates the pRF position and size based on the time course of the stimulus aperture and the measured BOLD time series. As illustrated in Appendix Figure A2.2, we model the pRF as a 2-D difference of Gaussians function described by four parameters (position: x, y , size: $\sigma_{center}, \sigma_{surround}$). We multiply each candidate pRF with the stimulus aperture at each point in time, resulting in a predicted time course of the neural activation. After convolution with the HRF, this yields a prediction of the BOLD response, given the candidate pRF. Next, the predicted BOLD response is compared to the measured BOLD time series, and the residual sum of squares (RSS) is used to assess the goodness-of-fit. We use a coarse-to-fine procedure to identify the optimal pRF parameters. We start with a large set of permutations of possible pRF parameters. For each recording site the optimal parameters from this large set are refined using a non-linear optimization routine. The pRF parameters that produce the prediction with the smallest RSS

are chosen for each recording site.

The analysis in this study differs from the typical pRF analysis because we use two different stimulus apertures to make the candidate time series predictions. This results in two different predictions for each recording site's time series. As an additional step at the end of the analysis we compare which of the predicted time series better explains the measured BOLD time series across recording sites in terms of the amount of variance explained. Appendix Figure A2.3 shows an example BOLD time series with the pRF model predictions for a recording site in area V1 of a single participant. As shown in the top panel (black dots: *measured time series*, blue line: *single bar prediction*, red line: *offset bars prediction*) the differences are quite small since the difference between the two stimulus sequences used to generate the predictions is small. However, looking at the difference between the two pRF predictions (bottom panel, green line) it is evident that the differences are mainly located at the points in the time series where the bar makes a horizontal (left-to-right, v.v.) or diagonal pass through the visual field. This is what we would expect since the binocular disparity is only present when the stimulus passes through the visual field in horizontal (left-to-right, v.v.) and diagonal directions.

Selecting voxels

In our main analysis we included all voxels whose best-fitting pRF model could explain more than 25% of the observed BOLD response variance (in addition to criteria such as eccentricity and size of the pRF) to exclude unresponsive voxels. We found however that many such voxels in areas beyond V2 could not reliably discriminate between the two control stimuli used in the experiment, although they still explained over 25% of response variance. To investigate cortical representations in these areas we ran an additional analysis that only used

The cyclopean eye in human visual cortex

voxels whose pRF models in our two control conditions could correctly discriminate which stimulus was shown. In order to be included in the analysis a voxel had to correctly discriminate between the two pRF models based on the original time series as well as explain at least 25% of the variance in the time series.

Appendix

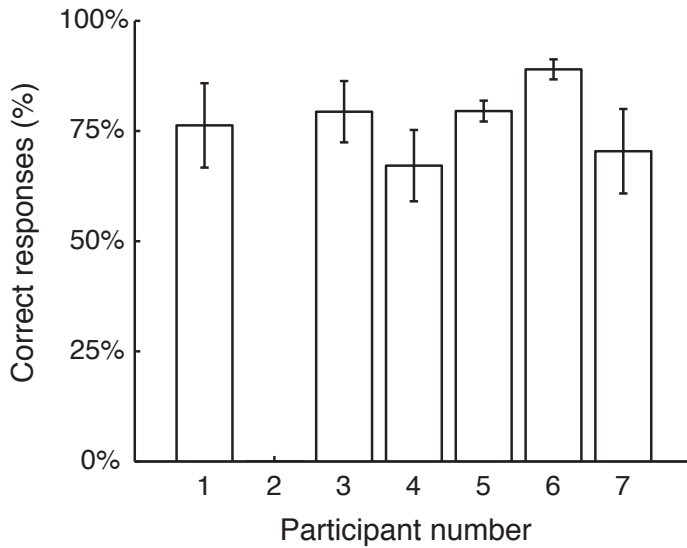


Figure A2.1 Behavioral results for all participants. At random intervals during the experiment the fixation dot's position in depth was changed briefly. Participants reported the direction of the change in position (towards or away) by pressing one of two buttons on the response box. The results are plotted as the percentage of correct responses during the experiment for each participant. Data for participant 2 is missing due to a technical problem with the response box. All error bars \pm s.e.m.

Single bar prediction

Offset bars prediction

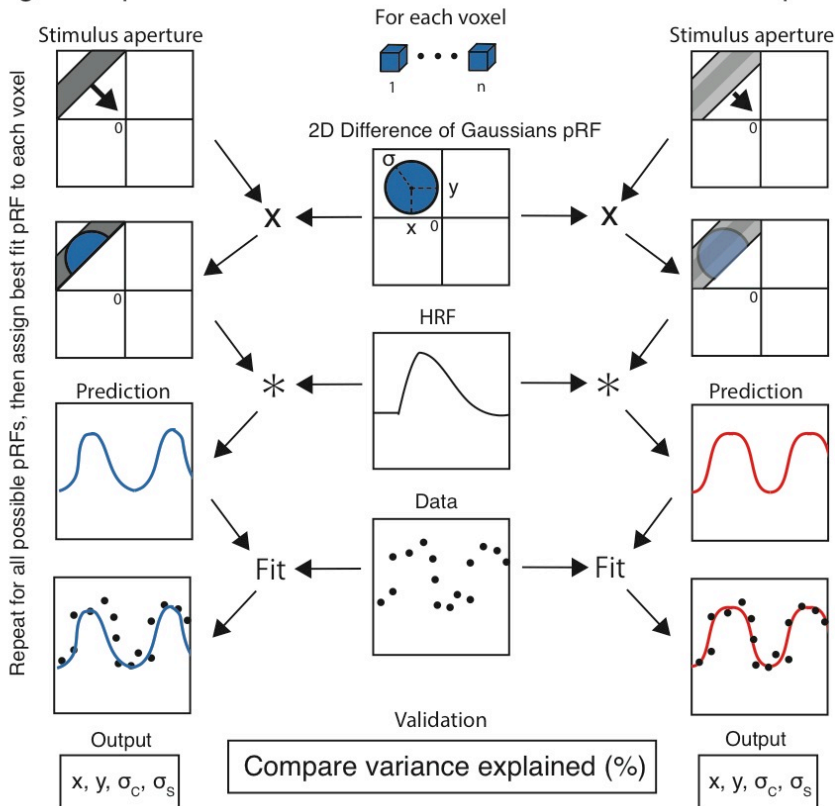


Figure A2.2 Schematic description of the pRF modeling analysis. Flowchart describing the pRF analysis for a single MRI recording site. We computed the overlap of the stimulus aperture with a model of the pRF (modeled as a 2-D Difference of Gaussians) for a given recording site and convolved the resulting time series with the haemodynamic response function (HRF) to provide a prediction of the measured time series for each recording site. Using different parameters for the modeled pRF we searched for the best fitting prediction to the measured data. When applying this method using different stimulus apertures, we can establish which model better predicts the observed data. The models are compared by the amount of variance explained in the observed BOLD time series.

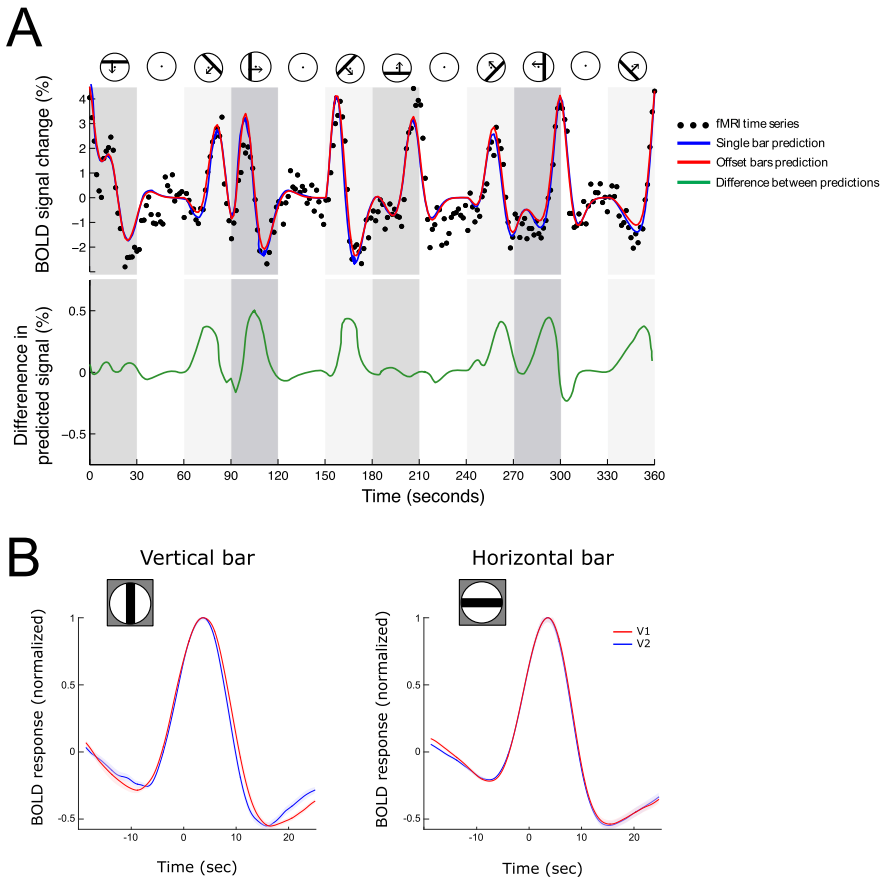


Figure A2.3 A: Examples of an observed V1 recording unit (voxel) time series and the predicted pRF model time series. pRF model predictions generated using two different stimulus apertures (single bar and offset bars) look relatively similar by eye and both predict a large proportion of the variance in the fMRI time series (panel 1). Panel 2 reveals that the major differences in the predicted time courses coincide with vertical and diagonal orientations of the bar stimuli. This is expected since the retinal positions of the stimulus in the two eyes differ for diagonal and vertical orientations of the stimulus, whereas no such difference in retinal position exists for the horizontal stimulus orientation. **B:** The observed HRF response averaged across voxels, stimulus repetitions and observers. The normalized BOLD response (vertical axis) is plotted as a function of time relative to the center of the pRF (horizontal axis). Because differences in pRF position between voxels result in differences in time courses we used a previously described method to align the BOLD response to the same point in time: the moment the stimulus passes through the center of each pRF (Dumoulin, Hess, May, Harvey, Rokers, & Barendregt, 2014). We observe a slightly broader HRF in visual area V1 compared to visual area V2 when the position-in-depth stimulus is oriented vertically, but not when it is oriented horizontally.

The cyclopean eye in human visual cortex

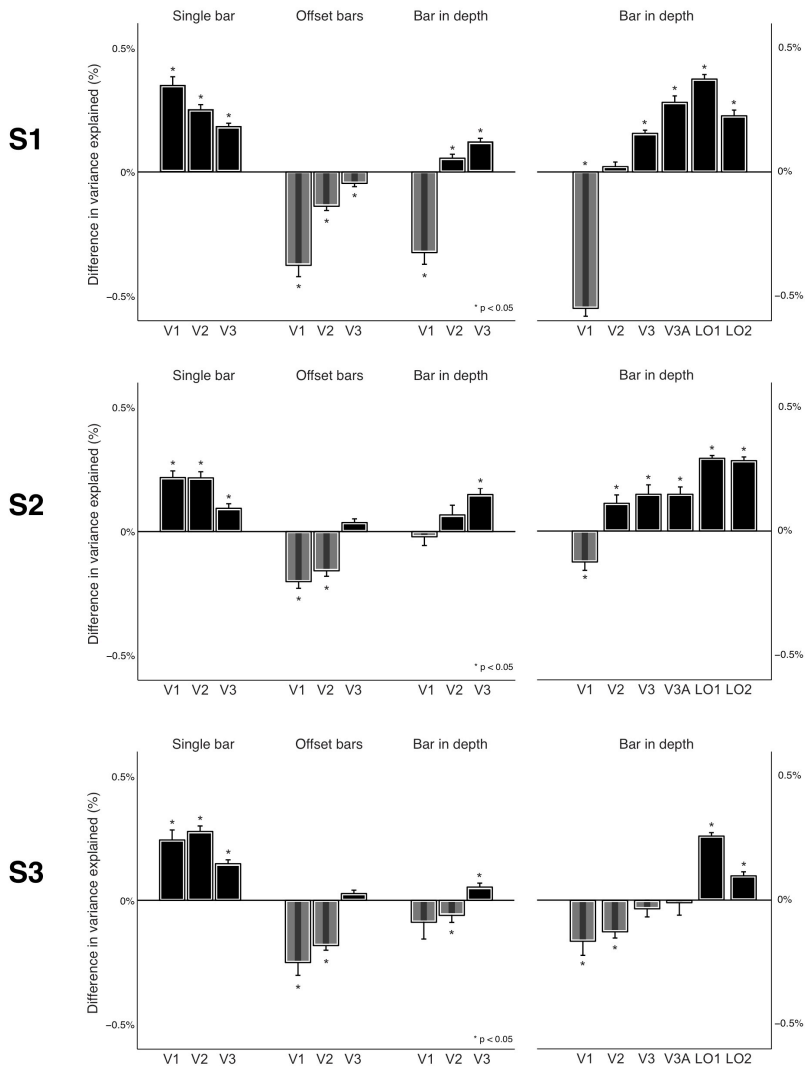


Figure A2.4 Individual participant results for participants S1-S3. Difference in variance explained between a model encoding a single stimulus position and a model encoding two offset retinal positions for the 3 datasets and three early visual areas. The solid black bars indicate that the data is best explained by a model encoding a single stimulus position and the striped bars indicate the data is best explained by a model encoding two offset retinal stimulus positions. As with **Figure 2.3B** in the main text, the right panel shows the difference in variance explained only for voxels that could correctly discriminate between the stimuli. All error bars \pm s.e.m.

Chapter 2

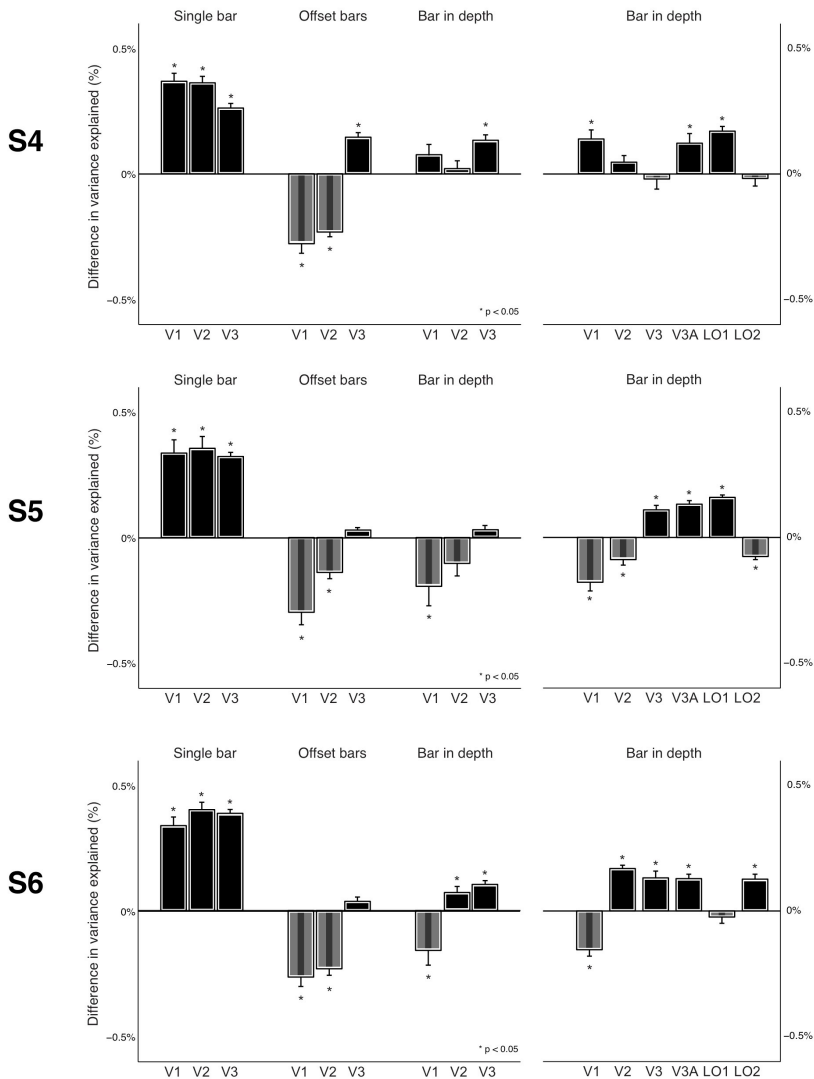


Figure A2.4 (cont.) Individual participant results for participants S4-S6. Difference in variance explained between a model encoding a single stimulus position and a model encoding two offset retinal positions for the 3 datasets and three early visual areas. The solid black bars indicate that the data is best explained by a model encoding a single stimulus position and the striped bars indicate the data is best explained by a model encoding two offset retinal stimulus positions. As with **Figure 2.3B** in the main text, the right panel shows the difference in variance explained only for voxels that could correctly discriminate between the stimuli. All error bars \pm s.e.m.

The cyclopean eye in human visual cortex

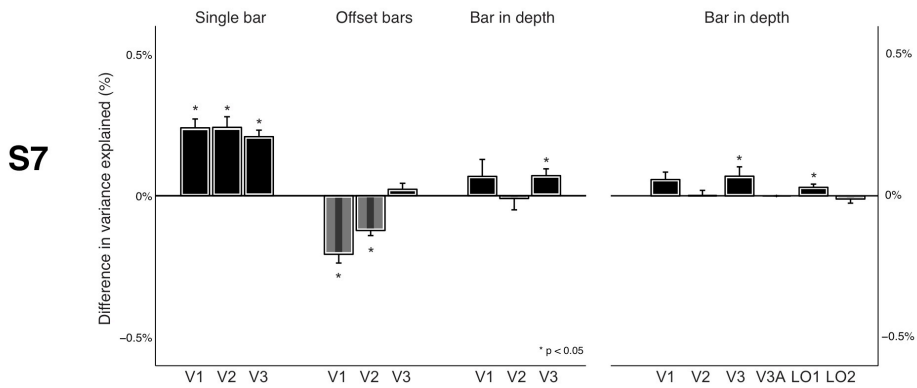


Figure A2.4 (cont.) Individual participant results for participant S7. Difference in variance explained between a model encoding a single stimulus position and a model encoding two offset retinal positions for the 3 datasets and three early visual areas. The solid black bars indicate that the data is best explained by a model encoding a single stimulus position and the striped bars indicate the data is best explained by a model encoding two offset retinal stimulus positions. As with **Figure 2.3B** in the main text, the right panel shows the difference in variance explained only for voxels that could correctly discriminate between the stimuli. All error bars \pm s.e.m.

Chapter 3

STEREOMOTION SCOTOMAS OCCUR AFTER BINOCULAR COMBINATION

Published as:

M Barendregt, SO Dumoulin & B Rokers (2014) Stereomotion scotomas occur after binocular combination. *Vision Research* **105**, 92-99

Acknowledgement of author contributions: MB, BR and SOD designed the experiment. MB collected the data and performed data analysis, under supervision of BR and SOD. All authors contributed to writing the manuscript.

Abstract

Stereomotion scotomas are a surprisingly common visual impairment that result in an observer's inability to accurately report the direction of an object's motion in depth in restricted parts of the visual field. In this study we investigated the role of binocular cues to motion in depth. Using stimuli containing only non-stationary cues to stereomotion, we measured sensitivity across the visual field and identified areas of significant impairment in stereomotion processing in over 50% of otherwise healthy observers. These impairments vary idiosyncratically in extent and location between observers. We established that these impairments occur for a variety of visual stimuli, as long as they share the property that stimulus motion is exclusively defined by interocular and velocity differences. We tested for concordant impairments at relatively early stages along the visual pathway, i.e. changes in sensitivity across the visual field to local eye-dominance, monocular motion or instantaneous binocular disparity. Although we find variability in sensitivity across the visual field of our observers for all visual tasks, this variability across visual field locations did not correlate with the impairments in stereomotion processing. We therefore conclude that these stereomotion scotomas are due to impaired processing of dynamic cues after the stage of binocular combination.

Introduction

Everyday activities such as playing sports, driving a car or just navigating the world depend on the ability to perceive motion in depth. Despite its importance, the ability to perceive motion in depth can be impaired in a large proportion of otherwise healthy observers (Hong & Regan, 1989; Regan, Erkelens, & Collewijn, 1986). These impairments are specific to regions of the observers' visual field in which they are not able to judge whether an object is moving towards or away, termed stereomotion scotomas (Richards & Regan, 1973). The nature and underlying cause of these visual impairments have received little attention and therefore remain poorly understood. We investigated whether these stereomotion scotomas are specific to either a deficit in early visual processing of the binocular cues to motion in depth or rather the result of deficient processing in a later stage of the visual hierarchy.

In natural scenes an object moving towards or away from an observer produces both monocular and binocular cues to motion in depth. We consider only binocular cues and their monocular constituent signals here because we are specifically interested in stereomotion processing. The visual system can use two binocular cues to motion in depth: changing disparity over time (CD) and interocular velocity differences (IOVD) (Harris, Nefs, & Grafton, 2008; Regan & Gray, 2009). The visual system processes these two cues independently (Rokers, Cormack, & Huk, 2009) and there is mounting evidence that the cues make independent contributions to the percept of motion in depth (Brooks & Stone, 2004; Brooks, 2002; Czuba, Rokers, Huk, & Cormack, 2010; Nefs, O'Hare, & Harris, 2010; Rokers, Cormack, & Huk, 2008; Shioiri, Nakajima, Kakehi, & Yaguchi, 2008; Shioiri, Saisho, & Yaguchi, 2000).

Stereomotion scotomas occur after binocular combination

In order to identify stereomotion scotomas we measured sensitivity to the direction of motion in depth across the visual field in our observers. To exclude possible contributions from instantaneous binocular disparity, we used a set of stimuli that were specifically designed to contain only non-stationary cues to stereomotion. Specifically, in previous work the stimulus consisted of a small rectangular bar that was moved back and forth in depth (Hong & Regan, 1989; Regan et al., 1986). Such a stimulus is confounded because it contains static cues to the direction of motion in depth (instantaneous disparity at the start and end of motion). To circumvent this issue, we used a drifting grating pattern within a Gaussian aperture. Because of the periodicity of the grating, instantaneous disparity would be uninformative of the direction of motion. In order to ensure that the measured sensitivity for stereomotion is not specific to certain stimulus parameters, we also used a different stimulus (moving dots) to independently verify the location of any stereomotion scotomas.

Next, we considered the possible underlying causes for stereomotion scotomas in early stages of visual processing. As illustrated in Figure 3.1 the binocular percept of 3D motion can be computed by processing monocular signals in two separate ways, corresponding to the two binocular cues to motion in depth (CD, IOVD). We hypothesized that a deficit in processing of either the monocular velocities ($V_{L,R}$) or binocular disparity (D_t) could be the underlying cause of the stereomotion scotomas, since either of those deficits could result in a less reliable stereomotion signal (V_{3D}). Another possible cause for the scotomas, binocular rivalry, is not directly represented in Figure 3.1, but would most likely occur prior to extracting these cues.

We were particularly interested in this question, since visual sensitivity for each of the constituent cues to stereomotion varies across the visual field. Stereomotion scotomas might therefore be the result of a specific impairment at

Chapter 3

one of these stages of stereomotion processing. Specifically, sensory eye dominance in binocular onset rivalry has shown to be anisotropic across the visual field (Carter & Cavanagh, 2007; Xu, He, & Leng, 2011). Additionally, there is variability in sensitivity to binocular disparity (Blakemore, 1970; Julesz, 1971; Westheimer & Truong, 1988), as well as directional anisotropy of motion sensitivity (Ball & Sekuler, 1980; Edwards & Badcock, 1993; Georgeson & Harris, 1978; Giaschi, Zwicker, Young, & Bjornson, 2007; Raymond, 1994) across the visual field. We therefore compared the variability in sensitivity to these cues with the variability in the locations of observers' stereomotion scotomas.

Briefly, we found evidence for stereomotion scotomas based on non-instantaneous cues in over 50% of our observers. The scotomas varied idiosyncratically in size and location between, but not within, individual observers. We found variability across the visual field in sensitivity at each of the three stages of stereomotion processing in our observers but these variations were not predictive of the location of the stereomotion scotomas. These results lead us to conclude that stereomotion scotomas are not due to binocular rivalry, and occur based on deficits in visual processing after the extraction of retinal motion and binocular disparity. The impairments therefore have to be due to impairments in the processing of the cues underlying stereomotion, i.e. the changing disparity (CD) and/or interocular velocity difference (IOVD) cues, later in the visual hierarchy.

Stereomotion scotomas occur after binocular combination

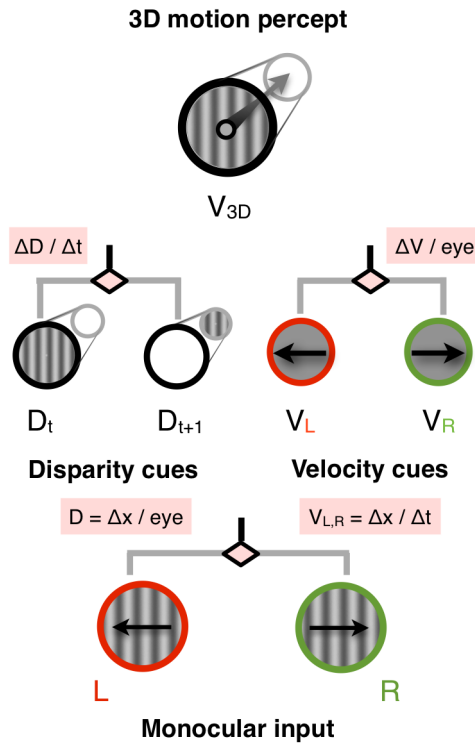


Figure 3.1 An estimate of motion in depth can be computed by processing binocular information in two ways. Based on the two retinal images the visual system can extract velocities for each eye ($V_{L,R}$) and compare these velocities to compute the motion in depth (V_{3D}) percept (formula in pink rectangle). The computation of motion in depth can also be based on disparity information. After computing the binocular disparity (D_t) from the retinal images the visual system could track the change in disparity over time (D_{t+1}) as a cue to motion in depth (formula in pink rectangle). A deficit in extracting the monocular velocities or in processing the binocular disparities is hypothesized as a possible cause for the stereomotion scotomas.

Methods

Observers

A total of 11 observers (1 female, ages 24-38) participated in the experiments. The participants gave informed consent and all had normal or corrected-to-normal vision. All were experienced psychophysical observers and naive to the purpose of the experiments, with the exception of the three authors. The experiments were carried out in accordance with the Code of Ethics of the World Medical Association (Declaration of Helsinki).

Apparatus & display

All stimuli were presented using a mirror stereoscope. The setup consisted of two 20" CRT displays (85Hz, 1024x768 pixels) with each display containing the image for one eye at a simulated viewing distance of 75 cm. The luminance of the two displays was linearized using standard gamma-correction procedures, and the mean luminance was 46.7 cd/m². The observer viewed the images through a set of mirrors that redirected each image to the corresponding eye. Vergence was facilitated by a 1/f noise background pattern. In addition a small fixation dot and a fixation cross of nonius lines was presented in the center of the display to help the observer maintain fixation and monitor vergence during the experiments. (See Figure 3.2 for an example of the stimulus display). The stimuli were generated using a Apple Mac Pro computer using Matlab (Mathworks, Natick, MA, USA) and the Psychophysics Toolbox 3 (Brainard, 1997; Kleiner, Brainard, Pelli, & Ingling, 2007; Pelli, 1997).

Stereomotion scotomas occur after binocular combination

Stimuli

The stimuli were presented within circular apertures (1.5° diameter) positioned within a 7.5° radius around fixation. The centers of the apertures ranged from 1.5° to 7.5° eccentricity in 5 equal steps and were laid out in a spoke-wheel pattern with 8 locations per ‘ring’ (see Figure 3.2). This arrangement provided a total of 40 testing locations across the visual field.

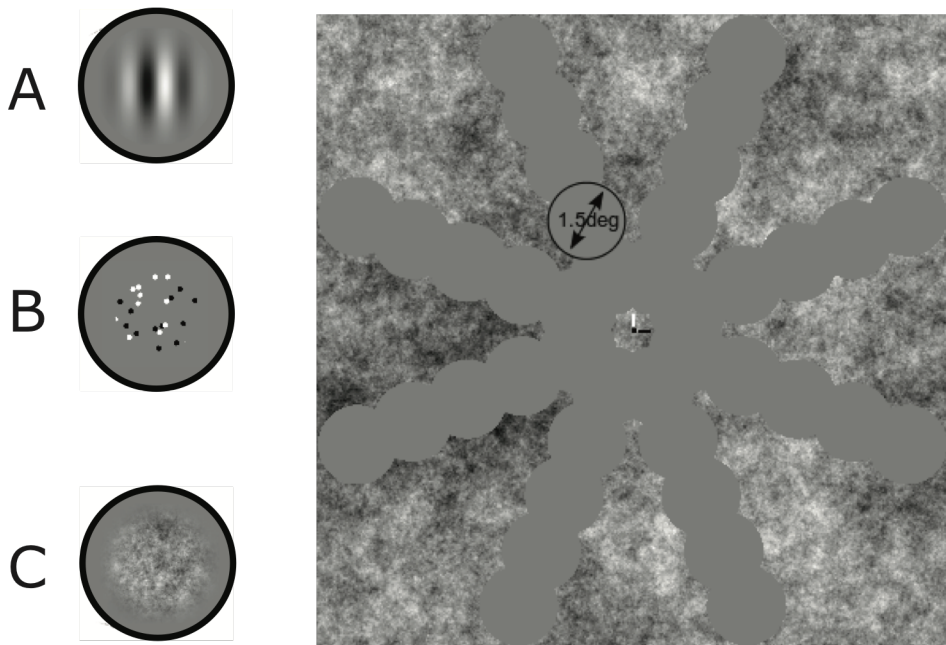


Figure 3.2 *Example of the stimulus display for one eye. Each eye's image contained 40 locations (gray circles) across the visual field where sensitivity would be assessed. The displays for the two eyes were identical except for the fixation cross and the stimulus. A: The stimulus for the stereomotion and ocular dominance experiments consisted of a sinusoidal grating pattern. B: In the stereomotion and lateral motion experiments, the stimulus consisted of randomly positioned black and white translating dots. C: In the static depth experiment the stimulus was a randomly generated circular patch of pink (1/f) noise with horizontal offset between the two eyes.*

Stereomotion sensitivity

We measured stereomotion sensitivity in three different experiments. In the first stereomotion sensitivity experiment, the stimulus consisted of a sinusoidal grating (2 cycles/°) drifting laterally at 4 cycles/sec within a stationary spatial envelope (2-dimensional Gaussian, sigma 0.25°, falling to 1% luminance at 0.56° eccentricity, Figure 3.2A). These stimulus parameters were used based on previous work which showed that stereomotion sensitivity is highest at a monocular speed of ~2 °/sec (Czuba et al., 2010) and our pilot data which showed that this spatial frequency produces the strongest percepts of motion in depth for this size of the Gaussian envelope.

In the second stereomotion experiment we used the same procedure as the first experiment but the stimulus consisted of moving dots rather than drifting grating patterns. A group of randomly distributed black and white dots (Figure 3.2B, dot diameter 0.06°) was presented moving laterally at 2 °/sec in opposite directions in the two eyes. Because the disparity range was limited this created a percept of the dots continuously wrapping through a cylindrical volume.

In the final stereomotion sensitivity experiment we used the exact same stimulus configuration as the first experiment (drifting grating, Gaussian aperture) but with varying contrast levels (5%, 7.5%, 10%, 20%, 100% contrast). Because the additional variable (contrast) increases the number of trials needed for each observer, we confined the stimulus to a single eccentricity 'ring' that would include a region of reduced stereomotion sensitivity (as measured by the previous two methods) in each observer. Because we had 5 levels of contrast as well as 5 different eccentricities in the previous experiments, this resulted in the same number of trials for this experiment and the previous ones.

Stereomotion scotomas occur after binocular combination

In order to identify a possible underlying cause for the impairments relatively early in the visual pathway, we conducted four experiments that measured extent of eye dominance (2 experiments), sensitivity to static binocular disparity, and sensitivity to lateral motion, in the same locations across the visual field. Movies of all stimuli used in the experiments have been included in the Appendix.

Eye dominance

To measure sensory eye dominance we used a binocular rivalry paradigm and two types of stimuli. The first stimulus was a stationary version of the 2 cycles/° grating pattern used in the stereomotion experiment (Figure 3.2A) but oriented $\pm 45^\circ$ (counter)clockwise in the two eyes. The second stimulus was the drifting 2 cycles/° grating pattern used previously, but instead of drifting horizontally, this grating drifted vertically, in opposite direction (up-/downward) in the two eyes. Both stimuli were designed to create binocular rivalry, instead of binocular fusion, so that in the absence of strong eye dominance the percept could alternate between the left- and right-eye stimuli.

Binocular disparity

To measure sensitivity to disparity-based static depth, a patch of randomly generated pink (1/f) noise (Figure 3.2C) was presented within the same Gaussian aperture as the grating stimuli. The use of a 1/f noise patch over a stationary grating was necessary because the periodicity of the latter would have rendered the disparity signal ambiguous (i.e. a binocular ‘match’ could be found in either direction). The patch was displaced, inside the aperture, between the two eyes to create a binocular disparity of $\pm 0.1^\circ$ (6 minutes of arc).

Lateral motion

In the motion sensitivity experiments the stimulus consisted of a set of randomly distributed black and white dots (Figure 3.2B, dot size 0.08°) contained within a 2° circular aperture centered on one of the 40 locations in the same way as in the other experiments. This larger diameter of the aperture was necessary because pilot experiments showed that a 1.5° aperture (which would correspond more closely to the Gaussian apertures) was too small to perform the task, even at 100% dot coherence. On each frame the dots would be repositioned at either a random location or according to a set direction (left or right) and displacement ($dx=0.3^\circ$, $dt=45ms$). The number of dots that would displace coherently was fixed at 50% (value based on pilot study using staircase-method) and the signal and noise dots were randomly selected on each frame-interval. A total of four sets of dots were presented interleaved to prevent 'streaks' and tracking of individual dots (Newsome & Pare, 1988). The dots were presented binocularly but with the exact same configuration in the two eyes.

Procedure and task

The stereoscope was initially adjusted so that the vergence demand was appropriate for the viewing distance given a typical interocular distance. Prior to each session, the observer made further adjustments so that the nonius markers were aligned both horizontally and vertically, and vergence was comfortable. Observers were instructed to maintain fixation at all times during the experiment.

All experiments followed a similar presentation procedure. In the stereomotion experiments the grating stimulus drifted (or dots moved) in opposite horizontal

Stereomotion scotomas occur after binocular combination

directions in the two eyes creating a binocular percept of motion drifting towards or away from the observer. On each trial the stimulus was presented for a single 250ms interval in one of the 40 possible locations. Observers were asked to maintain fixation at the center of the display at all times, so that this procedure mapped sensitivity to the stimuli across the visual field. After stimulus offset observers responded via a key press. For each observer, 20 repetitions of each of the 40 locations were pseudo-randomly distributed across trials, ensuring that the observer was unable to predict the location for any given trial. In the stereomotion experiments, the observer performed a 2-alternative forced-choice (2AFC) task on the direction of motion (towards/away) of the stimulus on each trial.

The binocular rivalry experiments followed a similar presentation procedure but with a longer stimulus duration (500ms). In pilot experiments we did not observe significant rivalry at the shorter 250ms duration used in the stereomotion assessment. To determine if rivalry nonetheless might be a contributing factor to the stereomotion scotomas, based on previous reports of variation in eye dominance across the visual field (Carter & Cavanagh, 2007; Stanley, Carter, & Forte, 2011), we assessed rivalry using the longer stimulus duration. The task for the observer was to indicate on each trial which of the two possible percepts (clockwise/counterclockwise orientation, upward/downward motion) was observed. If there was no exclusive dominance of one percept the observer was instructed to report the “more predominant” of the two.

In the static depth experiment the stimulus was presented for 250ms and the observer indicated whether the stimulus was perceived “in front” or “behind”

the plane of fixation, as defined by the fixation cross and the 1/f noise background.

The motion sensitivity experiment had a presentation duration of 500ms (the task proved too difficult at shorter durations) on each trial. The task for the observer was to report the perceived direction of motion (left/right) of the coherently moving dots.

Data analysis

In order to quantify the stereomotion sensitivity of each observer, the percentage of correct responses was computed for each location in the visual field. To determine the stability of the measured stereomotion sensitivity we tested each observer on three separate days and computed the Pearson correlation coefficient across locations between the separate datasets. We generally observed good session-to-session agreement and subsequently combined data from three sessions for each observer to increase statistical power. The percentages correct were then plotted in a visual field map (e.g. Figure 3.3) where each sample location is represented by a colored circle. A black contour marks locations where the percentage of correct responses was significantly different from chance ($p < 0.05$, uncorrected, binomial test). We opted to use an uncorrected statistical criterion because we were interested in identifying locations where performance did not differ significantly from chance. Adopting such a criterion makes us relatively conservative in classifying a location as lying within a stereomotion scotoma.

Each of the other experiments was also repeated on three separate days and then subsequently combined to increase statistical power. The data from these experiments were analyzed in the same manner as the stereomotion

Stereomotion scotomas occur after binocular combination

experiment, i.e. using the percentage of correct responses in each location of the visual field, with the caveat that for the binocular and motion rivalry experiments there was no 'correct' response. For these experiments we computed the percentage of correct responses to the stimulus presented in the left eye. This produced a percentage between 0% and 100%, where 100% (0%) indicates that the observer always reports the stimulus that was presented in the left (right) eye and 50% means that the observer's responses showed no bias of one eye over the other. Locations in the visual field where this value was significantly different from 50% ($p < 0.05$, uncorrected, binomial test) therefore indicated locations where one of the eyes was dominant.

Results

In the experiments described here we aimed to measure the sensitivity to stereomotion across the visual field for individual observers and to establish whether the location of deficits in stereomotion sensitivity was reproducible over multiple testing days.

Regions of stereomotion insensitivity in ~50% of observers

We quantified the sensitivity to stereomotion across the visual field for individual observers across three separate sessions using Gabor patterns (Figure 3.2A). We plotted the sensitivity in a visual field map for each observer, providing a visual reference for the relative sensitivity across the visual field. In Figure 3.3 the visual field maps for eight individual observers are shown. The colormap indicates the percentage of correct responses at each location in the visual field with 50% indicating total inability to determine direction of motion in depth (chance level) and 100% indicating perfect ability. A black contour indicates locations where the percentage correct is significantly different from chance ($p < 0.05$, uncorrected binomial test).

Figure 3.3A shows the visual field map for a single observer with accurate stereomotion discrimination performance in all measured locations (in all locations the percentage correct responses is significantly above chance). The variability in the percentage correct across locations is relatively small and only shows a slight decrease over the $1.5^\circ - 7.5^\circ$ range of eccentricity. A second observer is shown in panel (B) of Figure 3.3. For this observer the variation in percentage correct responses is much greater across the visual field. In the lower, central part of the visual field the observer was unable to reliably

Stereomotion scotomas occur after binocular combination

discriminate the direction of motion in depth, yet in the rest of the visual field and at the same eccentricities, this observer was perfectly able to do so (performance up to 100% in some locations). A third observer shown in Figure 3.3C has a region of poor stereomotion discrimination performance located very close to the center of the visual field (at 1.5° and 3° eccentricity), demonstrating that the decreased sensitivity is not an overall effect of visual field eccentricity. The other five observers shown in Figure 3.3 all have a region

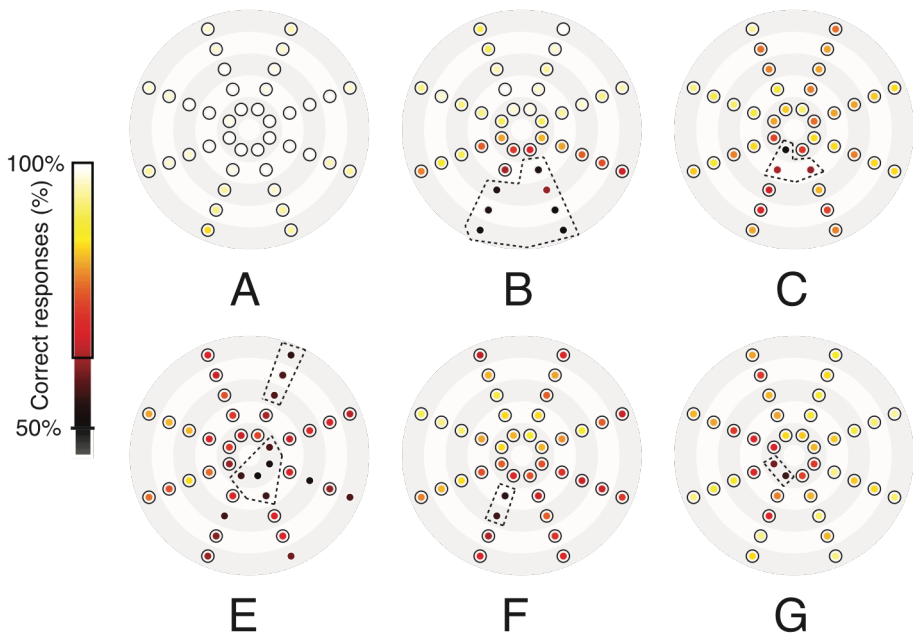


Figure 3.3 *Stereomotion sensitivity across the visual field for eight observers.* Points in the graph correspond to visual field locations on a range of eccentricities (1.5-7.5° in 5 equal steps, indicated by gray/white rings) and polar angles (8 steps of 45° per eccentricity). The colors indicate percentage of correct responses as shown in the colorbar. The black contour marks locations where the performance was significantly above chance, with the threshold as indicated by the black box in the colorbar. The observer in the top left figure has near perfect performance across the whole visual field, and is representative for 4 out of the 11 observers we tested. All of the 7 other observers have a distinct region (at different locations) in the visual field where the performance is not significantly different from chance.

of poor stereomotion discrimination performance in their visual field, although the locations and sizes differ between observers.

Measuring changes in stereomotion performance in terms of percentage correct has the potential to confound changes in sensitivity with changes in response bias. To exclude the possibility that our results are merely reflecting a difference in response bias across the visual field, we also computed d' as a direct measure of stereomotion sensitivity. The details and results are included in the appendix (Appendix Figures A3.1 and A3.2). We found that the percentage correct correlates very strongly with d' ($R^2 = 91\%$, $p < 0.0001$, $N = 8$) and only weakly with response bias ($R^2 = 4\%$, $p < 0.001$, $N = 8$).

We find stable impairments in stereomotion perception in 64% of our observers (7 out of 11, all shown in Figure 3.3 and Appendix Figure A3.1). Within the same observer performance could vary as much as 50%, from chance (50%) to ceiling performance (100% correct), at identical eccentricities. The location and size of the impairments varied idiosyncratically across observers and could be as close as 1.5° from fixation.

Locations of stereomotion insensitive regions are stable over time

To test the stability of the measured visual field over time, we tested each participants on three separate sessions divided over multiple days using the same stimulus (Figure 3.2A). These sessions were separated by at least a day and up to several weeks in some participants. Figure 3.4 shows visual field maps for three observers in three separate sessions. Any region indicated with dotted lines is the region of poor stereomotion discrimination as inferred from the combined data (see Figure 3.3A, B and F). Although there is session-to-session variability in the percentage correct responses within locations, the

Stereomotion scotomas occur after binocular combination

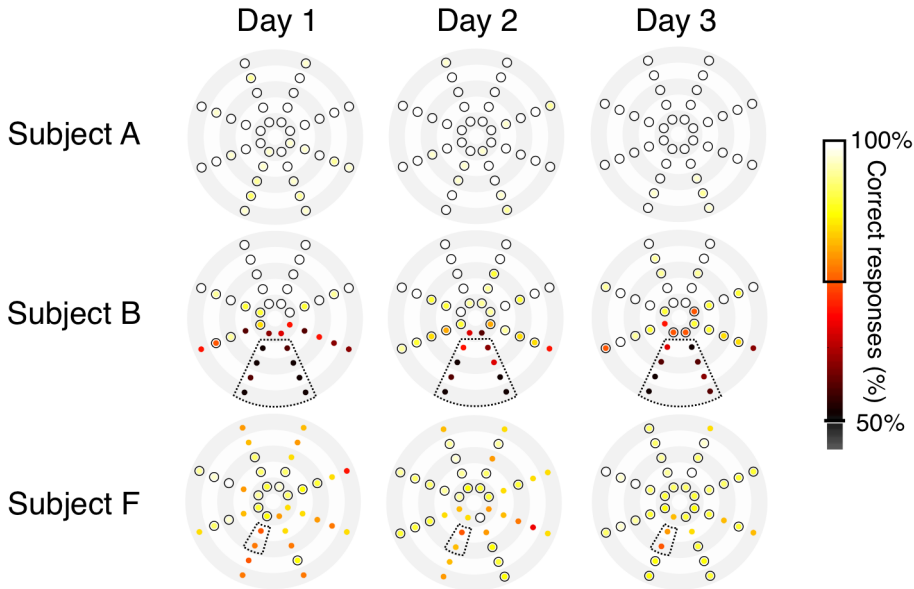


Figure 3.4 *Stereomotion sensitivity maps for three observers on three separate days with intervals ranging from one day to several weeks. The marked region indicates the location of possible stereomotion scotomas based on the cumulative data shown in figure 3.3. Although there is variation in the percentage of correct responses from session to session, locations within the scotoma (marked region) are not significantly different from chance in any of the sessions.*

threshold level is never reached for the locations that lie within the marked region. In general, we observe reliable session-to-session stability in all observers (correlation from 1st to 3rd session: $r = 0.60$, $p < 0.0001$, $N = 7$). Thus we conclude that the stereomotion scotomas are stable over time.

Locations of stereomotion insensitive regions are stable over stimulus parameters

In order to assess whether the measured sensitivity to stereomotion across the visual field is specific to the stimulus parameters used in this study, we repeated our visual field measurements using a stimulus with different characteristics (moving dots, Figure 3.2B). Figure 3.5 shows a comparison of the measured

stereomotion discrimination performance at a single eccentricity using the Gabor and moving dots stimuli for two observers (Figure 3.3E&F). Three observers participated in this moving dots experiment. Performance was correlated between the two different stimuli when combined across observers ($r = 0.68, p < 0.001$). These effects are on the same order as the session-to-session variability we observed within observers using the drifting grating stimuli.

To assess the stability of the scotomas as a function of stimulus contrast, we varied the contrast of the Gabor stimulus (Figure 3.2A) and measured a psychometric curve to quantify contrast sensitivity at 8 locations at a single eccentricity (Figure 3.5C). At very low contrasts (5-10% Michelson contrast) the performance decreases in all visual field positions, but above these values stereomotion sensitivity remained constant over a large range of contrasts (20%-100% Michelson contrast). This shows that sensitivity to stereomotion is not simply the result of different contrast sensitivity inside and outside the stereomotion scotoma. In summary, we found that the stereomotion scotomas were stable across different stimuli and a wide range of stimulus contrasts.

Potential early visual mechanisms underlying stereomotion scotomas

We considered early visual mechanisms involved in stereomotion processing (Figure 1) that could be impaired in the case of stereomotion scotomas. We identified and tested three mechanisms of early processing that might have been impaired: eye dominance, binocular disparity, and lateral motion. We quantified variability across the visual field of our participants for each of these three possible mechanisms in a series of experiments.

Stereomotion scotomas occur after binocular combination

Eye dominance

We measured sensory eye dominance in two related experiments, one using stationary and one using vertically drifting Gabor patterns (Figure 3.2A). Both experiments reveal significant variability in eye dominance across the visual field. In Figure 3.6A eye dominance is reported as the percentage of responses that correspond to the stimulus orientation or motion direction presented in each eye, ranging from 100% right dominant (observer always reported stimulus in right eye) to 100% left dominant (always reported stimulus in left eye). We compared eye dominance based on the stationary Gabor (orientation)

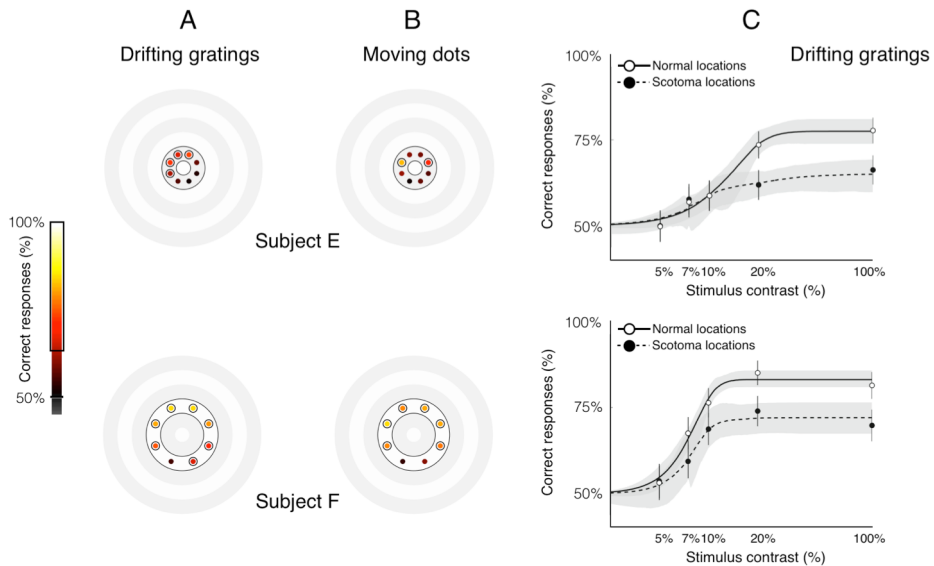


Figure 3.5 Comparison of stereomotion sensitivity in two observers as measured by three different tasks. All panels (A,B,C) display the results from the same two observers. A: Percentage of correct judgments when using a drifting grating. B: Percentage of correct judgments when using moving dots. Both panels A and B plot percentage of correct responses as a function of visual field position. The performance for the two different stimuli (A:grating vs B:dots) are significantly correlated $r = 0.63$ ($p < 0.0001$). C: Percentage of correct responses as a function of Michelson contrast (5%-100%). Here we presented the drifting grating pattern at different contrast levels. The two lines represent the average of the measurements taken at either the normal (open symbols) or scotoma locations (solid symbols, also in panel A&B). Performance remains relatively stable across a wide range (20-100%) of stimulus contrasts.

with eye dominance based on the drifting Gabor (motion) stimulus. We found a significant correlation between the two eye dominance experiments ($r=0.28$, $p<0.001$, $N=4$), suggesting that motion-based and orientation-based rivalry share a common mechanism. However, we did not find a significant correlation between the performance in the stereomotion experiment and eye dominance ($r=0.005$, $p=0.94$, $N=7$ for orientation rivalry and $r=0.08$, $p=0.32$, $N=4$ for motion rivalry).

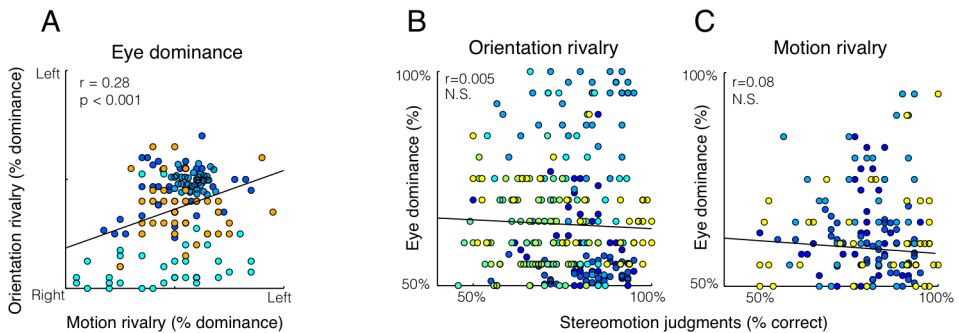


Figure 3.6 A: Measured eye dominance (in %) for 4 observers in two different experiments (different colors indicate different observers). The data shows a significant correlation between the results for the orientation stimulus (stationary grating pattern rotated $\pm 45^\circ$) and the motion stimulus (grating pattern drifting either up- or downward). B&C: Measured eye dominance (vertical axis) as a function of stereomotion discrimination in observers with a stereomotion scotoma. We did not find a significant correlation between the performance in stereomotion discrimination and eye dominance with either of the two stimuli used to measure eye dominance.

Binocular disparity

We quantified sensitivity to instantaneous binocular disparities by the percentage of correct responses when judging position in depth (near/far) for all observers with a stereomotion scotoma. We found that the sensitivity was stable over time (correlation from 1st to 3rd session: $r = 0.45$, $p < 0.0001$, $N=7$) but we found no significant correlation between discrimination performance in the binocular disparity experiment and the stereomotion experiment (Figure

Stereomotion scotomas occur after binocular combination

3.7A, $r=0.08$, $p = 0.81$, $N=7$). These results indicate that the variability in sensitivity to the binocular disparity cue is not predictive of the observed deficits in stereomotion processing.

Lateral motion

In Figure 3.7B we show the percentage of correct responses (between 50% and 100%) to the direction of motion (left/right) for 6 observers with a stereomotion scotoma (correlation from 1st to 3rd session: $r = 0.27$, $p < 0.05$, $N=6$). We did not find a significant correlation between performance in the lateral motion experiment and the stereomotion experiment ($r=0.01$, $p = 0.13$, $N=6$). These results indicate that the variability in sensitivity to lateral motion are not predictive of the observed deficits in stereomotion processing.

In order to exclude stimulus duration as an explanation of differences in task performance, we ran an additional version of the main experiment where we

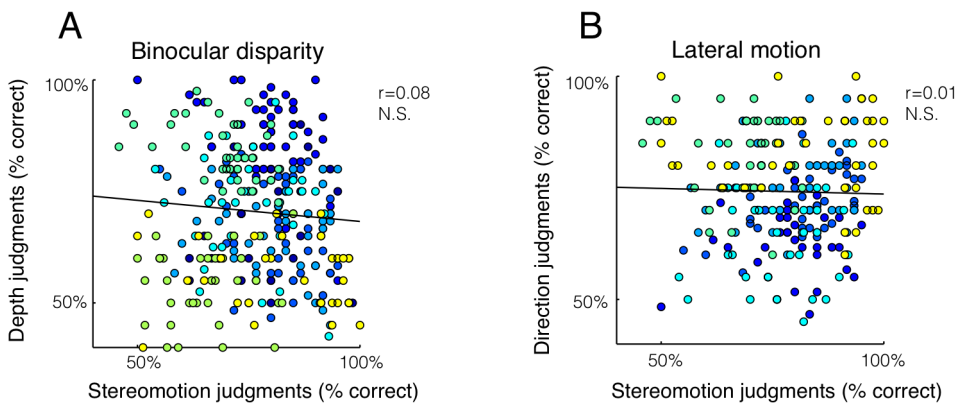


Figure 3.7 A: Performance on the depth discrimination task (judging position in depth) as a function of the performance on the stereomotion task (judging direction in depth) for all observers with a stereomotion scotoma. B: Same for the lateral motion direction judgment task. For both visual tasks we did not find a correlation between performance on the task and performance on the stereomotion discrimination task.

Chapter 3

presented the stimulus (drifting grating pattern) for 500ms. The results are included in the Appendix (Appendix Figure A3.3). The percentage correct at 250ms and 500ms presentations is significantly correlated ($R^2=0.89$, $p<0.0001$) demonstrating that a longer presentation time does not significantly alter the results.

In summary, we find clear evidence for local variation across the visual field in each of the three tested mechanisms. The results presented here are correlations over all subjects' data, however we also computed the individual correlations per subject and performed a GLM analysis. In all cases we do not find a systematic relationship between the variability in discrimination performance across the visual field for binocular rivalry, binocular disparity, or lateral motion and the location of stereomotion scotomas.

Discussion

Our results demonstrate that over 50% (7 out of 11) of otherwise healthy observers have impairments in the perception of 3D motion in regions of their visual field. We find that these stereomotion scotomas can vary idiosyncratically in eccentricity, polar angle and size between, but not within, observers. These scotomas are stable in size and position in the visual field within individual observers over time and a variety of stimulus parameters. We subsequently investigated possible causes of these common deficits in 3D motion perception relatively early in visual processing. Specifically, we hypothesized that either binocular rivalry, or deficits in the processing of either lateral motion or binocular disparity formed the basis of these deficits in 3D motion perception. Although the observers showed variability across the visual field for all three candidate mechanisms, none of these deficits in visual processing was predictive of the locations of the stereomotion scotomas.

We designed the stimuli so that instantaneous disparity was excluded as a possible cue. Nonperiodic stimuli will inherently contain such instantaneous disparity cues, and previous work did not explicitly distinguish between the instantaneous and time-varying cues (Hong & Regan, 1989; Regan et al., 1986; Richards & Regan, 1973). We showed that these instantaneous disparity cues are not the basis for the stereomotion deficits since the scotomas persist even when the cues are eliminated, and variability in sensitivity to instantaneous binocular disparity across the visual field does not predict stereomotion performance.

Some variability in measured performance across the visual field could be the result of an observers' inability to maintain fixation throughout the experiment. We did not explicitly monitor eye movements but using a short presentation

Chapter 3

time and randomizing the stimulus location on every trial ensured that eye movements would not be informative to the task. In fact, the significant session-to-session and stimulus-to-stimulus reliability of our findings would be unlikely if the differences in performance across the visual field were purely due to eye movements, and we therefore do not believe our results are driven by eye-movements.

All stimuli were presented at full contrast, except in the one experiment where we explicitly assessed stereomotion sensitivity as a function of stimulus contrast. When asked informally, all observers reported that they could easily see the stereomotion stimuli, in all but the lowest (5%) contrast condition, but that they were simply unable to judge their motion in depth. This indicates that the observers had no trouble perceiving motion in the stimuli but they specifically had trouble judging the direction of motion in depth. Some observers reported that they perceived lateral motion, as if binocular rivalry was occurring. Although, we did find regions of strong eye dominance in accordance with recent findings by Carter & Cavanagh (2007), our analysis showed that there was no systematic relationship between these percepts of binocular rivalry and the location of the stereomotion scotomas.

Other observers reported motion transparency, which can occur when two drifting gratings are superimposed (Adelson & Movshon, 1982; Wallach, 1935), and especially when the gratings differ in spatial frequency, relative direction, speed or contrast (Hupé & Rubin, 2004; Kim & Wilson, 1993; Kooi, De Valois, Switkes, & Grosf, 1992; Smith, 1992; Victor & Conte, 1992). A recent model has been proposed (Hedges, Stocker, & Simoncelli, 2011) that unifies those perceptual phenomena, but it is unclear why a propensity for perceptual coherence or transparency would vary across the visual field.

Stereomotion scotomas occur after binocular combination

Previous work has suggested that the perception of stereomotion might rely more on the processing of velocity rather than disparity cues. For example, sensitivity to changing disparity is often a poor predictor of 3D motion discrimination (Harris & Watamaniuk, 1995), and that psychophysical performance on velocity-isolating stimuli seems to better predict 3D motion performance away from fixation (Czuba et al., 2010). Of course our present findings suggest that sensitivity to lateral motion might be a poor predictor of the ability to perceive 3D motion as well, and care should be taken in attempting to isolate contributions of the constituent cues. Previous work (Nefs et al., 2010) demonstrated large inter-individual differences in the relative contributions of each cue to 3D motion perception. Therefore, it could be the case that the underlying cause for stereomotion scotomas is different across individuals. However, the inseparability of the changing disparity and interocular velocity cues to motion in depth in our current experiments precludes any strong inferences about their relative contribution based on our results.

In sum, we conclude that the commonly occurring stereomotion scotomas are due to deficits in relatively late stages of visual processing. While we do find variability of sensitivity to local ocular dominance, lateral motion sensitivity and static disparity sensitivity, these do not co-vary with the location of stereomotion scotomas. Given the hierarchical organization of the visual system (Essen & Maunsell, 1983), we posit that stereomotion scotomas are not the result of an impairment in the processing of the constituent cues, but rather the result of an impairment in the processing of the later stage cues underlying stereomotion proper, i.e. the changing disparity (CD) and/or interocular velocity difference (IOVD) cues.

Appendix

Estimation of stereomotion sensitivity

In addition to reporting performance in terms of percentage of correct responses, we also computed sensitivity in terms of d' . The values for d' were computed using the following equation:

$$d' = z(p(\text{towards response} \mid \text{towards presented})) - z(p(\text{towards response} \mid \text{away presented}))$$

Where $p(\text{towards response} \mid \text{towards presented})$ is the probability of the observer reporting the motion as towards, given that the presented motion was towards, $p(\text{towards response} \mid \text{away presented})$ is the probability of the observer reporting the motion as towards when the presented motion was away, and $z(p(\dots))$ is the conversion of a probability to the corresponding z score. In case any of these probabilities equaled 1, i.e. performance was 100% correct, we set the probability to 99.17%, or $1 - \frac{1}{2N}$, where N is 60.

In Figure A3.1, the visual fields are plotted the same way as Figure 3.3 in the main text with each dot representing a single location in the visual field and the color representing the value of d' at that location. The location of the stereomotion scotoma (dashed lines) for each observer has been transferred from Figure 3.3 for easy comparison of the performance measured by the percentage of correct responses and the sensitivity measured by d' .

We found a strong correlation ($R^2 = 91\%$, $p < 0.0001$) between the two measures of stereomotion sensitivity in our observers. This is further illustrated in Figure A3.2 where we plotted the individual data points for all observers from the two different measures. A linear fit through the data (solid black line, Figure A3.2 left panel) further illustrates the strong correlation between the two measurements.

Stereomotion scotomas occur after binocular combination

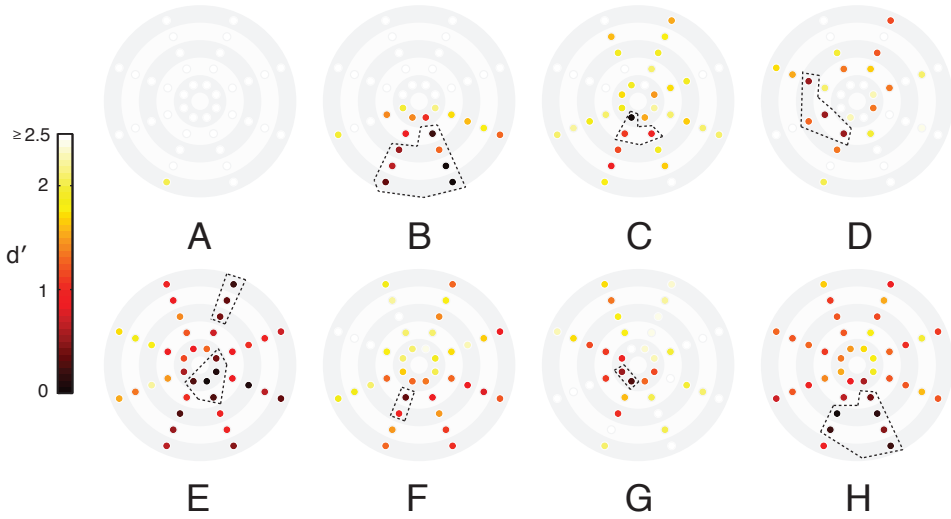


Figure A3.1 *Stereomotion sensitivity across the visual field.* The results are plotted in the same way as Figure 3.3, but here in terms of d' . We added the locations of the stereomotion scotomas (dashed lines) from Figure 3.3. Locations with low sensitivity (d') were in good agreement to locations of stereomotion scotomas identified based on discrimination performance (% correct) that was not significantly different from chance.

The right panel of Figure A3.2 shows the correlation between the performance as measured by percentage correct and the estimate of the response bias. We estimated the response bias by using the following equation:

$$\text{Bias} = -0.5 * (z(p(\text{towards response} | \text{towards presented})) + z(p(\text{towards response} | \text{away presented})))$$

We find a small correlation ($R^2 = 2\%$, $p < 0.01$) between the response bias and the performance as measured by percentage correct, indicating that there is a small increase in the response bias when the performance gets closer to chance level. The results demonstrate a small bias in our observers to report the direction of motion as towards more often than it was presented.

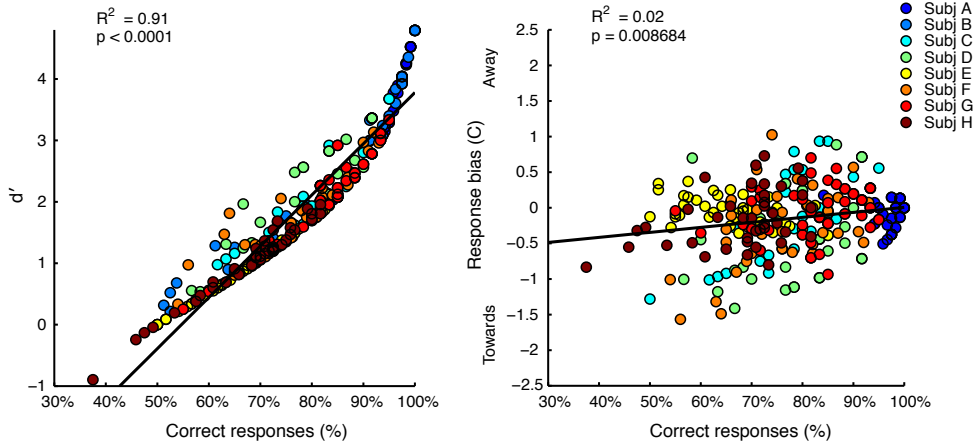


Figure A3.2 Left panel shows the correlation between stereomotion performance as measured by percentage correct (x-axis) and sensitivity as measured by d' (y-axis). The solid line indicates the best linear fit to the data. The analysis shows a variance explained (R^2) of 91% ($p < 0.0001$) indicating that these two measurements are highly correlated. The right panel shows the correlation between the stereomotion performance (x-axis) and an estimate of the response bias (y-axis). The solid line indicates the best fit through the data. The analysis shows a variance explained of 2% ($p < 0.01$) indicating a weak correlation between the two measurements.

Stereomotion scotomas do not vary with stimulus duration

A concern might be that the relatively short (250ms) presentation time of the stimuli in our main experiment contributes to the poor discrimination performance in stereomotion scotoma locations. To investigate whether the presentation time of the stimuli affects the performance in our experiments we ran an additional version of the first experiment (drifting Gabor pattern, observer judges direction of motion in depth) but with a presentation time of 500ms. Figure A3.3 shows the results we obtained in four observers (all part of the first experiment) both with a stimulus presentation time of 250ms (x-axis) and a presentation time of 500ms (y-axis). The results show a strong correlation ($R^2 = 89\%$, $p < 0.0001$) between the stereomotion performance measured with the two different presentation times. These results indicate that

Stereomotion scotomas occur after binocular combination

the poor performance in stereomotion scotoma locations cannot be the result of the stimulus presentation time.

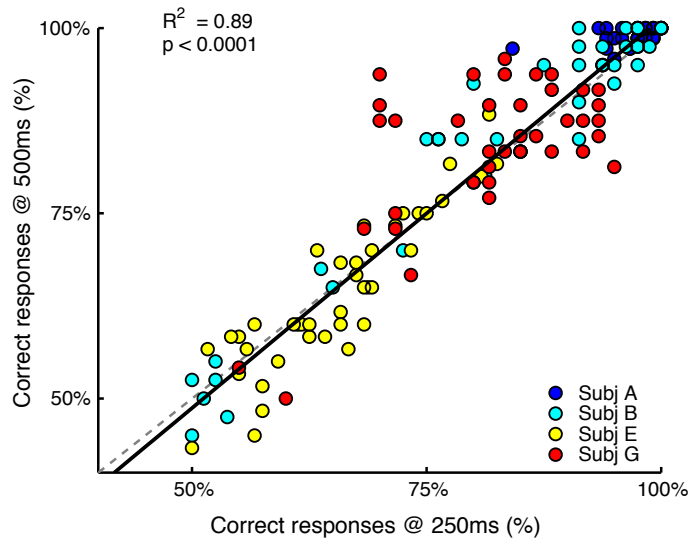


Figure A3.3 Comparison of performance on stereomotion discrimination task with stimulus presentation times of 250ms (x-axis) and 500ms (y-axis) in four observers (red, green, turquoise and blue dots). The solid black line is a linear fit through the data and illustrates that the performance as measured by a stimulus presented for 250ms is highly predictive of the performance when the stimulus is presented for 500ms ($R^2 = 0.89$, $p < 0.0001$). This shows that the inability to discriminate the direction of motion-in-depth in the stereomotion scotoma locations is not affected by stimulus presentation time.

Chapter 4

A NEURAL BASIS FOR MOTION AGNOSIA IN VISUAL CORTEX

In preparation as:

M Barendregt, B Rokers & SO Dumoulin (in preparation) Neural correlates of seen and unseen motion in depth.

Acknowledgement of author contributions: MB, BR and SOD and MB collected the data. MB performed data analysis under supervision of BR and SOD. MB wrote the manuscript and the other authors provided critical comments.

Abstract

Although the accurate perception of approaching and receding motion is critical for survival, over half of otherwise normal observers are unable to use binocular cues to distinguish approaching from receding motion in part of their visual field. This deficit is not due to impairments in early visual processing: binocular disparity and monocular motion detection are unaffected. Here, we investigate the neural basis of this deficit and the neural correlates of motion in depth perception. Participants performed direction judgments on moving dot stimuli across the visual field while in a MRI scanner. We found that neural responses in the middle temporal area (MT) and striate cortex (V1) are modulated by the deficit. We show that these modulations are due to the motion impairment per se in MT whereas they reflect the participants' response to the stimulus in V1. Our results establish the neural bases for a common visual motion impairment. Since the neural basis of the deficit is cortical, and there is no evidence for impaired processing at earlier stages, we conclude that the deficit should be considered a form of motion agnosia. Taken together these results provide new insights into the roles of V1 and MT in the perception of motion in depth.

Introduction

The ability to report the direction of moving stimuli often seems trivial and is generally very robust to stimulus manipulations (Newsome & Pare, 1988). Yet, over half of otherwise normal observers are not able to report the direction of motion in depth (towards/away) in part of their visual field (Barendregt, Dumoulin, & Rokers, 2014; Hong & Regan, 1989; Richards & Regan, 1973). This visual field deficit in motion perception appears to originate in visual cortex where motion signals from the two eyes are combined, and is unrelated to problems with the eyes or processing monocular motion information (Barendregt et al., 2014; Hong & Regan, 1989; Regan et al., 1986). While an observer with such a deficit in motion perception is not able to discriminate the direction of a moving stimulus, they are able to perceive that the stimulus moves (Barendregt et al., 2014). The deficit therefore seems better characterized as a form of visual agnosia (Farah, 2004), rather than motion blindness (scotoma).

Here, we aim to investigate the neural basis of this selective inability to perceive motion direction. The motion processing pathway is well-established in both human and non-human primates, starting with direction-selective neurons in primary (V1) and second (V2) visual cortex (Grunewald & Skoumbourdis, 2004; Livingstone & Hubel, 1988; Lu, Chen, Tanigawa, & Roe, 2010; Movshon & Newsome, 1996). From here the pathway continues to areas MT and MST (Maunsell & van Essen, 1983; Maunsell & Van Essen, 1983) which have a central role in the integration of visual motion (pattern motion, Huk & Heeger, 2002) and a well-described organization for direction-selectivity (Albright, Desimone, & Gross, 1984; DeAngelis & Newsome, 1999). While the physiology

of motion processing is generally well understood, much less is known about the role of area MT in the *perception* of motion (Richard, David, Born, & Bradley, 2005). Stimulation of area MT can influence the reported motion direction (Krug, Cicmil, Parker, & Cumming, 2013; Newsome & Pare, 1988) and some studies suggest that MT BOLD activity may reflect the perceived direction in motion aftereffects (He, Cohen, & Hu, 1998; Tootell et al., 1995), however this might also be the result of attention (Huk, Ress, & Heeger, 2001). Generally, it has been difficult to study the role of area MT in the perception of motion without confounds.

Motion agnosia provides an opportunity to investigate the neural correlates of the perception of motion since an identical physical stimulus can either elicit or fail to elicit a percept of motion direction in the same observer using a non-ambiguous stimulus. We therefore measured the responses of recording sites in area MT and other visual areas that might be involved in motion perception to stimuli moving in depth that were presented in a number of locations across the visual field. Because the agnosia for motion is limited to part of the visual field we can identify each recording sites' preferred location in the visual field (Dumoulin & Wandell, 2008; Engel et al., 1994; Sereno et al., 1995) and subsequently compare the response from recording sites with a preference for locations where the observer can not discriminate motion direction correctly to recording sites that prefer a location where the observer can discriminate motion direction.

One potential confound of the current study is that we might be looking at a general visual field defect rather than a defect that is specific for motion in depth. This would imply that any stimulus we present in different locations across the visual field might elicit the same pattern of results. Although our

Chapter 4

previous work on this visual field defect has shown that there are no corresponding deficits in other visual features (static disparity or lateral motion), the current study allows us to directly examine the neural responses to various stimuli rather than rely on behavioral reports. Therefore, we measured responses to both horizontally opposite binocular motion patterns (corresponding to real-world motion in depth) and vertically opposite binocular motion patterns (not corresponding to any real-world motion) in order to keep stimulus features as similar as possible.

We find that neural responses in both area MT and V1 are specifically modulated for motion in depth stimuli presented in locations where an observer is not able to judge motion direction. Using a combined analysis of behavioral and fMRI data we find that the differences in neural response in area MT are closely linked to motion agnosia per se. In contrast, the differences in area V1 appear to reflect the general ability to correctly judge motion direction, independent of the visual field location. Our results establish a neural basis for a common visual deficit and provide new insights into the neural correlates of motion perception.

Methods

Identifying motion agnosia

In order to identify participants with motion agnosia we adapted a previously described perimetry paradigm (Barendregt et al., 2014) for use inside the MRI scanner. Briefly, the experiment consists of presenting a small stimulus which moves through depth (towards/away) in one of 16 locations across the visual field. The participants performed a 2AFC task in which they report the perceived direction (towards/away) of the visual stimulus. By computing a percentage of correct responses for every measured location across the visual field we can identify regions in the visual field where a participant performance does not differ from chance (~50% correct). Such a region indicates that the participant is unable to report motion direction and therefore indicates a region of motion agnosia (Barendregt et al., 2014; Hong & Regan, 1989; Regan et al., 1986).

Participants

fMRI data were collected for seven participants with motion agnosia (one author, one female, aged 25-38). Other than the motion agnosia all participants had normal or corrected-to-normal visual acuity. Aside from one author, all participants were naïve to the purpose of the experiment. Experiments were approved by the Medical Ethics committee of University Medical Center Utrecht, undertaken with the written consent of each participant and were carried out in accordance with the Code of Ethics of the World Medical Association (Declaration of Helsinki).

Stimulus display

Visual stimuli were back-projected onto a screen (15x7.9 cm) located inside the bore. The participant viewed the display through custom-built prisms that allowed separate presentation for each eye. The total viewing distance from the participant to the display screen was 41 cm.

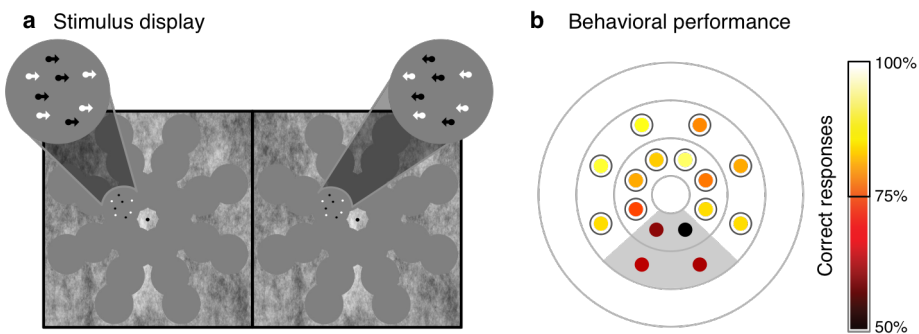


Figure 4.1 *The behavioral experiment participants performed inside the MRI. a: The stimulus configuration used in the MRI experiment. The left half of the display was only presented to the left eye and v.v. For every participant the stimuli (moving dots) would be presented in two of the three rings, depending on the visual field position of motion agnosia in the participant (as determined prior to the MRI experiment). On every trial the stimuli were presented in a semi-random selected location and the task for the participant was to report the perceived direction of motion in depth (towards/away) b: Behavioral results for one participant as measured during the MRI experiment. Each small dot corresponds to the same location in the stimulus display (a) and the color represents the percentage correct responses for that location in the participants' visual field. Locations where the participant was able to reliably report the direction of motion are indicated with a small circle ($P < 0.05$, binomial test). In the locations that lie inside the region highlighted in gray the participant was at chance level for the task. The locations in this regions are considered the motion agnosia locations for this participant.*

Magnetic resonance imaging

All MRI data was collected at the University Medical Centre Utrecht using a

A neural basis for motion agnosia in visual cortex

Philips 7 Tesla MRI scanner.

T1-weighted anatomical MRI data were acquired using a 32-channel head coil at a resolution of 0.98x0.98x1 mm. These were subsequently resampled to 1 mm isotropic resolution. Repetition time (TR) was 7 ms, echo time (TE) was 2.76 ms, and flip angle was 8 degrees.

For all participants T2*-weighted 2D echo planar images were acquired using a 32 channel head coil at a resolution of 1.97x1.97x2 mm resulting in a field of view of 190x190x50 mm. TR was 1500 ms, TE was 25 ms, and flip angle was 80 degrees. The acquired volume was always oriented perpendicular to the Calcarine sulcus providing coverage of the occipital lobe and posterior parts of the parietal and temporal lobes.

For the retinotopy scans, functional runs were each 248 time frames (372 seconds) in duration, of which the first eight time frames (12 seconds) were discarded to ensure the signal was at steady state. For the experimental scans, functional runs were 200 time frames (300 seconds) in duration, of which the first four time frames (6 seconds) were discarded in order to achieve a steady signal. Each participant was scanned in two sessions, a first session to acquire the T1 whole-brain anatomy and the retinotopy scans and the second session to acquire the experimental scans.

Processing of functional imaging scans

Functional scans were first compensated for head movement and motion artifacts (Nestares & Heeger, 2000). Subsequently, the functional images were averaged and aligned to the whole-brain anatomical scan. The alignment was done automatically (Nestares & Heeger, 2000) and afterwards checked and refined manually if needed.

Identification of visual areas

We determined the location of the different regions of interest (ROI) in visual cortex by identifying the visual field maps using a population receptive field (pRF) mapping technique (Dumoulin & Wandell, 2008; Zuiderbaan et al., 2012).

fMRI experiment

Inside the MRI scanner, participants performed an experiment, which was a slightly altered from a version previously used to identify motion agnosia (Barendregt et al., 2014). The participant was presented with a stimulus configuration consisting of a central fixation dot surrounded by three concentric rings of small (1.5°) circular apertures, so that largest eccentricity was 4.5° . An example of the stimulus display is shown in Figure 4.1.

Every trial lasted 2 TRs (3 seconds total) during which a set of 8 (half white) moving dots was shown for 1 second, with the exact stimulus onset randomly jittered to occur within the first TR. For every participant the stimulus could appear in one of 16 locations, on two of the three eccentricities in the stimulus display. The eccentricities for each participant were chosen such that they would intersect with their region of motion agnosia as determined prior to the fMRI experiment. The location in which the stimulus was presented on any trial was determined by a pseudo-random sequence that was optimized to reduce overlap in HRF responses between stimulus presentations.

In the main experiment, the direction of motion of the presented dots was horizontally opposite between the two eyes, which normally results in a percept of motion in depth (towards/away). The dots moved with a monocular speed of

0.6°/s per eye through a disparity range of $\pm 0.3^\circ$ (total range of 0.6° centered on 0°). Upon reaching the end of the volume a dot would be randomly repositioned (in x,y) on the opposite end of the volume. Every dot started at a random position (x,y,z) inside the volume. The instructions for the participant were to always fixate the centre of the display (central fixation dot) and to report the perceived direction of motion (toward or away) after every stimulus presentation.

In the attention experiment, the presented stimulus and method of presentation were identical to those in the main experiment. The only difference in this experiment is the task performed by the participant. The participant performed a previously described task (Barendregt, Harvey, Rokers, & Dumoulin, 2015) in which they had to report small changes in the position of the central fixation dot (i.e. closer to the observer or further away) that occurred at random intervals unrelated to the presentation of the motion stimuli. The average performance across participants on this fixation task was 74%.

For the vertical motion experiment, the direction of motion of the dots was vertically opposite (upward/downward), instead of horizontal, between the two eyes. Since such a stimulus does not elicit a motion in depth percept the task for the participant was to report which of the two motion directions (upward or downward) they perceived more. This task mainly served to keep the conditions of this experiment as close to the main experiment as possible.

Data analysis behavioral data

The behavioral data collected during the MID condition was converted into a percentage correct score for every position in the visual field (Barendregt et al., 2014). These scores are then plotted in a visual field plot for every participant

(Figure 4.2a and Appendix Figure A4.1) where the score at each position is represented by a colored dot. Positions where performance is significantly different from chance ($p < 0.05$, binomial test) are marked with a black contour. Because we are interested in identifying positions where performance does not differ from chance we opted to use an uncorrected criterion so that we are relatively conservative in classifying regions of motion agnosia.

Analysis of fMRI data based on stimulus locations

Since motion agnosia is defined in terms of locations in the visual field we needed to compute the responses to different visual field positions within each ROI. From the visual field map we have an estimate of the position (x,y) for every recording sites' population receptive field (pRF). Based on these parameters we select recording sites that have their pRF within one of the circular apertures around a stimulus location (Figure 4.1) and then subsequently group those recording sites based on their preferred stimulus location for the rest of the analysis. Each pRF also has an estimate for its size (σ) that was only used to exclude recording sites with a very large pRF size ($\sigma > 10^\circ$). We choose a conservative use of the pRF size estimate because this parameter is known to increase between visual areas and therefore excluding recording sites based on this parameter would affect later areas more than early areas. We also used a general linear model to only include recording sites that show a significant response to any stimulus presented in their preferred location across the entire experiment.

Computing the average HRF profile

In order to compute an average haemodynamic response function (HRF) for every participant, we first determined the preferred stimulus location for each recording site based on the visual field map that we obtained for every

participant (see above). Then we used the time course of the stimulus presentations at each location to deconvolve the HRF for every recording site and trial. Finally, we computed the average HRF for all recording sites with a preferred location in a particular visual field region (either the agnosia region or one or more of the control regions).

Comparing response amplitudes between visual field regions

We used a two-gamma function convolved with the time course of stimulus presentations to fit a general linear model to the BOLD time course of every recording site in order to estimate the BOLD response amplitude. Subsequently, we used a linear mixed effects model (*fitlme* in the Statistics Toolbox for Matlab) to quantitatively compare the response amplitudes of recording sites with different preferred stimulus locations. By using a linear mixed effects model we can account for individual differences in response amplitudes between participants while analyzing the responses of individual recording sites instead of working with averaged data.

Results

Determine the visual field location of motion agnosia

While we measured fMRI responses in visual cortex, participants viewed binocular motion stimuli at different locations in the visual field through a mirror stereoscope (Figure 4.1a). We determined the location of motion agnosia in our participants' visual field, based on the reported motion direction of the presented stimuli (towards/away) in the scanner. The percentage of correct responses at 16 locations across the visual field are shown in Figure 4.1b for a representative participant (results for all participants included in Appendix Figure A4.1). Each dot in the figure is one of the 16 locations where we assessed the participants' ability to report direction of motion in depth. Locations where an observers' performance is significantly different from chance ($P < 0.05$, binomial test) are marked with a black contour. In accordance with previous psychophysical studies we find that sensitivity to direction of motion varies across the visual field (Barendregt et al., 2014; Hong & Regan, 1989; Richards & Regan, 1973), as indicated by the color of the dots. For every participant, we find a distinct region in the visual field where performance is not significantly different from chance, highlighted in grey, indicating that they were not able to correctly perceive the movement direction of stimuli. It is important to note that while we find these impairments in motion perception in all the participants of this study, the position of these regions in the visual field varies across participants (see Appendix Figure A4.1). These findings are consistent with previous psychophysical results for each observer obtained using a stereoscope outside the scanner.

Motion agnosia evident in MT responses

Given what is known about the cortical processing of visual motion, a first candidate area for a neural basis of motion agnosia is the human middle temporal area (MT). We identified the preferred visual field position of recording sites in several areas of visual cortex based on a separate set of scans (Dumoulin & Wandell, 2008; Zuiderbaan et al., 2012). From previous work we know that the human middle temporal complex (MT+) is comprised of two visual field maps, referred to as TO-1 and TO-2, and these are thought to correspond to the macaque areas MT and MST (Amano, Wandell, & Dumoulin, 2009; Huk, Dougherty, & Heeger, 2002). Since recent work has demonstrated neuronal tuning for direction of motion in depth in area MT specifically (Czuba, Huk, Cormack, & Kohn, 2014; Rokers et al., 2009; Sanada & DeAngelis, 2014), we were first interested in the responses of this area.

We investigated the responses of area MT to stimuli presented in different visual field positions by computing the average BOLD response across recording sites that preferentially respond to either visual field positions inside (*affected location*) or outside (*unaffected locations*) the motion agnosia region of a participant. The results of this analysis are shown in Figure 4.2a for the single participant from Figure 4.1b (all participants are shown in Appendix Figure A4.2), where we plotted the average BOLD response in area MT to stimuli presented in the agnosia locations (black line). When compared to stimuli presented outside this region (other lines) we find a lower BOLD response for stimuli presented inside the agnosia locations.

In order to rule out any influence of global visual field asymmetries, e.g. upper versus lower visual field, we choose three regions of control locations that mirror the agnosia locations at a constant eccentricity. The BOLD response is

lower for stimuli presented in the agnosia locations, compared to each of the control locations across the visual field (t tests between locations, all $t > 3.59$, $P < 0.001$).

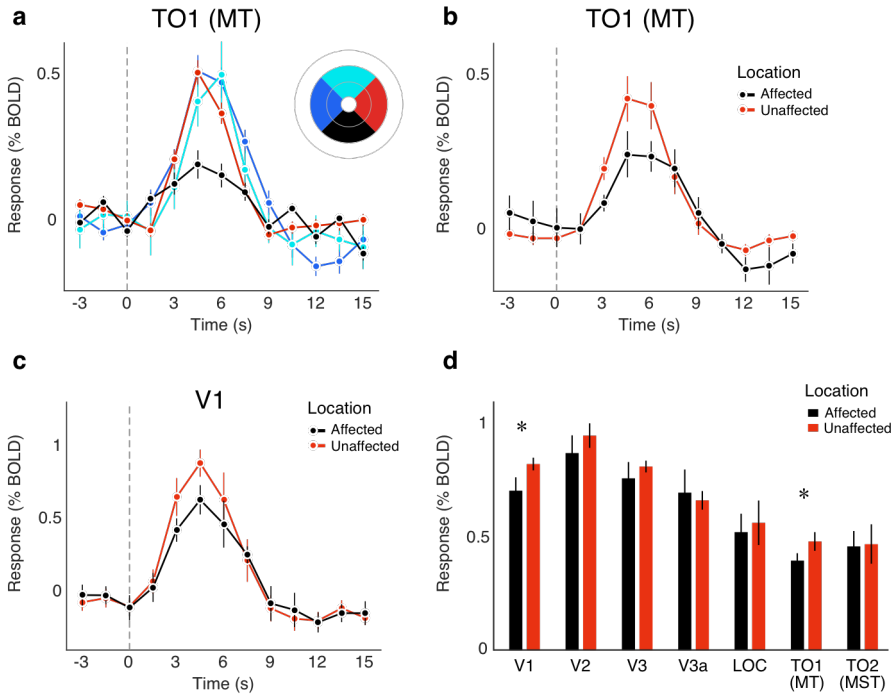


Figure 4.2 BOLD responses in area MT and V1 are modulated by motion agnosia. *a:* The average BOLD response profile in visual area TO1 (MT) for the participant shown in **Figure 1b**. Each line in the plot represents the average response of all recording sites in the visual area that preferred the correspondingly colored region in the visual field. Time (x -axis) is relative to the onset of a motion in depth stimulus (indicated by the dashed vertical line) presented in a location that falls within one of the colored regions. *b:* The average BOLD response profile in visual area TO1 (MT) across all participants. Each line represents the average response of recording sites that preferred either the affected location (black line) or any of the unaffected locations (red line). *c:* The average BOLD response profile in primary visual cortex (V1), across participants. We find a lower BOLD response for stimuli presented inside a motion agnosia region (black line) in area V1, similar to area MT. *d:* The average response amplitude to stimuli presented in either an agnosia (black bars) or control locations (red bars) across multiple areas in visual cortex (V1, V2, V3, V3a, LOC, MT and MST).

BOLD responses to the motion in depth stimuli were similar across participants. Therefore, we computed the average response to a stimulus presented inside a motion agnosia region (of any participant) and the average response in all the control regions. We find that the average response to a stimulus presented in the agnosia location is consistently lower compared to the average response for the control locations (Figure 4.2b) across all participants. Note that the visual field position of the agnosia and control regions differ between participants (Appendix Figure A4.1) and that, as a result, the only shared characteristic between the responses in each average is the ability or inability of the participant to consistently report the direction of a moving stimulus.

Agnosia-modulated responses also evident in primary visual cortex

While area MT is a likely candidate based on its role in motion in depth processing, we also investigated the neural correlates of motion agnosia in earlier visual areas. Because we know the visual field position of the impairment we can repeat the same analysis in other areas that contain a visual field map. In Figure 4.2c we plot the average BOLD response profile for recording sites in primary visual cortex (V1) that correspond to the agnosia location (black line) or a control location (red line). As for area MT, we find that in area V1 the response for stimuli presented inside a motion agnosia location is lower compared the control locations across the visual field.

Next, we extended the analysis to include multiple visual areas and used a linear mixed effects model to quantitatively compare the average response for stimuli presented in different visual field positions across visual cortex (V1, V2, V3, V3a, LOC, MT and MST, Figure 4.2d). We find a significantly lower response for stimuli presented in the agnosia locations across all observers in areas V1 and MT (V1: $F_{1,6} = 10.91$, $P = 0.017$, MT: $F_{1,4} = 15.08$, $P = 0.02$) but

Chapter 4

not in other visual areas (V2: $F_{1,6} = 4.46$, $P = 0.08$, V3: $F_{1,6} = 1.87$, $P = 0.222$, V3a: $F_{1,4} = 0.32$, $P = 0.601$, LOC: $F_{1,4} = 0.004$, $P = 0.95$, MST: $F_{1,5} = 0.03$, $P = 0.82$).

The observed differences are not a general visual deficit

A possible confound of our experiment is the specificity of the results we have obtained. In other words, it might be the case that any stimulus presented in the visual field locations we identified will result in a lower BOLD response compared to other locations. In order to test this possibility, we performed a control experiment using vertically, instead of horizontally, opposite motion (upward/downward) in the two eyes. These stimuli are matched for basic visual properties but, since opposite vertical directions of motion in the two eyes do not correspond to real world motion, the stimuli are not informative to the visual system.

We computed the average BOLD responses to the vertically opposite motion stimulus presented in the same locations across the visual field (Figure 4.3a). Contrary to the previous experiments we find no difference between the BOLD responses for the agnosia location and control locations in any visual area (V1: $F_{1,6} = 3.89$, $P = 0.096$, V2: $F_{1,5} = 2.24$, $P = 0.185$, V3: $F_{1,4} = 2.57$, $P = 0.183$, V3a: $F_{1,5} = 0.55$, $P = 0.491$, LOC: $F_{1,4} = 0.96$, $P = 0.382$, MT: $F_{1,3} = 0.53$, $P = 0.532$, MST: $F_{1,3} = 0.53$, $P = 0.532$). Based on these results we conclude that the differences we find in the previous experiments are specific to motion signals that correspond to approaching/receding motion and not due to a general visual deficit.

Spatial attention does not explain the observed effects

Since motion agnosia has so far only been demonstrated behaviorally, the influence of the task that the observer performs is of potential concern.

Although our previous work on motion agnosia always used a randomized order of presenting stimuli across the visual field (Barendregt et al., 2014) to account for attentional effects, attention has been shown to affect the responses measured in MT+ in several studies (Huk et al., 2001; Klein, Harvey, & Dumoulin, 2014; Womelsdorf, Anton-Erxleben, Pieper, & Treue, 2006). In order to rule out that we are simply measuring differences in spatial attention we included an additional experiment to test whether motion agnosia-related differences in the neuronal response are independent from the task that the observer performs.

Stimuli that elicit a 3D motion percept may draw more attention than those that do not. In order to exclude this possibility, we repeated the experiment with the same stimuli but now included a challenging fixation task. The participants were instructed to monitor the central fixation dot and report small changes in its position in depth that were temporally and spatially unrelated to the moving dot stimuli that were being shown (Barendregt et al., 2015). The average performance on the fixation task was 74% correct, indicating that the task was challenging enough to keep attention in the center.

In Figure 4.3b we show the results for this experiment for the different locations (agnosia and controls) across all measured visual areas. Although the task for the participant is now unrelated to the location and content of the motion stimulus, we again find that the BOLD response is significantly lower for the agnosia locations in visual areas V1 and MT+ (V1: $F_{1,6} = 15.93$, $P = 0.003$, V2: $F_{1,6} = 4.37$, $P = 0.07$, V3: $F_{1,6} = 5.84$, $P = 0.039$, V3a: $F_{1,6} = 0.82$, $P = 0.4$,

Chapter 4

LOC: $F_{1,5} = 0.46$, $P = 0.523$, MT: $F_{1,5} = 17.54$, $P = 0.01$, MST: $F_{1,6} = 3.48$, $P = 0.11$). This shows that our previous finding is independent of the task the participant is performing and cannot be explained by attentional effects.

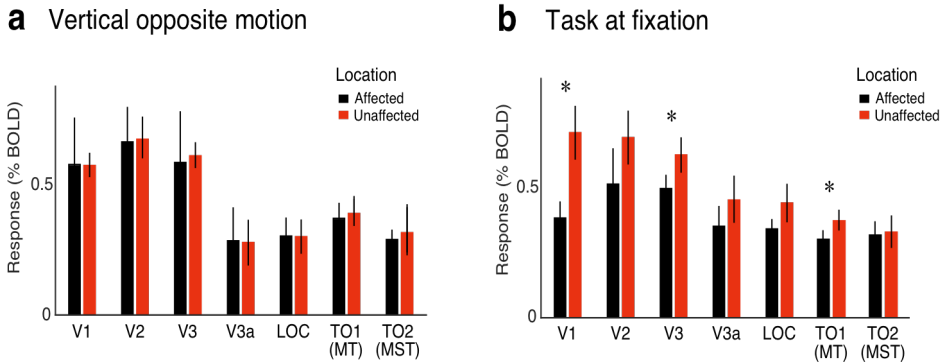


Figure 4.3 a: The average BOLD response to vertically opposite motion in affected (black bars) and unaffected (red bars) locations across participants and visual areas. In contrast to the main experiment (**Figure 4.2d**) where horizontally opposite motion was presented, we don't find any differences in the responses between affected and unaffected locations (all $F < 3.89$, all $P > 0.09$). This indicates that the observed differences in the main experiment are due to a deficit in motion in depth perception and not a general visual deficit. **b:** To exclude the possibility that our findings are due to attentional influences, we repeated the main experiment with identical stimuli but the participant monitors the position of the fixation point, rather than the direction of the motion in depth stimuli. We again find that the BOLD responses in areas V1 and MT are significantly modulated by motion agnosia (V1: $F_{1,6} = 15.93$, $P = 0.003$, MT: $F_{1,6} = 9.43$, $P = 0.013$), demonstrating that these differences are independent from the task that is performed.

Response in V1 predicts behavioral performance in unaffected, but not affected locations

While the involvement of the motion processing area MT in motion agnosia was expected, the differences in response we find in primary visual cortex are more surprising. Participants with motion agnosia are not able to report on the direction of motion of a presented stimulus but they have no difficulty seeing the stimulus per se. Therefore, we would not immediately expect to find an effect of motion agnosia at the level of primary visual cortex.

To further investigate the nature of these effects in V1 and MT, we combined the measured fMRI responses with the behavioral data that was collected at the same time. Across all visual areas we compared the average BOLD response in the agnosia location with the average BOLD response in the control locations for trials where the participant reported either the correct or the incorrect direction of motion (Appendix Figure A4.4). We find that the average response in area V1 is significantly lower when the participant reports the incorrect motion direction compared to reporting the correct direction ($t_{1938} = 2.34$, $P = 0.019$). Further, there is no difference between the V1 responses for trials that were reported incorrectly and trials that were presented in the agnosia region, regardless of the reported direction (Correct/incorrect: $F_{1,2520} = 1.26$, $P = 0.261$, Agnosia/control: $F_{1,14} = 1.84$, $P = 0.197$).

The same analysis in area MT (Appendix Figure A4.4) gives a very different result. In this area we find no difference based on the correctness of the reported motion direction ($F_{1,2354} = 1.17$, $P = 0.28$) but only based on whether or not the stimulus was presented in the agnosia region ($F_{1,14} = 18.67$, $P = 7 \times 10^{-4}$). This suggests that the modulation of neural responses in area MT is based

Chapter 4

on the processing of the physical stimulus and relatively independent from the percept of the stimulus.

Discussion

Our results demonstrate a neural basis for the inability to judge motion direction (motion agnosia) in human visual cortex. We find that neural responses in primary visual cortex (V1) and area MT are reduced in amplitude when stimuli are presented in visual field locations where an observer can't report the direction of moving stimulus. While we find a clear effect of motion agnosia on the responses in both area V1 and area MT, the effects appear to have different origins. By combining the fMRI data with simultaneously collected behavioral data we find that the responses in V1 are lower for both stimuli presented in agnosia locations and locations where the stimulus direction was misreported, even in the unaffected locations. Conversely, for area MT we find that the responses only differ based on whether a stimulus is presented in a motion agnosia region or not. Using a number of control locations in the visual field we also demonstrated that these differences are not due to global visual field asymmetries or a general visual deficit.

Our results in the human middle temporal area (MT) show that the neural responses in this area can be significantly modulated by the presence or absence of motion agnosia at different visual field locations. While this result is in itself not surprising given the role of MT in human motion processing (Richard et al., 2005) and the well-established selectivity for motion in depth (Czuba et al., 2014; Rokers et al., 2009; Sanada & DeAngelis, 2014), it does provide some new insights into the role of area MT in the perception of motion. In particular, by combining behavior and neuroimaging we show that the BOLD response in MT is only influenced by the presented location of the visual stimulus and not by whether or not the participant can report the correct direction of motion.

Chapter 4

The responses in human area MT therefore might reflect whether the binocular motion signals can be integrated properly into a coherent motion in depth percept and not whether the observer can subsequently report this percept correctly.

Previous studies on the relation between MT activity and the perception of motion have produced conflicting results (Richard et al., 2005). Using bi-stable stimuli (Brouwer & van Ee, 2007), transparent motion (Castelo-Branco et al., 2002) or adaptation (He et al., 1998; Tootell et al., 1995) previous studies have found that responses in MT reflect the perceived motion direction of a stimulus rather than the physical stimulus properties. However, studies have also shown that some of those results are based on attention (Huk et al., 2001) and that MT might in fact respond to local rather than global motion (Hedges, Stocker, et al., 2011; Hedges, Gartshteyn, et al., 2011). Because we used highly localized stimuli to compare the responses of different subpopulations of MT along with the observers general ability to report a percept we find evidence that area MT responds to the binocular integration of motion signals and not the percept of motion per se.

The exact role of primary visual cortex (V1) in the perception of motion has been troublesome to pinpoint in humans. Human V1 shows little adaptation to motion direction (Huk & Heeger, 2002) and while motion-direction can be decoded from V1 with high accuracy (Kamitani & Tong, 2006; Serences & Boynton, 2007) it has recently been shown that this is based on the stimulus aperture rather than the absolute direction of motion (H. X. Wang, Merriam, Freeman, & Heeger, 2014). Even more so than for lateral motion, V1 typically shows very little sensitivity to motion in depth (Rokers et al., 2009). In this context the fact that we find a modulation of the V1 response by the presence of

motion agnosia is unexpected. However, our additional analysis of the behavior suggests that the differences in area V1 can be interpreted as an increased BOLD response for trials where the observer correctly perceives the motion direction of the stimulus. This finding is consistent with results showing that activity in V1 can predict whether a visual stimulus is sufficiently processed to be reported (Ress, Backus, & Heeger, 2000; H Supèr, Spekreijse, & Lamme, 2001; Hans Supèr, van der Togt, Spekreijse, & Lamme, 2003). Further, our results fit with the role that V1 is thought to play in visual awareness (Covey & Walsh, 2000; Silvanto, Covey, Lavie, & Walsh, 2005).

A potential concern for any visual field mapping study is the effect of eye movements on the results. In all experiments we instructed the participants to fixate the central fixation dot, regardless of the task they were performing. While we did not explicitly monitor eye movements to verify that the participants maintained fixation the the pattern of behavioral results that we obtained are highly unlikely if participants were fixating the presented stimulus location on every trial (performance would be close to uniform). Further, since we find identical results regardless of the spatial location of the task (the stimulus location or the fixation location) our data cannot be explained by eye movements.

The inability to discriminate the direction of motion in depth is considered here to be a form of visual agnosia. This is a different approach from previous studies on this subject, those by our own lab included, where this has been described as a form of motion blindness (Barendregt et al., 2014; Hong & Regan, 1989; Regan et al., 1986). The difference is that agnosia is not a deficit in perception but in discrimination (Farah, 2004) and this better describes the deficit we investigate here. Although the prevalence of motion agnosia (>50%)

Chapter 4

is much higher compared to other forms of visual agnosia, a study by Kennerknecht et al (Kennerknecht et al., 2006) indicates that congenital agnosia might be more common than previously thought because it often goes unnoticed. Another difference between agnosia for motion and for other features is that motion agnosia does not extend across the whole visual field. This is most likely due to the fact that motion is processed much earlier in the visual hierarchy, where receptive fields are much smaller, compared to most other visual features that are known to be affected by agnosia.

In conclusion, we reveal the neural correlates of a common visual impairment, motion agnosia, in human visual areas V1 and MT. Further we provide new evidence for the respective roles that each of these two area play in the perception and awareness of visual motion. These findings therefore have implications for our current understanding of motion processing in general and motion agnosia in particular.

Appendix

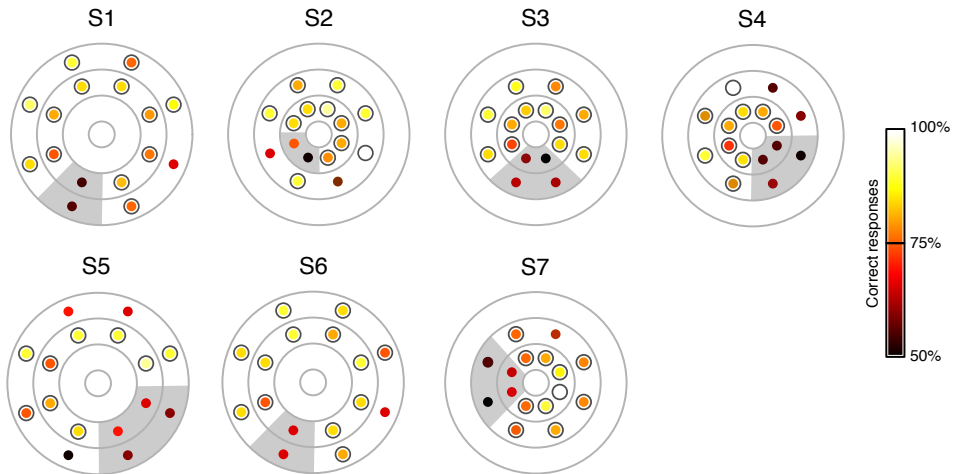


Figure A4.1 Behavioral results across the visual field as measured inside the MRI scanner for all participants. The 16 colored dots represent the locations where the participant performed a motion discrimination (approaching vs receding) judgment. The color of each dot indicates their performance and the black circles identify the locations where a participant was able to correctly judge motion direction above chance level ($P < 0.05$, binomial test). The grey shaded region in each participants' visual field indicates the region where the participant is unable to perform a motion direction judgment above chance level.

Chapter 4

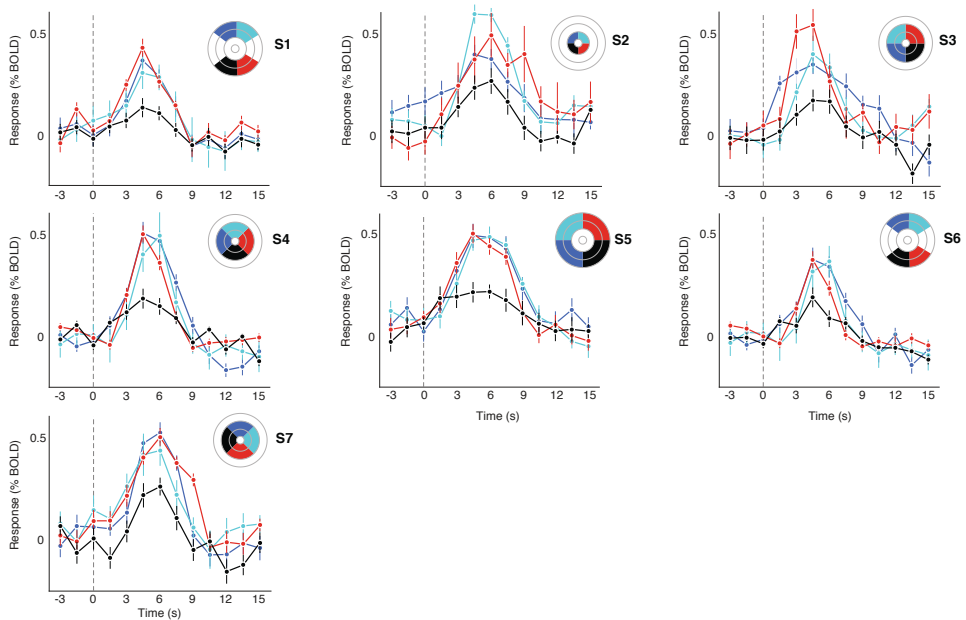


Figure A4.2 The average HRF in visual area MT for stimuli presented inside (black line) and outside (other colours) the affected region in all participants. The three coloured lines represent the average response to stimuli presented in the three regions indicated in the visual field plot of each participant. We find that the HRF amplitude in the affected region (black) is consistently lower compared to all the other locations showing that our results cannot be explained by global visual field asymmetries.

A neural basis for motion agnosia in visual cortex

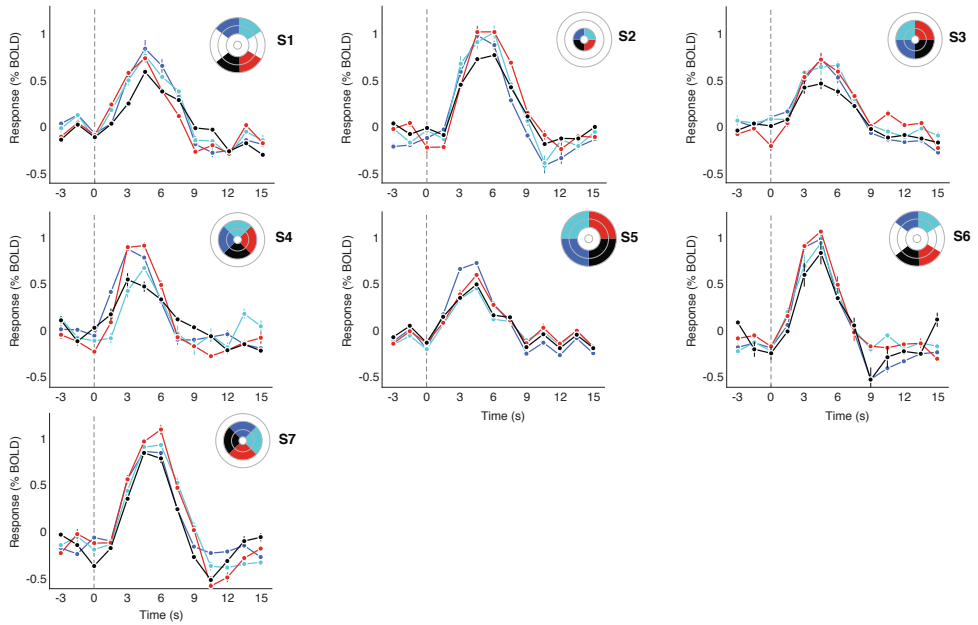


Figure A4.3 The average HRF in visual area V1 for stimuli presented inside (black line) and outside (other colours) the affected region in all participants. The three coloured lines represent the average response to stimuli presented in the three regions indicated in the visual field plot of each participant. We find that the HRF amplitude in the affected region (black) is generally lower compared to all the other locations showing that our results cannot be explained by global visual field asymmetries.

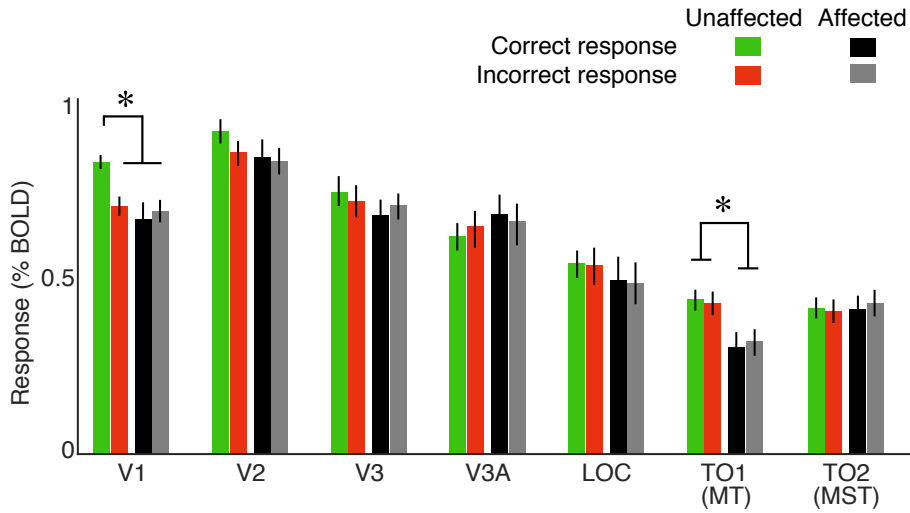


Figure A4.4 The average BOLD response across seven visual areas (V1, V2, V3, V3a, LOC, TO1/2) for correct and incorrect responses in either affected or unaffected visual field locations. We find that in area V1 there is only a significant increase in BOLD response for correct responses in unaffected visual field locations, whereas in area TO-1 (MT) we find a significantly higher BOLD response in unaffected locations independent from the response given.

Chapter 5

MOTION AGNOSIA IS THE RESULT OF IMPAIRED VELOCITY PROCESSING

Accepted as:

M Barendregt, B Rokers & SO Dumoulin (2016) Impaired velocity processing reveals an agnosia for motion in depth. *Psychological Science*

Acknowledgement of author contributions: MB designed the experiment and collected the data. MB performed data analysis under supervision of BR and SOD. MB wrote the manuscript and the other authors provided critical comments.

Abstract

Many individuals with intact form- and color perception are unable to discriminate the direction of three-dimensional motion in parts of the visual field. This deficit has been labeled a stereomotion scotoma, but it has remained unclear whether the origin is ocular, visual, or cognitive. We hypothesized that the impairment is due to a failure in the processing of one of the binocular cues to 3D motion: either changes in binocular disparity or interocular velocity differences. We found that sensitivity to interocular velocity differences, but not to changes in binocular disparity, varied systematically with the locations of stereomotion scotomas in the visual field. These results show that an individual's inability to interpret motion in depth is due to a failure in the neural mechanisms that combine velocity signals from the two eyes. Our results uncover the existence of a prevalent but previously unrecognized agnosia specific to the perception of visual motion.

Introduction

Under general viewing conditions, judging the direction of two-dimensional (2D) motion is trivial. However, under the exact same conditions the perception of motion in depth (approaching/receding) can be severely impaired. These impairments are traditionally termed stereomotion scotomas, because the deficits are typically not complete but rather confined to a part of the observers' visual field (Hong & Regan, 1989; Richards & Regan, 1973). The impairments occur in over 50% of otherwise healthy observers, are stable over time, and are not predicted by impairments in the processing of monocular information (Barendregt et al., 2014). The underlying cause of these stereomotion scotomas has remained elusive.

Our previous work suggests that the deficit underlying stereomotion scotomas must originate near the stage where signals from the two eyes are combined (Barendregt et al., 2014), and there are only two known binocular cues to motion in depth, (1) changes in binocular disparity over time (CD), and (2) interocular velocity differences (IOVD). Under natural viewing conditions, these two cues tend to co-occur, with the primary functional difference arising due to a difference in the order of operations. For CD, binocular disparity for an object is computed first, followed by computation of the change in disparity over time (Cumming & Parker, 1994; Regan, 1993); for IOVD, change in monocular object position (velocity) is computed first, and the difference in velocity is computed subsequently (Harris et al., 2008; Regan & Gray, 2009; Shioiri et al., 2000).

Motion agnosia is the result of impaired velocity processing

Even though these two cues occur simultaneously in most viewing situations, it is possible to isolate the cues in an experimental setting. Julesz (1971) designed a *dynamic random dot (DRDS)* stimulus that contains changes in binocular disparity over time, but no coherent motion in either retinal image. Conversely, anti-correlated (Rokers et al., 2008) or uncorrelated (Shioiri et al., 2000) stimuli can be created that contain coherent motion in each retinal image but disrupt the processing of changes in binocular disparity over time. Both types of stimuli still support the perception of motion in depth.

Thus, we set out to identify the neural impairment that underlies stereomotion scotomas, by measuring sensitivity to motion in depth across the visual field in a number of observers with no obvious retinal impairments. We then used cue-isolating stimuli to evaluate the relative contribution of the two motion in depth mechanisms. We showed that at the spatial scales at which stereomotion scotomas occur, the CD cue contributes little to the perception of motion in depth. Instead, the variation in sensitivity to the direction of motion in depth across the visual field is well-predicted by the sensitivity to the IOVD cue. These findings indicate that stereomotion scotomas are caused by a failure in the combination of retinal motion signals from the two eyes in visual cortex. Since we identify a clear neural basis for this visual deficit we argue that these impairments are more correctly described as motion agnosia, a previously unrecognized form of apperceptive visual agnosia.

Methods

Observers

A total of 11 observers (1 female, ages 24-35) participated in the experiment. The participants gave informed consent. All had normal or corrected-to-normal vision and were able to judge position in depth in stereo displays. All participants were experienced psychophysical observers and all but one (one of the authors) were naive to the purpose of the experiments. Our sample size was based on the assumption of a relatively large ($r^2 \sim 0.25$) within-subject effect size. The experiments were carried out in accordance with the Code of Ethics of the World Medical Association (Declaration of Helsinki).

Apparatus & display

Stimuli were presented on two 20" CRT displays (60Hz, 1024x768) with each display containing the image for one of the eyes at a simulated viewing distance of 75cm. Using a mirror stereoscope, in which a set of mirrors redirected each image to the corresponding eye, the observer fused both images into a single binocular image. A pink noise ($1/f$) background pattern was presented throughout the experiment to facilitate vergence. The stimuli were generated using a Apple Mac Pro computer using Matlab (Mathworks, Natick, MA, USA) and the Psychophysics Toolbox 3 (Brainard, 1997; Kleiner et al., 2007; Pelli, 1997). The experimental setup used here has previously been described in more detail (Barendregt et al., 2014).

Motion agnosia is the result of impaired velocity processing

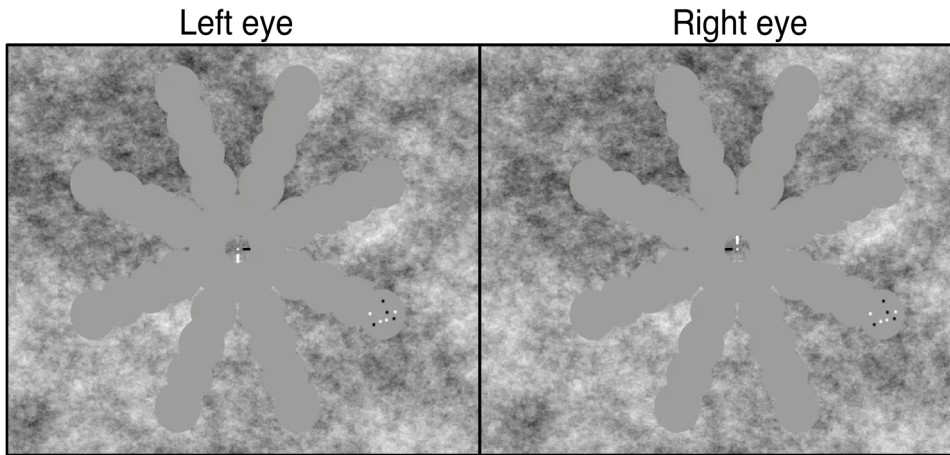


Figure 5.1 *Illustration of the stimulus display for the left and right eyes. Stimuli were presented at one of 40 locations ranging from 1.5° to 7.5° eccentricity in 5 equal steps and with 8 locations per 'ring'. In these example images a stimulus is displayed in one location in the lower right visual field.*

Stimuli

The stimuli were presented within circular apertures (1.5° diameter) positioned within an 8.25° radius around fixation. The centers of the apertures ranged from 1.5° to 7.5° eccentricity in 5 equal steps and were laid out in a spoke-wheel pattern with 8 locations per 'ring' (**Figure 5.1**). This arrangement provided a total of 40 testing locations across the visual field.

Each stimulus consisted of a set of dots, half white and half black, randomly positioned within the gray background (46.7 cd/m²) aperture. During each trial the dots moved in opposite directions between the two eyes consistent with a monocular speed of 0.6°/s. The dots were randomly repositioned whenever they reached a binocular disparity of $\pm 0.3^\circ$. The starting position of the dots was chosen such that they would not move beyond the edge of the aperture in

either monocular image. In every condition all dots shared the same position in depth so that the stimulus defined a single plane that moved through depth.

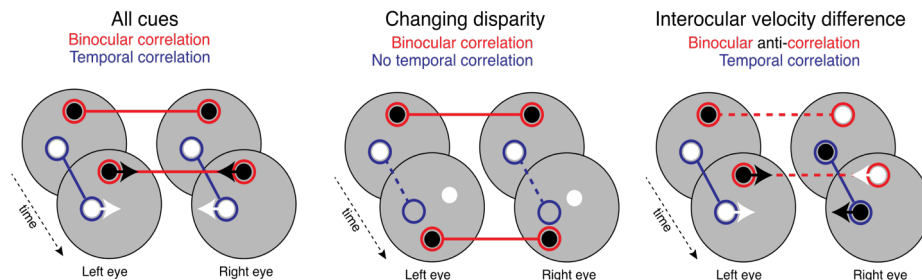


Figure 5.2 *Illustration of the stimuli used in the experiment.* In our FULL stimulus condition the left and right eyes images are both binocularly and temporally correlated. To isolate the fundamental binocular cues to motion in depth, the CD stimulus isolates the changing disparity over time by randomly repositioning dots on every frame while systematically changing the binocular disparity. In the IOVD stimulus we anti-correlated the dots in the left and right eye images, that is corresponding dots had opposite contrast in the two eyes. While anti-correlation of the dots does not remove the disparity information entirely, the information is greatly degraded relative to the velocity information.

We used three main stimulus conditions in these experiments (**Figure 5.2**). In the FULL stimulus condition, the position of each dot is correlated both between the eyes (binocular correlation) and from frame-to-frame (temporal correlation), so that it contained both CD and IOVD cues. To isolate the changing disparity cue in the CD stimulus we randomly reposition the dots in the image-plane on every frame while coherently increasing/decreasing their binocular disparity. Perceptually the resulting stimulus looks like the static of a poorly tuned television moving through depth. To isolate the velocity component in the IOVD stimulus we anti-correlated the dots in the two eyes, which greatly reduces the percept of position in depth. This stimulus still contains interocular velocity differences, and we had previously shown that

Motion agnosia is the result of impaired velocity processing

observers retain the ability to judge the direction of motion in depth for such stimuli (Rokers et al., 2008).

Procedure

The stereoscope was initially adjusted to accommodate the typical interocular distance. Prior to each session the observer could make further changes if needed so that the nonius markers in the display appeared aligned both horizontally and vertically. Observers were instructed to maintain continuous fixation on the center of the display using a central fixation dot.

The experimental paradigm was a block design where each block comprised a complete sampling of the visual field for one stimulus condition. A total of 800 trials (40 locations x 20 repetitions) were presented during each block with the location of the stimulus pseudo-randomly distributed across trials. As a result, observers could not predict in which visual field location the stimulus would appear on any given trial.

On every trial a stimulus that randomly moved either towards or away from the observer was presented for 500ms. During each trial the stimulus would move through a cylindrical volume (based on the maximal disparity) and would “wrap around” when it reached either extreme (near/far) of the volume. The instantaneous disparity at any point throughout the trial could not serve as a potential cue to the direction of motion in depth, in any of the experiments. For the main experiment, parameters were such that the randomly chosen starting position of the plane in depth was always equal to the ending position. For experiments with slower (0.3°/s) and faster (1.2°/s) speeds, we chose to keep all other parameters (such as the size of the volume) identical to the main experiment. As a result, the dots in these stimuli would wrap around either

more (1.2°/s) or less (0.3°/s) frequently. In all experiments, we chose the starting position in depth of the dot plane on each trial randomly, so that starting (or ending) position could not serve as a cue to motion in depth. Note also that due to the stimulus wrapping, the starting and ending position of the dot plane would be identical in all but the slow (0.3°/s) condition.

Depending on the stimulus, observers reported either the perceived direction of motion, or the perceived position in depth after stimulus offset by pressing one of two keys, thus performing a two alternative forced choice (2AFC) task.

Data analysis

The data collected in the 2AFC task was converted into a percentage correct score for every position in the visual field. We also assessed sensitivity by calculating d-prime. Since the results were essentially identical using either measure we report all further analyses in terms of the percentage correct scores of the observers.

To assess the contribution of the velocity and disparity cues to 3D motion perception, we fitted a linear mixed effects model to the percentage correct scores. To account for any overall differences in task performance between observers, we entered observer as a random effect and performance on the different stimuli as fixed effects. All linear models were fitted using the `fitlme` function in the Statistics Toolbox for Matlab and we used restricted maximum likelihood to obtain a less biased estimate of the variances.

We fitted a model to the data obtained for every cue separately to assess how well the performance on a single cue can predict the performance on a stimulus containing both cues (FULL condition). Further, to directly compare the models

Motion agnosia is the result of impaired velocity processing

obtained for different stimulus speeds, we used a likelihood ratio test. We tested the assumption that the observed responses are more likely to occur under one model compared to the other model. Using the compare function in the Statistics Toolbox for Matlab we computed a p-value to determine if the likelihood ratio of two linear models significantly deviated from a reference chi-squared distribution.

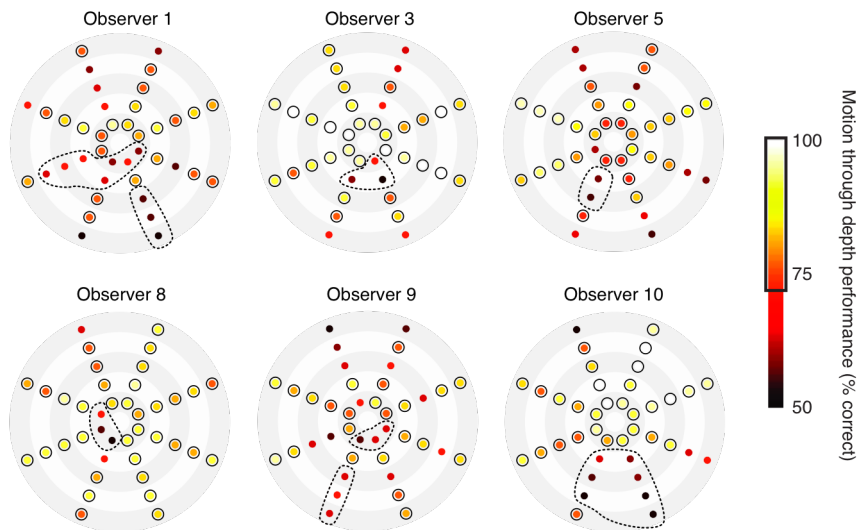


Figure 5.3 *Sensitivity to motion in depth across the visual field for six observers with stereomotion scotomas.* Each plot shows the visual field for a single observer with the color of each dot representing the percentage of correct responses in that location. A black circle around a dot indicates performance that was significantly different from chance. While performance may be variable across the visual field, we consistently identify locations where the performance is not different from chance in each of these observers, indicating a stereomotion scotoma (dotted regions).

Results

We measured sensitivity to motion in depth across the visual field and aimed to evaluate the relative contribution of the binocular cues, *changing disparity (CD)* and *interocular velocity differences (IOVD)*, to motion sensitivity.

Substantial variability of 3D motion sensitivity across the visual field

The percentage of correct responses across the visual field for six of our 11 observers to the FULL condition stimulus is shown in **Figure 5.3**. Sensitivity to motion in depth varies greatly across the visual field with motion discrimination reaching near perfect performance (white dots) in some locations, while dropping to performance at or close to chance (black dots) in other locations of the visual field. In some cases, these drops in performance are abrupt, producing either near perfect or random performance in adjacent locations, which are separated by 1.5° of visual angle (center-to-center), for example, see Observer 3.

In short, we identify locations in the visual field where the observer is not able to discriminate between a stimulus moving towards or away, indicating a stereomotion scotoma (dotted regions). In previous work we showed that these regions are stable over time, and persist across a range of stimulus parameters such as duration and contrast. Moreover, the impairments are specific to the perception of motion in depth. Changes in sensitivity across the visual field to binocular rivalry, static disparity and lateral motion do not explain the location of these impairments (Barendregt et al., 2014; Hong & Regan, 1989; Regan et al., 1986).

Motion agnosia is the result of impaired velocity processing

The changing disparity over time cue does not predict differences in motion sensitivity

Changes in disparity over time that occur when an object moves towards (or away from) the observer have traditionally been considered the primary cue to motion in depth, with a smaller role for interocular velocity differences (Cumming & Parker, 1994; Nefs et al., 2010). To assess if the location of the stereomotion scotomas can be explained by a local deficit in the processing of changing disparity cues, we measured the sensitivity to motion in depth using a stimulus that isolated the changes in disparity. In **Figure 5.4A** we show the sensitivity to motion in depth as measured by a stimulus isolating the changes in disparity (CD) and as measured using a stimulus containing both binocular cues (FULL) for three observers with stereomotion scotomas. The locations of stereomotion scotomas as measured by the FULL stimulus are indicated by a black dotted region in the left column of figures as well as by a light grey dotted region in the middle column.

The same data for the other observers is included in Appendix Figure A5.1. We find that the sensitivity to the CD stimulus is generally poor across the whole visual field and there are no regions with systematically lower sensitivity that correspond to a stereomotion scotoma.

To quantify how well the sensitivity to motion in depth as measured by the FULL stimulus is predicted by the CD stimulus we fit a mixed effects linear model to the combined data of all observers. **Figure 5.4B** shows the result of this linear fit where the performance measured using the FULL stimulus is plotted as a function of the performance predicted by the CD stimulus. Colored

lines indicate the fits of individual observers and the thick black line shows the fit of the overall data. Sensitivity to the CD cue did not significantly predict the sensitivity to motion in depth across the visual field ($F(1,75) = 2.55, p = 0.115$) as measured by a stimulus that contains both binocular cues, suggesting that stereomotion scotomas are not due to variability of sensitivity to CD across the visual field.

Poor sensitivity to changing disparity is not caused by diminished sensitivity to static disparity

Our results suggest that the changes in disparity over time do not serve as a cue to motion in depth in the spatially restricted stimulus conditions that reveal the existence of stereomotion scotomas. These results are consistent with previous findings that changing disparity cues require a large field stimulus to be effective (Czuba, Rokers, Huk, & Cormack, 2012). We wished however, to exclude the possibility that the relatively poor performance in our observers was due to the stimulus containing poor cues to binocular disparity, on which the extraction of changing disparity cues necessarily depends. This is a concern especially given that we refresh the location of the dots in the CD stimulus on each display frame (approx. every 17ms).

To evaluate the sensitivity to static disparity in our stimulus arrangement, we therefore conducted a control experiment. We presented the stimulus previously used to isolate the CD cue but at a constant depth (at 0.15° disparity, half-way through the trajectory the motion stimulus would traverse) either near or far relative to the fixation point. Note that in this stimulus, we still refreshed all dots on each frame, but the plane defined by the dots did not move through depth. The task for the observer was to indicate the stimulus position in depth on every stimulus presentation. We find that all observers are able to perform

Motion agnosia is the result of impaired velocity processing

this task at better than chance levels across nearly all tested locations (right column of **Figure 5.4A**). To test whether the sensitivity of an observer to static

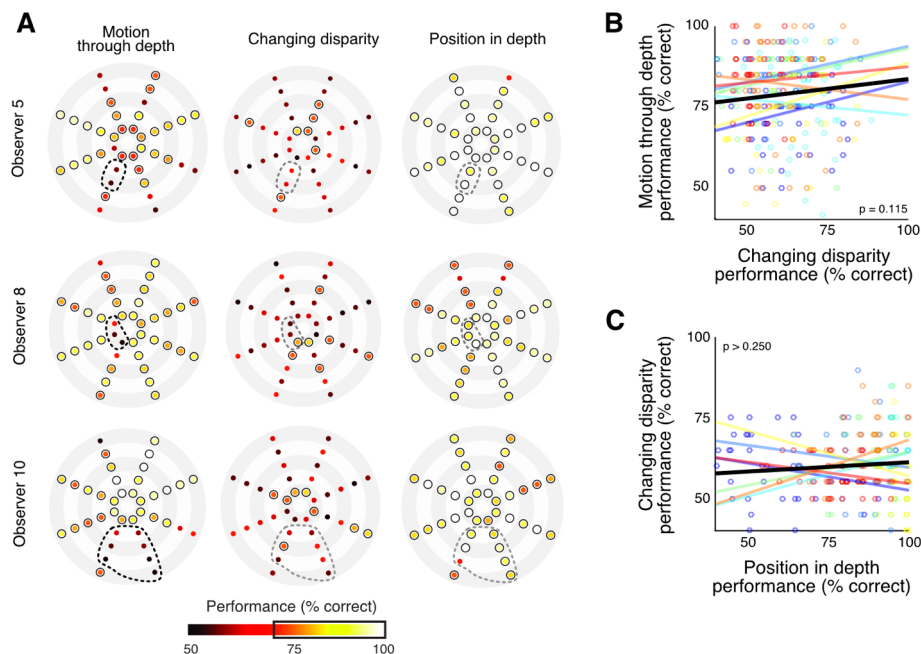


Figure 5.4 Sensitivity to binocular disparity does not predict the location of stereomotion scotomas **A:** Sensitivity to 3D motion and binocular disparity stimuli across the visual field in three representative observers. Left column: the sensitivity as measured by the FULL stimulus. Middle column: sensitivity as measured using the changing disparity (CD) stimulus. While the location of the scotoma is easily identified in each of the left-column figures (black dotted regions), performance based on the CD stimulus (middle column) is generally low, and does not predict the stereomotion scotoma location. Right column: the sensitivity to static disparity across the visual field for each observer, indicating that the relatively poor performance based on the CD stimulus is not due to an inability to extract binocular disparity signals from the visual display. The results for all observers are shown in supplementary Figure S1. **B:** Sensitivity to 3D motion measured with the FULL stimulus as a function of sensitivity to the CD cue. Performance on the CD cue does not significantly predict sensitivity to motion in depth ($F(1,75) = 2.55, p = 0.115$). The colored lines indicate fits for individual observers and the thick black line indicates the overall fit based on a mixed effects linear model. **C:** Sensitivity to the CD cue as a function of sensitivity to static disparity. Sensitivity to static disparity does not significantly predict sensitivity to changing disparity across the visual field ($F(1,4.2) = 0.89, p > 0.250$). The colored lines indicate fits for individual observers and the thick black line indicates the overall fit based on a mixed effects linear model.

disparity is predictive of their performance on the CD stimulus we fit a linear model using the data obtained with both stimuli. Sensitivity to static disparity did not significantly predict the sensitivity to changing disparity ($F(1,4.2) = 0.89, p > 0.250$) across the visual field (**Figure 5.4C**).

Taken together these results lead us to conclude that the CD cue is not predictive of the sensitivity to motion in depth across the visual field at the, relatively small, spatial scale of the stimuli used here. In addition, we conclude that the sensitivity to disparity per se is not impaired and that the generally poor performance we find on the CD stimulus task is not caused by a problem detecting disparity in our displays.

Sensitivity to motion in depth is predicted by sensitivity to the IOVD cue

Next we investigated the failure to combine velocity signals from the two eyes as a potential cause for stereomotion scotomas. Aside from changes in disparity, it has been shown that the visual system can rely on a second binocular cue to motion in depth: *interocular velocity differences*. **Figure 5.5A** shows the sensitivity to motion in depth for three observers in whom we identified a stereomotion scotoma (left column, indicated by black dotted region). An inability to combine velocity signals from the two eyes seems to underlie these visual deficits. When we present a stimulus in which binocular disparity is disrupted, but interocular velocity signals are present, locations of poor performance match those of the stereomotion scotomas (right column, indicated by the grey dotted region). The same data for the other observers is included in Appendix Figure A5.2.

A linear regression analysis to quantify how well the sensitivity measured by the FULL stimulus is predicted by the sensitivity as measured by the IOVD stimulus,

Motion agnosia is the result of impaired velocity processing

reveals that the sensitivity to the IOVD cue significantly predicts motion in depth sensitivity ($F(1,7.3) = 17.29, p = 0.004$). To illustrate, **Figure 5.5B** plots the sensitivity as measured in the FULL condition as a function of the sensitivity measured using the IOVD stimulus. The colored lines represent the fits for individual observers and the thick black line represents the overall fit to the data.

Thus, the location of a stereomotion scotoma, as measured by a stimulus containing all binocular cues to motion in depth, is best predicted by the sensitivity of an observer to the IOVD cue across the visual field. The sensitivity to the CD cue is uniformly poor across the visual field and therefore does not predict the scotoma location.

Findings are robust across stimulus speed

Previous studies suggest that the sensitivity to the CD and IOVD cues depends on the monocular speed of the stimulus, and that the peak sensitivity for both cues is different (Czuba et al., 2010; Wardle & Alais, 2013). Specifically, the mechanisms that underlie the CD cue seem to prefer slower speeds compared to the IOVD mechanisms. We specifically chose the monocular speed (0.6 °/s) in our experiments because it is closer to peak CD than peak IOVD sensitivity. Naturally this leaves open the possibility that the existence of stereomotion scotomas is specific to a particular speed, or that the underlying neural cause varies depending on stimulus speed.

We therefore repeated all of our experiments at both halved (0.3 °/s) and doubled monocular speeds (1.2 °/s). For each speed we tested whether the CD or IOVD sensitivities were more predictive of the sensitivity to the FULL cue stimulus. **Figure 5.6** plots the linear fit of the FULL cue performance (y-axis) as

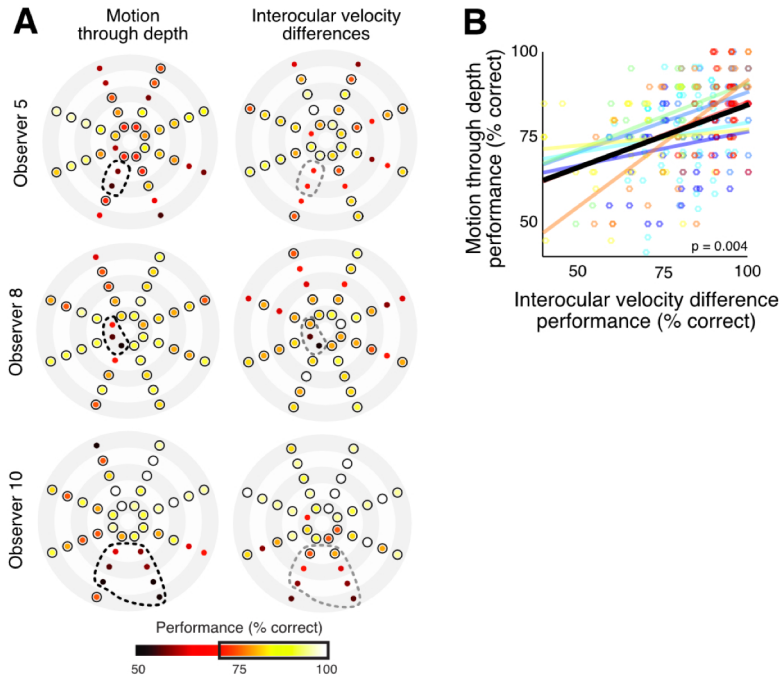


Figure 5.5 Sensitivity to interocular velocity differences predicts location of stereomotion scotoma **A:** Sensitivity to 3D motion and interocular velocity differences (IOVD) across the visual field in three representative observers. Left column: sensitivity to 3D motion as measured by the FULL stimulus. Right column: sensitivity as measured using the IOVD stimulus. The stereomotion scotoma as identified in each of the left-column figures (black dotted regions) match locations of poor performance in the right-column figures (grey dotted regions), suggesting that impairments in motion in depth perception are related to deficits in the processing of IOVD cues. The results for all observers are shown in supplementary Figure S2. **B:** Sensitivity to 3D motion measured with the FULL stimulus as a function of sensitivity to the IOVD stimulus. Sensitivity to the IOVD stimulus significantly predicts sensitivity to the FULL stimulus ($F(1,7.3) = 17.29, p = 0.004$). The colored lines indicate fits for individual observers and the thick black line indicates the overall fit based on a mixed effects linear model.

Motion agnosia is the result of impaired velocity processing

a function CD (gray line) or IOVD (black line) cue performance (x-axis) for all three different monocular speeds. CD cue sensitivity did not significantly predict the FULL cue sensitivity at any monocular stimulus speed (0.3 °/s: $F(1,6.5) = 2.59, p = 0.15$, 0.6 °/s: $F(1,75) = 2.55, p = 0.115$, 1.2 °/s: $F(1,92.7) = 0.41, p > 0.250$). Conversely we find that the sensitivity to the IOVD cue significantly predicts the sensitivity to the FULL cue at all three stimulus speeds (0.3 °/s: $F(1,7.1) = 26.04, p = 0.001$, 0.6 °/s: $F(1,7.3) = 17.29, p = 0.004$, 1.2 °/s: $F(1,6.3) = 72.20, p < 0.001$). Further, using a likelihood ratio test to compare the CD and IOVD linear models we find that for all speeds, sensitivity to the IOVD cue is infinitely better at explaining FULL cue performance (0.3 °/s: $LR = 81.26, p \sim 0$, 0.6 °/s: $LR = 73.33, p \sim 0$, 1.2 °/s: $LR = 71.06, p \sim 0$). In addition, sensitivity to motion in depth based on the CD cue does not generally improve with lower speeds.

The individual cues in combination do not better predict stereomotion sensitivity

In normal viewing situations the two binocular cues are both present. Therefore, the contribution of the CD cue might not be significant when considered separately, but it might contribute in a combined model. To test this, we fitted a linear model using both the performance as measured by the CD stimulus and the performance as measured by the IOVD stimulus. Using an ANOVA we tested the contribution of the two cues in this combined model. Across all three stimulus speeds we do not find a significant contribution of CD stimulus sensitivity to the model (0.3 °/s: $F(1,11.4) = 1.66, p = 0.22$, 0.6 °/s: $F(1,5.8) = 0.91, p > 0.250$, 1.2 °/s: $F(1,85.9) = 0.80, p > 0.250$). Conversely, we find that sensitivity to the IOVD stimulus does contribute significantly to the model at each speed (0.3 °/s: $F(1,6.8) = 28.59, p = 0.001$, 0.6 °/s: $F(1,6.3) = 56.57, p < 0.001$, 1.2 °/s: $F(1,6.5) = 73.12, p < 0.001$). Further, we do not find

that the combined model is better at predicting the sensitivity to stereomotion compared to a model that is only based on the IOVD cue (likelihood ratio test, *all p values* > 0.88).

Motion sensitivity per se is not the underlying cause of stereomotion scotomas

We find that the sensitivity to interocular differences in retinal velocity is strongly predictive of an observer's sensitivity to motion in depth. Previously, we demonstrated that sensitivity to 2D motion (left/right) is generally not predictive of sensitivity to motion in depth (Barendregt et al., 2014). In supplementary figure S3 we included the results of a 2D motion discrimination task that was performed in the previous study by four observers that also participated in this study. Using a linear mixed effects regression we found that performance on the 2D motion discrimination task is not predictive of the performance on the motion in depth task ($F(1,4) = 0.79, p = 0.43$).

Taken together, our results lead us to conclude that the sensitivity to interocular velocity differences is a strong predictor of sensitivity to motion in depth. We fail to find a significant contribution of the changing disparity cue to the perception of motion in depth at the spatial scales of our stimulus design, even when we combine both cues in the same model. Finally, the ability to predict 3D motion sensitivity based on the IOVD cue is relatively independent of stimulus speed, even at very slow speeds optimized for the CD stimulus.

Motion agnosia is the result of impaired velocity processing

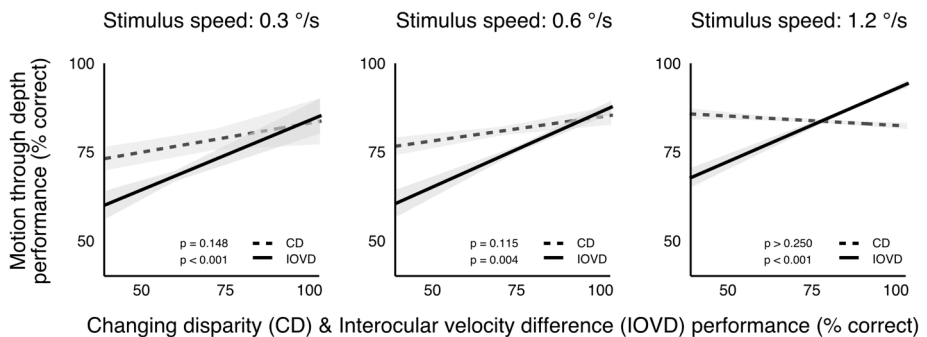


Figure 5.6 *Sensitivity to the IOVD cue, but not the CD cue, predicts sensitivity to 3D motion across a range of monocular speeds. Each panel shows the relationship of sensitivity to 3D motion as measured by the FULL stimulus and sensitivity to the CD (dashed line) or IOVD (solid line) stimulus. From left to right the panels represent data collected using a stimulus with a monocular speed of 0.3°/s, 0.6°/s and 1.2°/s. We find that sensitivity to the IOVD stimulus significantly predicts 3D motion sensitivity at each speed (all $p < 0.005$). In contrast, sensitivity to the CD stimulus does not significantly predict sensitivity to 3D motion at any speed (all $p > 0.1$). Shaded gray regions represent 95% confidence interval of the linear fit.*

Discussion

We investigated the cause of stereomotion scotomas, a surprisingly prevalent deficit in the processing of visual motion, that occurs in over 50% of otherwise healthy observers (Barendregt et al., 2014; Hong & Regan, 1989). Since stereomotion scotomas are not associated with any clear retinal impairment or a deficit in the processing of monocular information, we investigated if stereomotion scotomas might result from failures in the processing of one or both of the known binocular cues to motion in depth. We did not find a significant contribution of the changing disparity (CD) cue to the sizable motion impairments in these observers. Instead, we find that the visual field location of deficits in motion perception is best predicted from deficits in the sensitivity to the interocular velocity difference (IOVD) cue. Taken together our results show that the cause of stereomotion scotomas is a deficit in the binocular combination of retinal velocity cues.

Relation to previous work on stereomotion scotomas

The present work shows that the impairments in the perception of motion in depth occur specifically as a result of impairments in processing visual cues that vary over time. While previous work (Hong & Regan, 1989; Richards & Regan, 1973) has provided evidence for the existence of the impairment, it did not explicitly distinguish between instantaneous and time-varying cues to motion in depth. Moreover, we focused on the contribution of binocular cues because our previous work (Barendregt et al., 2014) suggested that stereomotion scotomas are due to a failure at or after the stage of binocular combination. Since there are two binocular cues to motion in depth, this implied that the deficit had to

Motion agnosia is the result of impaired velocity processing

be due to a problem in processing either the *changing disparity over time* or *interocular velocity difference* cue (or both).

The inability to detect motion in depth from CD cues is not due to an inability to extract the binocular disparity signals

We emphasize that the observers in our experiments had no trouble detecting binocular disparity per se, despite the short presentation time of each display frame (~17 ms). In a control condition where observers had to judge position in depth of a stationary stimulus with the same presentation time, we found that all observers were easily able to perform this task across the visual field. This is consistent with previous reports that stereopsis per se is mainly limited by monocular luminance mechanisms (Gheorghiu & Erkelens, 2005b). However, previous studies have also shown that the temporal frequencies that can be used for the perception of motion from disparity are quite low (Gheorghiu & Erkelens, 2005a; Kane, Guan, & Banks, 2014). Thus, the poor performance in detecting motion from changes in disparity is not the result of limitations in extracting binocular disparity signals per se, but instead derives from poor sensitivity to the changing binocular disparity cue in displays that use fast temporal updating and a small spatial extent that can expose these deficits in motion perception.

Contributions of the changing disparity cue to motion perception

Previous work has suggested that these deficits in motion perception exist even when (static) binocular disparity cues are present (Hong & Regan, 1989). Taken together with the current result that observers perform poorly when detecting motion from the CD cue stimulus, this would seem to suggest that binocular disparity cues do not appear to contribute significantly to motion in depth perception at all.

We note however that disparity cues can contribute to the perception of motion in depth, but such contributions seem restricted to situations where the motion is slow (Czuba et al., 2010) and spans a large part of the visual field (Czuba et al., 2012; Sakano, Allison, & Howard, 2012). A careful investigation of the role of stimulus size on the perception of motion in depth from changing binocular disparity would therefore be beneficial.

Contributions of the interocular velocity difference cue to motion perception

Our results indicate that deficits in motion perception are closely linked to an observer's ability to utilize interocular velocity difference cues in visual displays. When we isolate the contribution of IOVD cues by eliminating instantaneous binocular disparity as a cue, and disrupting the changing disparity cues, the resulting behavior is highly predictive of the behavioral performance measured using stimuli containing all binocular cues. Given that monocular motion processing appears unimpaired under the same viewing conditions (Barendregt et al., 2014), the problem is likely not in the motion signals per se, or a binocular imbalance, but rather a failure in the integration of motion signals from the two eyes. Thus our findings show that the underlying cause of stereomotion scotomas is a failure to combine velocity signals between the eyes, pointing to a deficit in visual cortical areas involved in motion processing.

Alternative explanations

One might consider that these deficits are not due to a failure in motion processing, but to other factors, such as stimulus contrast. While there is some evidence that motion in depth perception is more sensitive to stimulus contrast compared to similar 2D motion stimuli (Fulvio, Rosen, & Rokers, 2015), previous work explicitly investigating the effects of stimulus contrast in visual displays very similar to the ones used here has shown that these specific

Motion agnosia is the result of impaired velocity processing

deficits in motion in depth perception are relatively robust to contrast (Barendregt et al., 2014).

We did not explicitly monitor observers' eye movements in these experiments. The short presentation duration and the randomized order of the stimulus locations ensured that making eye movements would not be informative to the task. Importantly, if observers had been actively making eye movements towards the presented locations, we should expect their performance to be either close to uniform across the visual field or declining as a function of eccentricity. Moreover, we would not expect significant correlations across the different stimulus types and speeds. Since we did not find such a pattern of results in any of our observers, we feel confident that observers making eye movements towards the stimulus location cannot explain our results.

Motion agnosia

We propose that the deficit associated with stereomotion scotomas should be considered a previously unrecognized type of visual agnosia. While a scotoma is a localized loss of visual acuity or a blind spot, visual agnosias are characterized by an inability to discriminate a specific feature of visual stimuli, in the presence of normal basic visual function. The visual field deficit described here is identified by an inability to discriminate the direction of motion in depth, but affected individuals are not blind in those parts; rather, they are unable to interpret what they see.

Visual agnosia is frequently associated with cortical lesion (Riddoch, 1917), but this is not a necessary condition. For example, prosopagnosia exists in the absence of any lesion, and is in part congenital (Kennerknecht et al., 2006). Unlike other such deficits, the motion agnosia we describe here is quite common – based on our results, they occur in over 50% of the normal

population – and typically restricted to part of the visual field. A likely reason for this restriction of the agnosia in the visual field are the smaller receptive field size of motion in depth sensitive neurons, compared to neurons sensitive to other visual properties, such as objects or faces. It is currently not known if other forms of visual agnosia also occur in a spatially-restricted form, but our results suggest that this might be an interesting avenue of further research.

Identifying the neural mechanisms involved in visual agnosias is often complicated by the fact that a large number of visual cues contribute to visual perception (Avidan, Hasson, Malach, & Behrmann, 2005). However, since there are only two cues that support the binocular perception of motion in depth, we were in a unique situation to investigate the underlying neural cause of this particular form of visual agnosia. Future work should incorporate these findings with the existing knowledge on the cortical processing of motion in depth to elucidate what cortical processes might lead to this visual deficit.

Conclusion

In sum, we studied a prevalent form of visual agnosia in which > 50% of otherwise healthy observers are unable to judge the direction of motion in depth in part of their visual field. We do not find that changing disparity cues contribute significantly to the perception of motion in depth for these particular stimulus configurations. Instead, we find that the cause for such motion agnosia is a failure to properly combine retinal velocity signals in visual cortex. These findings contribute to our understanding of visual motion perception and identify the underlying cause for a specific type of visual agnosia.

Motion agnosia is the result of impaired velocity processing

Appendix

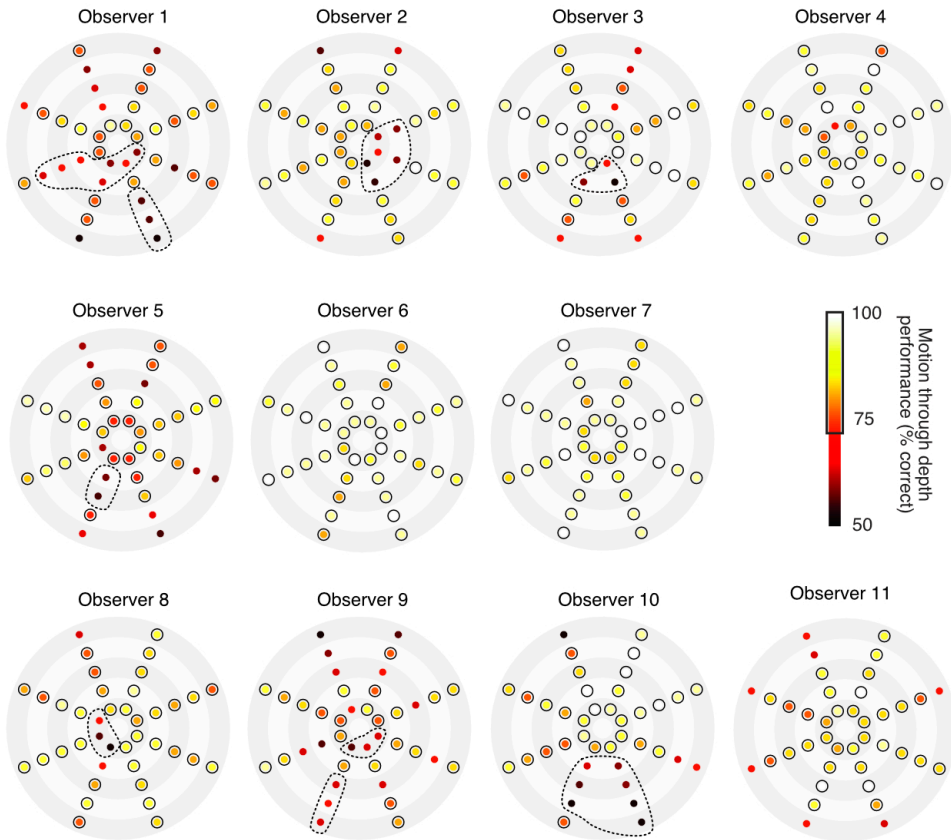


Figure A5.1 Sensitivity to changing disparity measured across the visual field for all observers in our study. The dotted lines indicate the location of the 3D motion blindness region for an observer, as determined by their performance on a task with a stimulus containing multiple cues to 3D motion (Figure 5.3). Observers 4, 6, 7 and 11 did not have a stereomotion scotoma in their visual field.

Chapter 5

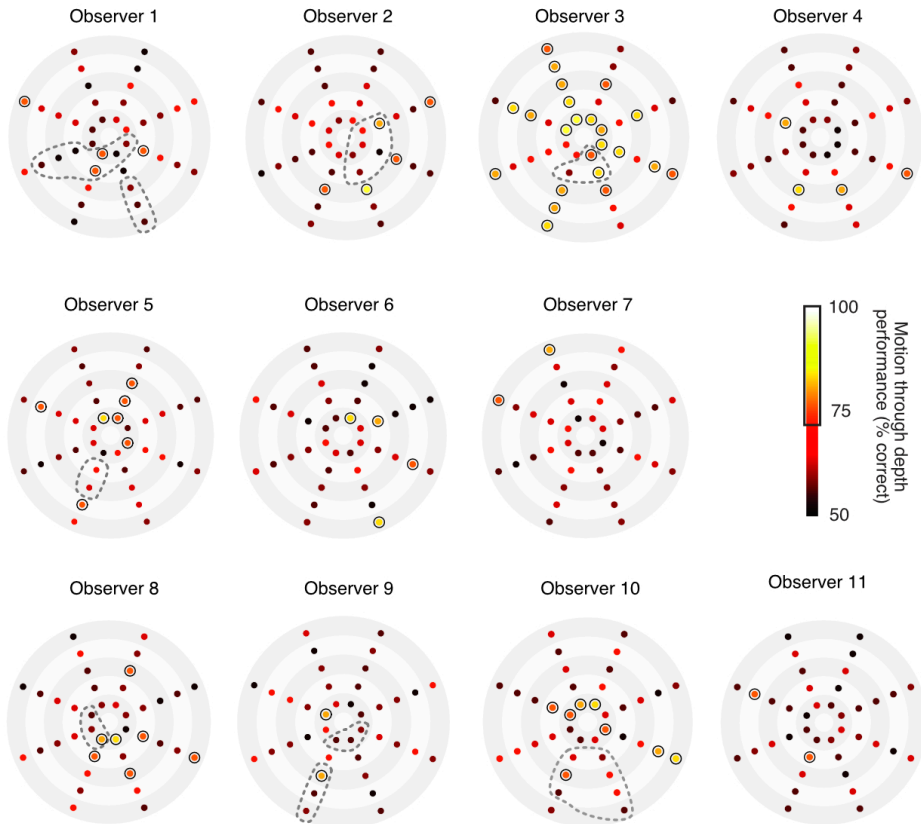


Figure A5.2 Sensitivity to changing disparity measured across the visual field for all six observers with 3D motion blindness. The light grey dotted lines indicate the location of the 3D motion blindness region for each observer, as determined by their performance on a task with a stimulus containing multiple cues to 3D motion (**Figure 5.3**). Observers 4, 6, 7 and 11 did not have a stereomotion scotoma in their visual field.

Motion agnosia is the result of impaired velocity processing

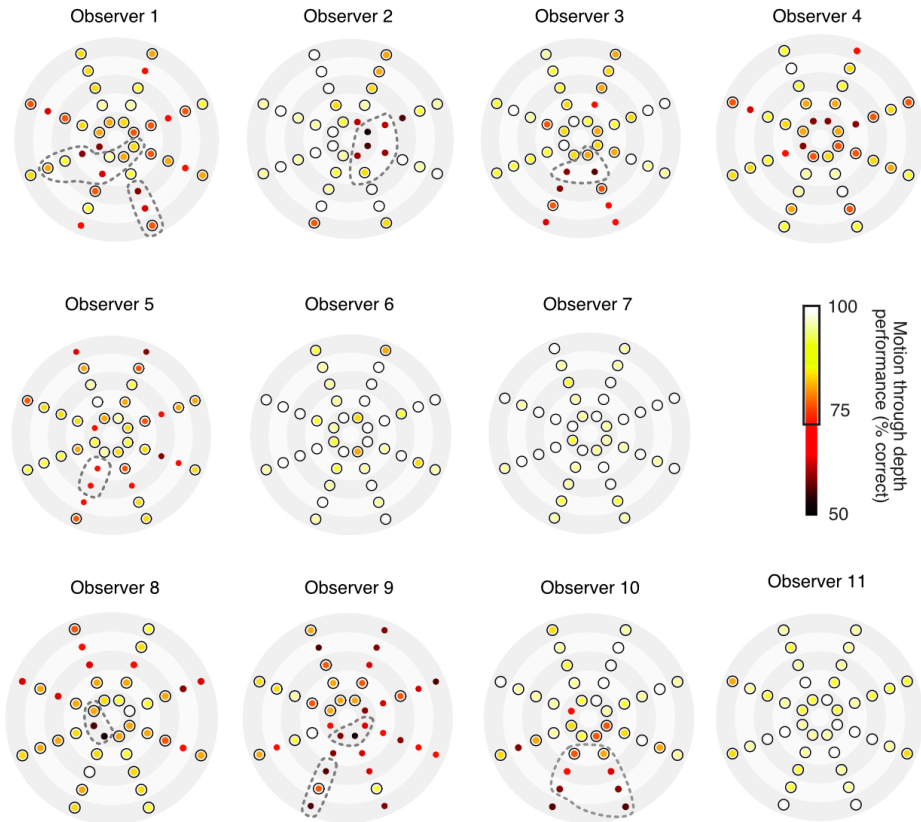


Figure A5.3 Sensitivity to interocular velocity differences measured across the visual field for all six observers with 3D motion blindness. The light grey dotted lines indicate the location of the 3D motion blindness region for each observer, as determined by their performance on a task with a stimulus containing multiple cues to 3D motion (**Figure 5.3**). Observers 4, 6, 7 and 11 did not have a stereomotion scotoma in their visual field.

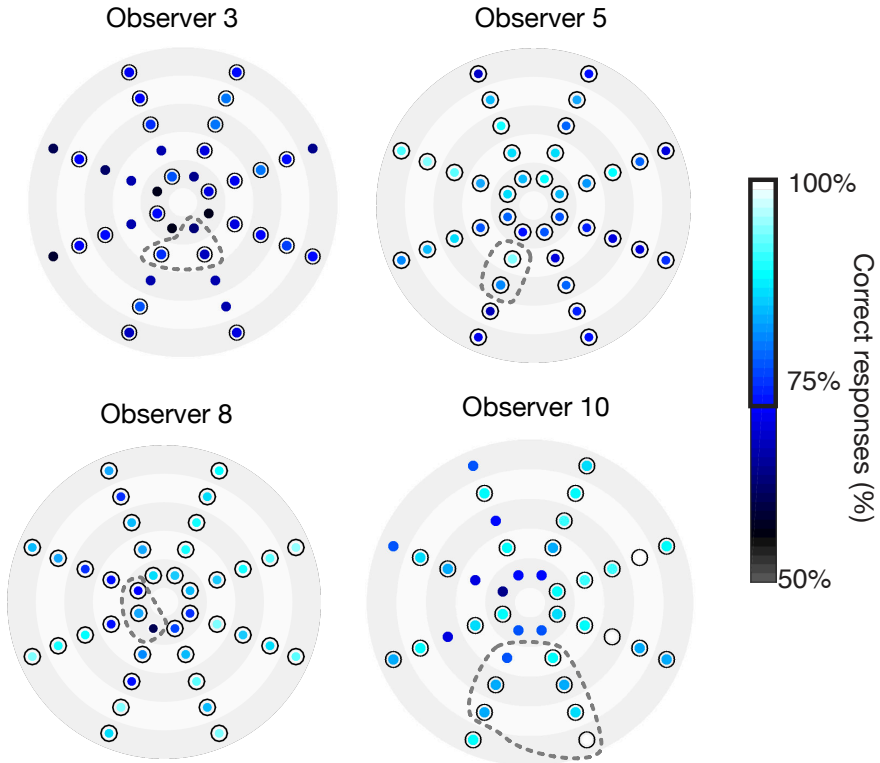


Figure A5.4 Sensitivity to lateral (2D) motion measured across the visual field. Data shown is from a previous publication with the same observers as the current study (Barendregt et al., 2014). The task for the observer was to judge the direction of motion (left/right) of a subset of coherently moving dots (50%) between randomly moving dots. The grey lines indicate a region of 3D motion blindness for an observer, as based on the data in **Figure 5.3**.

Chapter 6

SUMMARY AND CONCLUSIONS

Summary per chapter

Chapter 2

The two images our eyes have of the world are combined by the brain into a single, cyclopean view. In this chapter we set out to identify where in the brain this transformation from retinal images to a cyclopean image occurs. Using computational neuroimaging techniques, we show that the representation of the visual world is based on the retinal images in the first visual area, primary visual cortex, but is then subsequently transformed into a representation of the cyclopean image in the second visual area. We also find that in all later visual areas, the cyclopean representation is maintained. These results shed light on how our single, cyclopean view of the world is constructed based on the input from our eyes.

Chapter 3

In this chapter we set out to characterize an odd visual deficit in binocular motion perception: the inability to report the direction of motion of a stimulus that moves in depth. In our experiments we find that over half of the participants are unable to discriminate between approaching and receding motion in a part of their visual field. Although the position of the deficit varies widely between participants, we demonstrate that these visual field deficits do not change in position over time but always occur at the same position for every participant. Using a set of control experiments we show that there are no corresponding visual field deficits in the discrimination of static disparity or lateral motion as well as no evidence for strong eye dominance at these visual field positions. In sum, we therefore conclude that this deficit in motion

Chapter 6

perception likely originates at the stage in visual processing where the monocular signals from the two eyes are integrated.

Chapter 4

After describing the inability to report motion direction using behavioral methods, we set out to identify a neural basis for this visual deficit in this chapter. The fact that the deficit is confined to a particular location in the visual field allows us to directly investigate neural responses at a relatively fine level using the visual field maps in the brain. Comparing the responses for affected locations with control locations, in the same participant, we find a significant modulation of the neural response in two important visual areas. We find that the neural responses in an important area for motion processing, the human middle temporal complex, are significantly modulated by the inability to discriminate motion direction at a seemingly low level of visual processing. In addition, we also find a clear influence on responses in primary visual cortex. These results provide the first evidence for the neural basis of this deficit in motion perception and show that this deficit can best be characterized as motion agnosia. The results also provide new insights into the roles of primary visual cortex and the middle temporal complex in the perception of motion.

Chapter 5

A source of much recent debate in the literature is the role of two visual cues, *changing disparity over time* and *interocular velocity differences*, in the perception of motion in depth. In this chapter we evaluate the role of these two cues in motion agnosia. Using a variation of the behavioral experiment described in Chapter 2 we measure sensitivity to each of the two cues across the visual field in participants with motion agnosia. We find that only the velocity-based cue, and not the disparity-based cue, is predictive of the location of motion agnosia

Summary and conclusions

in the visual field. These results show that motion agnosia is primarily a deficit of processing the velocity-based cue to motion in depth.

General discussion

A large part of research in the field of neuroscience is concerned with describing and understanding how the brain represents the outside world based on the sensory input. In this thesis we used the binocularity of human vision to study sensory representations in visual cortex. Binocular vision is a fundamental property of the human visual system and plays a significant role in the perception of depth. Because the retina is a two-dimensional surface on which visual information from the outside world projects, all information about the third dimension has to be inferred from these retinal projections. As a consequence, the visual system has to perform a number of computations to build up the interpretation that we end up perceiving. In this thesis the aim was to gain a better understanding of the underlying computations that form the basis for the binocular perception of motion in depth (3D motion). Using a combination of behavioral and neuroimaging methods we investigated the representation of monocular and binocular representations in human visual cortex (Chapter 2) and the neural mechanisms involved in motion perception using motion agnosia (Chapters 3, 4 and 5).

The nature of internal representations of the outside world

The idea that the information from the two retinal images is combined in early visual cortex is not new (Hubel & Wiesel, 1962). From studies in cats and non-human primates we know that binocular neurons in primary visual cortex respond to inputs from both eyes and can detect binocular disparities (Blasdel & Fitzpatrick, 1984; Hubel et al., 2013; Hubel & Wiesel, 1962). However, this does not tell us how the human visual system builds an internal representation of the outside world: based on the retinal images or on the cyclopean image. In

Summary and conclusions

Chapter 2 we demonstrate, using a combination of fMRI and computational modeling, that the human visual system contains two distinct internal representations in primary visual cortex. These representations are then transformed into a single, cyclopean representation of the visual world in extrastriate cortex. An important distinction here is in the way this transformation could be carried out. One possibility would be that the positions of objects in the V1 representation are simply averaged into a single position in the V2 representation. However, our results suggest that this is not what happens. Rather, the two positions of an object in the V1 representation are transformed into the position of the object in the cyclopean image (see Figure 2.4 for an illustration of this difference). This shows that in extrastriate visual areas, an object is represented at a position that is largely independent from the position of the object on the two retinas.

Our results on the representation of binocular visual information demonstrate a fundamentally different cortical representation of the outside world by the primary visual cortex and the extrastriate areas. These results build on the idea that the processing of visual information is governed by a hierarchical structure where different cortical areas sequentially process different features of the sensory input (Essen & Maunsell, 1983). Traditionally, the view has been that the primary and secondary visual areas perform similar operations on the sensory input but on different spatial scales due to the increase in average receptive field size between the two areas (Smith, Singh, Williams, & Greenlee, 2001; Zeki, 1978). However, the results in this thesis contribute to a growing body of work that demonstrate a distinct role for the secondary visual area (V2) in visual processing (G. Chen et al., 2008; M. Chen et al., 2014; Dumoulin et al., 2014; Freeman et al., 2013). Importantly, we find that the internal representation of the sensory information in V2 moves away from reflecting the

sensory organ (retina) and instead transforms into a representation that is more relevant to guide interactions with the outside world.

Why motion agnosia should not be considered a stereomotion scotoma

In this thesis, the inability to discriminate the direction of motion in depth has been described both as a form of blindness (stereomotion scotoma) and a form of agnosia (motion agnosia). In this thesis we skew towards using the latter term but as is evident from Chapter 3 this point of view has evolved over time. The original term ‘stereomotion scotoma’ to describe the deficit emphasizes the limited spatial extent in the visual field (Richards & Regan, 1973). The term ‘scotoma’ typically refers to a region in the visual field that has a reduction in or an absence of visual acuity. It is therefore often used in ophthalmological literature and practice to describe such regions in the visual field of patients with retinal or macular defects, thereby linking the term mostly to different forms of (near-)blindness.

However, in the case of motion agnosia the most salient aspect of the deficit is not the spatial extent but rather the phenomenology of the behavior. The deficit is clearly not a form of blindness in the sense that the observer is unable to perceive a visual stimulus. Rather, the observer can perceive the stimulus *and* often even that it moves but in spite of this can not discriminate the direction of motion. This points to a problem with visual discrimination, rather than a problem with visual perception per se. Visual agnosia is defined as the inability to discriminate specific visual features, such as faces or objects, in spite of having normal visual input. Therefore, classifying the visual deficit that is studied in this thesis as a motion agnosia better captures the phenomenology of the deficit.

How motion agnosia informs the understanding of cortical motion processing

How do the results in this thesis fit within the existing models of binocular motion in depth perception? In recent years, attempts to incorporate the processing of motion in depth with the existing models of two-dimensional motion processing have demonstrated that most of the cortical processing is apparently done by area MT (Czuba et al., 2014; DeAngelis & Newsome, 1999; Rokers et al., 2009; Sanada & DeAngelis, 2014). Our finding that area MT is involved in motion agnosia therefore fits with our current understanding of cortical motion processing but also adds more evidence for an inconsistency in that understanding.

As illustrated in Figure 3.1, the current view of how the brain determines direction of motion in depth is that there are two binocular cues the brain utilizes in order to extract the 3D motion direction of visual input. Visual area MT has been shown to process both of those cues (Rokers et al., 2009), yet the relative roles and contributions of the disparity- and the velocity-based cues to 3D motion remain unclear (Czuba et al., 2010, 2012; Nefs & Harris, 2010; Nefs et al., 2010; Sakano & Allison, 2014). In contrast, our results on the mechanisms that might be defective in motion agnosia provide a very clear answer in that only a deficit in the velocity-based cue leads to motion agnosia. Visual area MT has been shown to be the location in cortex where the velocity-based cue is processed (Rokers et al., 2009), yet this means that this area should have information about the eye of origin of the incoming motion signals (Rokers, Czuba, Cormack, & Huk, 2011) in order to be able to compute a difference between the velocity signals in each eye (Shioiri et al., 2000). Since the traditional view holds that the signals from the two eyes are combined in primary visual cortex, and our results in Chapter 2 support this, it is currently

unclear how area MT is able to perform these computations. While there are suggestions that area MT might receive direct projections from subcortical structures that could in theory provide eye-specific visual input (Sincich, Park, Wohlgemuth, & Horton, 2004), it remains an open problem and provides a promising avenue for future research.

What motion agnosia contributes to the study of visual agnosia

Our results on motion agnosia provide strong evidence for a well-defined neural basis of a novel form of visual agnosia. It has traditionally been difficult to pinpoint the neural origins of the various known forms of visual agnosia since there are often multiple visual features involved that interact in unknown ways (Avidan et al., 2005; Bridge et al., 2013). In contrast to complex shapes or faces, motion is processed in the earliest stages of the cortical visual hierarchy and has also been much more thoroughly studied in both non-human primates and humans. Even though our understanding of motion processing is far from complete, as discussed above, the reduction in complexity of the features and processes involved combined with the much higher prevalence in the population means that the study of motion agnosia provides a very useful tool in the study of visual agnosia in general. As one example, the fact that we show that motion agnosia is not a complete deficit but rather varies across the visual field suggests that this might also hold for other forms of visual agnosia, something that has not yet been explicitly studied.

Where the findings of this thesis contribute outside of basic science

The results that we discuss in this thesis potentially have broader applications beyond the laboratory. The knowledge of exactly where in the brain the human visual system integrates the information from the two eyes is valuable for the study and possible treatment of various disorders of binocular vision, such as

Summary and conclusions

amblyopia (lazy eye). Since disorders like amblyopia are often the result of a deficit of the neural pathways rather than the eyes itself, it is very important to have a complete understanding of how the visual pathways in the human brain interact and ultimately lead to our perception of the environment. Our findings regarding the neural basis and binocular mechanisms involved in motion agnosia provide a novel opportunity to study visual agnosia and can inform new models of the neural basis of other forms of agnosia. Therefore, the results in this thesis could ultimately contribute to a better understanding and inform potential treatments of both visual disorders like amblyopia as well as disorders such as agnosia. Aside from clinical implications, the high prevalence of motion agnosia should also have implications for the general population. In particular, the fact that such a high proportion of people have difficulty discriminating motion direction means that activities involving fast motion, such as driving a car or playing sports, could benefit from the study of this deficit.

Appendix

NEDERLANDSE SAMENVATTING

Hoofdstuk 2

De twee beelden van de wereld in onze twee ogen worden door het brein samengevoegd tot een enkel, cyclopisch beeld. In dit hoofdstuk is het doel om erachter te komen waar in het brein deze overgang van de twee beelden op de retina naar een cyclopisch beeld plaats vindt. Met behulp van computationele neuroimaging methoden tonen we aan dat de interne representatie van de visuele wereld in het eerste visuele hersengebied, primaire visuele schors, is gebaseerd op de retinale beelden maar dat deze vervolgens transformeert naar een cyclopische representatie in het tweede visuele hersengebied. Tevens vinden we dat in alle volgende visuele hersengebieden, deze cyclopische representatie blijft behouden. Deze resultaten geven inzicht in hoe ons brein het enkele, cyclopische beeld dat we van de wereld waarnemen samenstelt op basis van de beelden die via de ogen binnenkomen.

Hoofdstuk 3

In dit hoofdstuk onderzoeken we een vreemde visuele afwijking bij het binoculair waarnemen van beweging: niet in staat zijn de bewegingsrichting te duiden wanneer een stimulus in diepte beweegt. In onze experiment vinden we dat meer dan de helft van de deelnemers niet in staat is om beweging naar zich toe te onderscheiden van beweging van zich af, in een gedeelte van hun gezichtsveld. Hoewel de positie van deze afwijking in het gezichtsveld sterk varieert tussen deelnemers, vinden we dat de positie altijd hetzelfde is ongeacht hoe vaak we dit bij een deelnemer meten. Met behulp van een aantal controle experimenten tonen we aan dat er geen corresponderende afwijkingen zijn in het onderscheiden van positie in diepte (binoculaire dispariteit) of zijdelingse beweging. Tevens vinden we geen bewijs dat oog dominantie een rol speelt. Uiteindelijk concluderen we hieruit dat de origine van deze afwijking bij het

waarnemen van beweging in diepte zich waarschijnlijk bevindt in het stadium waar het brein de signalen van de twee ogen samenvoegt.

Hoofdstuk 4

Nadat we (in Hoofdstuk 3) een visuele afwijking bij het waarnemen van beweging hebben beschreven, gaan we in dit hoofdstuk op zoek naar een neurale oorsprong voor deze afwijking. Omdat de afwijking zich altijd limiteert tot een gedeelte van het gezichtsveld kunnen we gebruik maken van de kaart van het gezichtsveld in het brein. Als we de hersenactiviteit voor aangetaste locaties vergelijken met de activatie voor niet-aangetaste, control locaties dan zien we dat de activatie significant wordt beïnvloed in twee belangrijke visuele hersengebieden. In het hersengebied dat traditioneel wordt geassocieerd met het verwerken van bewegingsinformatie, vinden dat de activatie sterk verminderd onder de invloed van het niet kunnen onderscheiden van de bewegingsrichting. Daarnaast vinden we ook een sterke invloed in de primaire visuele hersenschors, hoewel deze effecten meer veroorzaakt lijken te worden door het wel of niet juist kunnen antwoorden tijdens een taak. Deze resultaten tonen het eerste directe bewijs voor een neurale oorsprong voor deze visuele afwijking en tonen aan dat deze afwijking het beste kan worden gekarakteriseerd als een vorm van agnosie: bewegingsagnosie.

Hoofdstuk 5

Een bron van veel recente discussie in de literatuur is de rol van twee visuele cues, verandering in dispariteit over tijd en interoculaire snelheidsverschillen, in de waarneming van beweging in diepte. In dit hoofdstuk evalueren we de rol van deze twee cues in bewegingsagnosie. Met een variant van het gedragsexperiment beschreven in Hoofdstuk 2 meten we gevoeligheid voor elk van de twee signalen in het gezichtsveld van deelnemers met

Nederlandse samenvatting

bewegingsagnosie. We vinden dat alleen de op snelheid gebaseerde cue en niet de dispariteit-gebaseerde cue, voorspellend is voor de locatie van bewegingsagnosie in het gezichtsveld. Deze resultaten tonen dat bewegingsagnosie vooral wordt veroorzaakt door een verstoring in de verwerking van de snelheid-gebaseerde cue.

Appendix

LIST OF REFERENCES

List of references

- Adelson, E., & Movshon, J. (1982). Phenomenal coherence of moving visual patterns. *Nature*, *300*, 523–525.
- Albright, T. D., Desimone, R., & Gross, C. G. (1984). Columnar organization of directionally selective cells in visual area MT of the macaque. *Journal of Neurophysiology*, *51*, 16–31. <http://doi.org/6693933>
- Allen, B., Haun, A. M., Hanley, T., Green, C. S., Rokers, B., & Allen, C. B. (2015). Optimal Combination of the Binocular Cues to 3D Motion. *Investigative Ophthalmology & Visual Science*, *56*(12), 7589. <http://doi.org/10.1167/iovs.15-17696>
- Amano, K., Wandell, B. A., & Dumoulin, S. O. (2009). Visual Field Maps, Population Receptive Field Sizes, and Visual Field Coverage in the Human MT+ Complex. *Journal of Neurophysiology*, *102*(5), 2704–2718. <http://doi.org/10.1152/jn.00102.2009>
- Avidan, G., Hasson, U., Malach, R., & Behrmann, M. (2005). Detailed exploration of face-related processing in congenital prosopagnosia: 2. Functional neuroimaging findings. *Journal of Cognitive Neuroscience*, *17*(7), 1150–1167. <http://doi.org/10.1162/0898929054475154>
- Ball, K., & Sekuler, R. (1980). Human vision favors centrifugal motion. *Perception*, *9*(3), 317–25.
- Barendregt, M., Dumoulin, S. O., & Rokers, B. (2014). Stereomotion scotomas occur after binocular combination. *Vision Research*, *105*, 92–99. <http://doi.org/10.1016/j.visres.2014.09.008>
- Barendregt, M., Harvey, B. M., Rokers, B., & Dumoulin, S. O. (2015). Transformation from a Retinal to a Cyclopean Representation in Human Visual Cortex. *Current Biology*, *25*(15), 1982–1987. <http://doi.org/10.1016/j.cub.2015.06.003>
- Blakemore, C. (1970). The range and scope of binocular depth discrimination in man. *The Journal of Physiology*, *211*, 599–622.

Appendix

- Blasdel, G., & Fitzpatrick, D. (1984). Physiological organization of layer 4 in macaque striate cortex. *The Journal of Neuroscience*, *4*(3), 880–895.
- Brainard, D. (1997). The psychophysics toolbox. *Spatial Vision*, *10*(4), 433–436.
- Bridge, H., Thomas, O. M., Minini, L., Cavina-Pratesi, C., Milner, A. D., & Parker, A. J. (2013). Structural and Functional Changes across the Visual Cortex of a Patient with Visual Form Agnosia. *The Journal of Neuroscience*, *33* (31), 12779–12791. <http://doi.org/10.1523/JNEUROSCI.4853-12.2013>
- Brooks, K. R. (2002). Interocular velocity difference contributes to stereomotion speed perception. *Journal of Vision*, *2*(3), 218–31. <http://doi.org/10.1167/2.3.2>
- Brooks, K. R., & Stone, L. (2004). Stereomotion speed perception : Contributions from both changing disparity and interocular velocity difference over a range of relative disparities. *Journal of Vision*, *4*(12), 1061–1079. <http://doi.org/10.1167/4.12.6>
- Brouwer, G. J., & van Ee, R. (2007). Visual cortex allows prediction of perceptual states during ambiguous structure-from-motion. *The Journal of Neuroscience : The Official Journal of the Society for Neuroscience*, *27*(5), 1015–1023. <http://doi.org/10.1523/JNEUROSCI.4593-06.2007>
- Carter, O., & Cavanagh, P. (2007). Onset rivalry: Brief presentation isolates an early independent phase of perceptual competition. *PLoS One*, *2*(4). <http://doi.org/10.1371/journal.pone.0000343>
- Casagrande, V. A., & Boyd, J. D. (1996). The neural architecture of binocular vision. *Eye (London, England)*, *10* (Pt 2), 153–60. <http://doi.org/10.1038/eye.1996.40>
- Castelo-Branco, M., Formisano, E., Backes, W., Zanella, F., Neuenschwander, S., Singer, W., & Goebel, R. (2002). Activity patterns in human motion-sensitive areas depend on the interpretation of global motion. *Proceedings*

List of references

- of the National Academy of Sciences of the United States of America*, 99(21), 13914–13919. <http://doi.org/10.1073/pnas.202049999>
- Chen, G., Lu, H. D., & Roe, A. W. (2008). A map for horizontal disparity in monkey V2. *Neuron*, 58(3), 442–50.
<http://doi.org/10.1016/j.neuron.2008.02.032>
- Chen, M., Li, P., Zhu, S., Han, C., Xu, H., Fang, Y., ... Lu, H. D. (2014). An Orientation Map for Motion Boundaries in Macaque V2. *Cerebral Cortex*, 26(1), 279–287. <http://doi.org/10.1093/cercor/bhu235>
- Cowey, A., & Walsh, V. (2000). Magnetically induced phosphenes in sighted, blind and blindsighted observers. *Neuroreport*, 11(14), 3269–3273.
<http://doi.org/10.1097/00001756-200009280-00044>
- Cumming, B. G., & Parker, A. J. (1994). Binocular mechanisms for detecting motion-in-depth. *Vision Research*, 34(4), 483–495.
- Czuba, T. B., Huk, A. C., Cormack, L., & Kohn, A. (2014). Area MT encodes three-dimensional motion. *The Journal of Neuroscience*, 34(47), 15522–15533. <http://doi.org/10.1523/JNEUROSCI.1081-14.2014>
- Czuba, T. B., Rokers, B., Huk, A. C., & Cormack, L. K. (2010). Speed and eccentricity tuning reveal a central role for the velocity-based cue to 3D visual motion. *Journal of Neurophysiology*, 104(5), 2886–99.
<http://doi.org/10.1152/jn.00585.2009>
- Czuba, T. B., Rokers, B., Huk, A. C., & Cormack, L. K. (2012). To CD or not to CD: Is there a 3D motion aftereffect based on changing disparities? *Journal of Vision*, 12, 7–7. <http://doi.org/10.1167/12.4.7>
- d’Avossa, G., Tosetti, M., Crespi, S., Biagi, L., Burr, D. C., & Morrone, M. C. (2007). Spatiotopic selectivity of BOLD responses to visual motion in human area MT. *Nature Neuroscience*, 10, 249–255.
<http://doi.org/10.1038/nn1824>
- DeAngelis, G. C., & Newsome, W. T. (1999). Organization of disparity-selective

Appendix

- neurons in macaque area MT. *The Journal of Neuroscience*, 19(4), 1398–415.
- Dumoulin, S. O., Hess, R., May, K., Harvey, B., Rokers, B., & Barendregt, M. (2014). Contour extracting networks in early extrastriate cortex. *Journal of Vision*, 14(5), 1–14. <http://doi.org/10.1167/14.5.18>.doi
- Dumoulin, S. O., & Wandell, B. A. (2008). Population receptive field estimates in human visual cortex. *NeuroImage*, 39(2), 647–60. <http://doi.org/10.1016/j.neuroimage.2007.09.034>
- Edwards, M., & Badcock, D. R. (1993). Asymmetries in the sensitivity to motion in depth: a centripetal bias. *Perception*, 22(9), 1013–23.
- Engel, S., Rumelhart, D., & Wandell, B. (1994). fMRI of human visual cortex. *Nature*, 369, 525.
- Erkelens, C. J., & Van Ee, R. (2002). The role of the cyclopean eye in vision: Sometimes inappropriate, always irrelevant. *Vision Research*, 42, 1157–1163. [http://doi.org/10.1016/S0042-6989\(01\)00280-2](http://doi.org/10.1016/S0042-6989(01)00280-2)
- Essen, D. Van, & Maunsell, J. (1983). Hierarchical organization and functional streams in the visual cortex. *Trends in Neurosciences*, 6(9), 370–375.
- Farah, M. (2004). *Visual Agnosia*. Visual Agnosia. Cambridge, MA, US: MIT Press.
- Freeman, J., Ziemba, C. M., Heeger, D. J., Simoncelli, E. P., & Movshon, J. A. (2013). A functional and perceptual signature of the second visual area in primates. *Nature Neuroscience*, 16(7), 974–81. <http://doi.org/10.1038/nn.3402>
- Fulvio, J. M., Rosen, M. L., & Rokers, B. (2015). Sensory uncertainty leads to systematic misperception of the direction of motion in depth. *Attention, Perception, & Psychophysics*, 77(5), 1685–1696. <http://doi.org/10.3758/s13414-015-0881-x>
- Gardner, J. L., Merriam, E. P., Movshon, J. A., & Heeger, D. J. (2008). Maps of

List of references

- visual space in human occipital cortex are retinotopic, not spatiotopic. *The Journal of Neuroscience : The Official Journal of the Society for Neuroscience*, 28(15), 3988–99. <http://doi.org/10.1523/JNEUROSCI.5476-07.2008>
- Georgeson, M. A., & Harris, M. G. (1978). Apparent foveofugal drift of counterphase gratings. *Perception*, 7(5), 527–36.
- Gheorghiu, E., & Erkelens, C. J. (2005a). Differences in perceived depth for temporally correlated and uncorrelated dynamic random-dot stereograms. *Vision Research*, 45(12), 1603–1614. <http://doi.org/10.1016/j.visres.2004.12.005>
- Gheorghiu, E., & Erkelens, C. J. (2005b). Temporal properties of disparity processing revealed by dynamic random-dot stereograms. *Perception*, 34(10), 1205–1219. <http://doi.org/10.1068/p5404>
- Giaschi, D., Zwicker, A., Young, S. A., & Bjornson, B. (2007). The role of cortical area V5/MT+ in speed-tuned directional anisotropies in global motion perception. *Vision Research*, 47(7), 887–98. <http://doi.org/10.1016/j.visres.2006.12.017>
- Grunewald, A., & Skoumbourdis, E. K. (2004). The integration of multiple stimulus features by V1 neurons. *The Journal of Neuroscience : The Official Journal of the Society for Neuroscience*, 24(41), 9185–94. <http://doi.org/10.1523/JNEUROSCI.1884-04.2004>
- Harris, J. M., Nefs, H. T., & Grafton, C. E. (2008). Binocular vision and motion-in-depth. *Spatial Vision*, 21(6), 531–547. <http://doi.org/10.1163/156856808786451462>
- Harris, J. M., & Watamaniuk, S. N. J. (1995). Speed discrimination of motion-in-depth using binocular cues. *Vision Research*, 35(7), 885–896.
- Harvey, B. M., Klein, B. P., Petridou, N., & Dumoulin, S. O. (2013). Topographic representation of numerosity in the human parietal cortex. *Science*, 341(6150), 1123–6. <http://doi.org/10.1126/science.1239052>

Appendix

- Hayhow, W. R. (1958). The cytoarchitecture of the lateral geniculate body in the cat in relation to the distribution of crossed and uncrossed optic fibers. *The Journal of Comparative Neurology*, *110*(1), 1–63.
- He, S., Cohen, E. R., & Hu, X. (1998). Close correlation between activity in brain area MT/V5 and the perception of a visual motion aftereffect. *Current Biology : CB*, *8*, 1215–1218. [http://doi.org/10.1016/S0960-9822\(07\)00512-X](http://doi.org/10.1016/S0960-9822(07)00512-X)
- Hedges, J. H., Gartshteyn, Y., Kohn, A., Rust, N. C., Shadlen, M. N., Newsome, W. T., & Movshon, J. A. (2011). Dissociation of neuronal and psychophysical responses to local and global motion. *Current Biology*, *21*(23), 2023–2028. <http://doi.org/10.1016/j.cub.2011.10.049>
- Hedges, J. H., Stocker, A. A., & Simoncelli, E. P. (2011). Optimal inference explains the perceptual coherence of visual motion stimuli, *11*, 1–16. <http://doi.org/10.1167/11.6.14>
- Hong, X., & Regan, D. (1989). Visual field defects for unidirectional and oscillatory motion in depth. *Vision Research*, *29*(7), 809–19.
- Hubel, D. H., & Wiesel, T. N. (1962). Receptive fields, binocular interaction and functional architecture in the cat's visual cortex. *The Journal of Physiology*, *160*(38), 106–54. <http://doi.org/10.1523/JNEUROSCI.1991-09.2009>
- Hubel, D. H., Wiesel, T. N., Yeagle, E. M., Lafer-Sousa, R., & Conway, B. R. (2013). Binocular Stereoscopy in Visual Areas V-2, V-3, and V-3A of the Macaque Monkey. *Cerebral Cortex*, *25*(4), 959–971. <http://doi.org/10.1093/cercor/bht288>
- Huk, A. C., Dougherty, R. F., & Heeger, D. J. (2002). Retinotopy and functional subdivision of human areas MT and MST. *The Journal of Neuroscience : The Official Journal of the Society for Neuroscience*, *22*(16), 7195–205. <http://doi.org/20026661>
- Huk, A. C., & Heeger, D. J. (2002). Pattern-motion responses in human visual

List of references

- cortex. *Nature Neuroscience*, 5(1), 72–75. <http://doi.org/10.1038/nn774>
- Huk, A. C., Ress, D., & Heeger, D. J. (2001). Neuronal basis of the motion aftereffect reconsidered. *Neuron*, 32(1), 161–172. [http://doi.org/10.1016/S0896-6273\(01\)00452-4](http://doi.org/10.1016/S0896-6273(01)00452-4)
- Hupé, J.-M., & Rubin, N. (2004). The oblique plaid effect. *Vision Research*, 44(5), 489–500.
- Inouye, T. (1909). *Die Sehstörungen bei Schussverletzungen der kortikalen Sehsphäre*. Leipzig: Engelmann.
- Julesz, B. (1971). *Foundations of cyclopean perception*. Oxford, England: U. Chicago Press.
- Kamitani, Y., & Tong, F. (2006). Decoding Seen and Attended Motion Directions from Activity in the Human Visual Cortex. *Current Biology*, 16(11), 1096–1102. <http://doi.org/10.1016/j.cub.2006.04.003>
- Kane, D., Guan, P., & Banks, M. S. (2014). The limits of human stereopsis in space and time. *The Journal of Neuroscience : The Official Journal of the Society for Neuroscience*, 34(4), 1397–408. <http://doi.org/10.1523/JNEUROSCI.1652-13.2014>
- Kennerknecht, I., Grueter, T., Welling, B., Wentzek, S., Horst, J., Edwards, S., & Grueter, M. (2006). First report of prevalence of non-syndromic hereditary prosopagnosia (HPA). *American Journal of Medical Genetics, Part A*, 140(15), 1617–1622. <http://doi.org/10.1002/ajmg.a.31343>
- Kim, J., & Wilson, H. R. (1993). Dependence of plaid motion coherence on component grating directions. *Vision Research*, 33(17), 2479–2489.
- Klein, B. P., Harvey, B. M., & Dumoulin, S. O. (2014). Attraction of position preference by spatial attention throughout human visual cortex. *Neuron*, 84(1), 227–237. <http://doi.org/10.1016/j.neuron.2014.08.047>
- Kleiner, M., Brainard, D., Pelli, D. G., & Ingling, A. (2007). What's new in Psychtoolbox-3. *Perception*, 36(ECVP abstract supplement).

Appendix

- Kooi, F. L., De Valois, K. K., Switkes, E., & Grosop, D. H. (1992). Higher-order factors influencing the perception of sliding and coherence of a plaid. *Perception*, *21*(5), 583–98.
- Krug, K., Cicmil, N., Parker, A., & Cumming, B. G. (2013). A Causal Role for V5 / MT Neurons Coding Motion-Disparity Conjunctions in Resolving Perceptual Ambiguity. *Current Biology*, *23*(15), 1454–1459.
<http://doi.org/10.1016/j.cub.2013.06.023>
- Livingstone, M., & Hubel, D. (1988). Segregation of form, color, movement, and depth: anatomy, physiology, and perception. *Science*, *240*(4853), 740–749. <http://doi.org/10.1126/science.3283936>
- Lu, H., Chen, G., Tanigawa, H., & Roe, A. (2010). A Motion Direction Map in Macaque V2. *Neuron*, *68*(5), 1002–1013.
<http://doi.org/10.1016/j.neuron.2010.11.020>
- Maunsell, J. H., & Van Essen, D. C. (1983). Functional properties of neurons in middle temporal visual area of the macaque monkey. I. Selectivity for stimulus direction, speed, and orientation. *Journal of Neurophysiology*, *49*(5), 1127–47.
- Maunsell, J. H., & van Essen, D. C. (1983). The connections of the middle temporal visual area (MT) and their relationship to a cortical hierarchy in the macaque monkey. *The Journal of Neuroscience : The Official Journal of the Society for Neuroscience*, *3*(12), 2563–2586.
- Movshon, J. A., & Newsome, W. T. (1996). Visual response properties of striate cortical neurons projecting to area MT in macaque monkeys. *Journal of Neuroscience*, *16*(23), 7733–7741. <http://doi.org/10.1167/9.8.752>
- Nefs, H. T., & Harris, J. M. (2010). What Visual Information is Used for Stereoscopic Depth Displacement Discrimination? *Perception*, *39* (6), 727–744. <http://doi.org/10.1068/p6284>
- Nefs, H. T., O'Hare, L., & Harris, J. M. (2010). Two independent mechanisms

List of references

- for motion-in-depth perception: evidence from individual differences. *Frontiers in Psychology*, 1(October), 155.
<http://doi.org/10.3389/fpsyg.2010.00155>
- Nestares, O., & Heeger, D. J. (2000). Robust multiresolution alignment of MRI brain volumes. *Magnetic Resonance in Medicine*, 43(5), 705–15.
- Newsome, W. T., & Pare, E. (1988). A selective impairment of motion perception following lesions of the middle temporal visual area (MT). *The Journal of Neuroscience*, 8(6), 2201–2211.
- Ono, H., Mapp, A. P., & Howard, I. P. (2002). The cyclopean eye in vision: The new and old data continue to hit you right between the eyes. *Vision Research*, 42, 1307–1324. [http://doi.org/10.1016/S0042-6989\(01\)00281-4](http://doi.org/10.1016/S0042-6989(01)00281-4)
- Parker, A. J., & Yang, Y. (1989). Spatial properties of disparity pooling in human stereo vision. *Vision Research*, 29(11), 1525–1538.
[http://doi.org/10.1016/0042-6989\(89\)90136-3](http://doi.org/10.1016/0042-6989(89)90136-3)
- Pelli, D. G. (1997). The VideoToolbox software for visual psychophysics: Transforming numbers into movies. *Spatial Vision*, 10(4), 437–442.
- Qian, N., & Zhu, Y. (1997). Physiological computation of binocular disparity. *Vision Research*, 37(13), 1811–1827. [http://doi.org/10.1016/S0042-6989\(96\)00331-8](http://doi.org/10.1016/S0042-6989(96)00331-8)
- Raymond, J. (1994). Directional anisotropy of motion sensitivity across the visual field. *Vision Research*, 34(8), 1029–1037.
- Regan, D. (1993). Binocular Correlates of the Direction of Motion in Depth. *Vision Research*, 33(16), 2359–2360.
- Regan, D., Erkelens, C. J., & Collewijn, H. (1986). Visual field defects for vergence eye movements and for stereomotion perception. *Investigative Ophthalmology & Visual Science*, 27(5), 806–19.
- Regan, D., & Gray, R. (2009). Binocular processing of motion: some unresolved

Appendix

- questions. *Spatial Vision*, 22(1), 1–43.
<http://doi.org/10.1163/156856809786618501>
- Ress, D., Backus, B. T., & Heeger, D. J. (2000). Activity in primary visual cortex predicts performance in a visual detection task. *Nature Neuroscience*, 3(9), 940–945. <http://doi.org/10.1038/78856>
- Richard, T. B., David, C. B., Born, R. T., & Bradley, D. C. (2005). Structure and Function of Visual Area Mt. *Annual Review of Neuroscience*, 28, 157–89.
<http://doi.org/10.1146/annurev.neuro.26.041002.131052>
- Richards, W., & Regan, D. (1973). A stereo field map with implications for disparity processing. *Investigative Ophthalmology & Visual Science*, 12(12), 904–909.
- Riddoch, G. (1917). On the Relative Perceptions of Movement and a Stationary Object in Certain Visual Disturbances due to Occipital Injuries. *Proceedings of the Royal Society of Medicine*, 10(Neurol Sect), 13–34.
- Rokers, B., Cormack, L., & Huk, A. C. (2009). Disparity-and velocity-based signals for three-dimensional motion perception in human MT+. *Nature Neuroscience*, 12(8), 1050–1055. <http://doi.org/10.1038/nn.2343>
- Rokers, B., Cormack, L. K., & Huk, A. C. (2008). Strong percepts of motion through depth without strong percepts of position in depth. *Journal of Vision*, 8(4), 1–10. <http://doi.org/10.1167/8.4.6.Introduction>
- Rokers, B., Czuba, T. B., Cormack, L. K., & Huk, A. C. (2011). Motion processing with two eyes in three dimensions. *Journal of Vision*, 11, 1–19.
<http://doi.org/10.1167/11.2.10.Introduction>
- Sakano, Y., & Allison, R. (2014). Aftereffect of motion-in-depth based on binocular cues: Effects of adaptation duration, interocular correlation, and temporal correlation. *Journal of Vision*, 14, 1–14.
<http://doi.org/10.1167/14.8.21.doi>
- Sakano, Y., Allison, R. S., & Howard, I. P. (2012). Motion aftereffect in depth

List of references

- based on binocular information. *Journal of Vision*, 12(1), 11–11.
<http://doi.org/10.1167/12.1.11>
- Sanada, T. M., & DeAngelis, G. C. (2014). Neural Representation of Motion-In-Depth in Area MT. *Journal of Neuroscience*, 34(47), 15508–15521.
<http://doi.org/10.1523/JNEUROSCI.1072-14.2014>
- Serences, J. T., & Boynton, G. M. (2007). The representation of behavioral choice for motion in human visual cortex. *Journal of Neuroscience*, 27(47), 12893–12899. <http://doi.org/27/47/12893>
[pii]\r10.1523/JNEUROSCI.4021-07.2007
- Sereno, M. I., Dale, A. M., Reppas, J. B., Kwong, K. K., Belliveau, J. W., Brady, T. J., Rosen, B.R. & Tootell, R. B. (1995). Borders of multiple visual areas in humans revealed by functional magnetic resonance imaging. *Science*, 268(5212), 889–93. <http://doi.org/10.1126/science.7754376>
- Shioiri, S., Nakajima, T., Kakehi, D., & Yaguchi, H. (2008). Differences in temporal frequency tuning between the two binocular mechanisms for seeing motion in depth. *Journal of the Optical Society of America. A*, 25(7), 1574–85.
- Shioiri, S., Saisho, H., & Yaguchi, H. (2000). Motion in depth based on interocular velocity differences. *Vision Research*, 40, 2565–2572.
- Silvanto, J., Cowey, A., Lavie, N., & Walsh, V. (2005). Striate cortex (V1) activity gates awareness of motion. *Nature Neuroscience*, 8(2), 143–4.
<http://doi.org/10.1038/nn1379>
- Sincich, L. L. C., Park, K. F. K., Wohlgemuth, M. J. M., & Horton, J. C. J. (2004). Bypassing V1: a direct geniculate input to area MT. *Nature Neuroscience*, 7(10), 1123–8. <http://doi.org/10.1038/nn1318>
- Smith, A. T. (1992). Coherence of plaids comprising components of disparate spatial frequencies. *Vision Research*, 32(2), 393–397.
- Smith, A. T., Singh, K. D., Williams, A. L., & Greenlee, M. W. (2001). Estimating

Appendix

- Receptive Field Size from fMRI Data in Human Striate and Extrastriate Visual Cortex. *Cerebral Cortex*, 11 (12), 1182–1190.
<http://doi.org/10.1093/cercor/11.12.1182>
- Stanley, J., Carter, O., & Forte, J. (2011). Color and luminance influence, but can not explain, binocular rivalry onset bias. *PLoS One*, 6(5).
<http://doi.org/10.1371/journal.pone.0018978>
- Supèr, H., Spekreijse, H., & Lamme, V. A. (2001). Two distinct modes of sensory processing observed in monkey primary visual cortex (V1). *Nature Neuroscience*, 4(3), 304–10. <http://doi.org/10.1038/85170>
- Supèr, H., van der Togt, C., Spekreijse, H., & Lamme, V. A. F. (2003). Internal state of monkey primary visual cortex (V1) predicts figure-ground perception. *The Journal of Neuroscience : The Official Journal of the Society for Neuroscience*, 23(8), 3407–3414. <http://doi.org/10.1523/JNEUROSCI.2383-03.2003> [pii]
- Talbot, S., & Marshall, W. (1941). Physiological studies on neural Mechanisms of localization and discrimination. *Amer. J. Ophthalmology*, 24, 1255–1264.
- Tong, F., & Engel, S. (2001). Interocular rivalry revealed in the human cortical blind-spot representation. *Nature*, 411, 195–199.
- Tootell, R. B., Reppas, J. B., Dale, A. M., Look, R. B., Sereno, M. I., Malach, R., Brady, T.J. & Rosen, B. R. (1995). Visual motion aftereffect in human cortical area MT revealed by functional magnetic resonance imaging. *Nature*, 375, 139–41. <http://doi.org/10.1038/375139a0>
- Victor, J. D., & Conte, M. M. (1992). Coherence and transparency of moving plaids composed of Fourier and non-Fourier gratings. *Perception & Psychophysics*, 52(4), 403–414. <http://doi.org/10.3758/BF03206700>
- Wallach, H. (1935). On the visually perceived direction of motion. *Psychologische Forschung*, 20, 325–380.
- Wandell, B. A., Brewer, A. A., & Dougherty, R. F. (2005). Visual field map clusters in human cortex. *Philosophical Transactions of the Royal Society of London B*, 360(1367), 1317–1332. <http://doi.org/10.1098/rstb.2005.0077>

List of references

- London. Series B, Biological Sciences*, 360(1456), 693–707.
<http://doi.org/10.1098/rstb.2005.1628>
- Wandell, B. A., Dumoulin, S. O., & Brewer, A. A. (2007). Visual Field Maps in Human Cortex. *Neuron*, 56(2), 366–383.
<http://doi.org/10.1016/j.neuron.2007.10.012>
- Wang, H. X., Merriam, E. P., Freeman, J., & Heeger, D. J. (2014). Motion Direction Biases and Decoding in Human Visual Cortex. *Journal of Neuroscience*, 34(37), 12601–12615.
<http://doi.org/10.1523/JNEUROSCI.1034-14.2014>
- Wang, L., Mruczek, R. E. B., Arcaro, M. J., & Kastner, S. (2015). Probabilistic maps of visual topography in human cortex. *Cerebral Cortex*, 25(10), 3911–3931. <http://doi.org/10.1093/cercor/bhu277>
- Wardle, S., & Alais, D. (2013). Evidence for speed sensitivity to motion in depth from binocular cues. *Journal of Vision*, 13(1), 1–16.
<http://doi.org/10.1167/13.1.17.Introduction>
- Westheimer, G., & Truong, T. T. (1988). Target crowding in foveal and peripheral stereoacuity. *American Journal of Optometry and Physiological Optics*, 65(5), 395–9.
- Wheatstone, C. (1838). Contributions to the physiology of vision. Part II. On some remarkable, and hitherto unobserved, phenomena of binocular vision. *Proceedings of the Royal Society of London*, 6, 138–141
- Womelsdorf, T., Anton-Erxleben, K., Pieper, F., & Treue, S. (2006). Dynamic shifts of visual receptive fields in cortical area MT by spatial attention. *Nature Neuroscience*, 9(9), 1156–1160. <http://doi.org/10.1038/nn1748>
- Xu, J. P., He, Z. J., & Leng, T. (2011). A binocular perimetry study of the causes and implications of sensory eye dominance. *Vision Research*, 51(23-24), 2386–2397. <http://doi.org/10.1016/j.visres.2011.09.012>
- Zeki, S. M. (1978). Uniformity and diversity of structure and function in rhesus

Appendix

monkey prestriate visual cortex. *The Journal of Physiology*, 277(1978), 273–90.

Zuiderbaan, W., Harvey, B. M., & Dumoulin, S. O. (2012). Modeling center-surround configurations in population receptive fields using fMRI. *Journal of Vision*, 12(3), 10. <http://doi.org/10.1167/12.3.10>

Appendix

ACKNOWLEDGEMENTS

Acknowledgements

Although science is very often a solitary endeavor, spending long hours staring at a computer screen waiting for another ‘aha’ moment, there are a lot of people that were directly or indirectly involved in making this thesis happen. Since I will certainly forget to mention someone, I’ll begin with a general thanks to everyone that supported me during the course of my PhD years. In particular, I would like to thank all the anonymous participants (you know who you are) that spend many hours in the experiments that make up the body for this thesis.

Serge, met mijn master-stage in jouw lab werd ik ingewijd in de wondere wereld van fMRI en pRF modellen. Ondanks dat je het de afgelopen jaren steeds drukker kreeg met onderwijs geven en het managen van je lab, maakte je altijd tijd om even over onderzoek te praten omdat je zo naar eigen zeggen toch nog wat ‘echte wetenschap’ kon bedrijven. Bedankt voor alle kennis en inzichten die je me hebt gegeven en ik weet zeker dat we elkaar nog zeer regelmatig tegen zullen komen.

Bas, ik heb nog nooit zoveel tegen mijn computer zitten praten als in de afgelopen jaren. Hoewel er een oceaan tussen ons in zat, was je altijd snel beschikbaar om wat code te debuggen of over een analyse te discussiëren. Je hebt me geleerd dat het bij onderzoek altijd belangrijk is naar het grotere plaatje te kijken. Ik ben heel dankbaar voor de ervaring die ik in Madison heb kunnen opdoen en ik zal het perfectioneren van de figuren van een paper tot diep in nacht gaan missen.

Frans, hoewel je met een gerust hart de begeleiding aan Serge & Bas overliet, was zonder jou dit hele project niet mogelijk geweest.

Ben, you were always happy to critically discuss ongoing projects and participate in the most tedious experiments. I also appreciate the advice that you were always happy to provide on less science-related matters.

Appendix

Wietske, hoewel het niet altijd over de leukste dingen kon gaan denk ik met veel plezier terug aan onze gesprekken. Als ik in de toekomst even wat frustratie over studenten kwijt moet dan weet ik je te vinden.

Alessio, it was great working with you and if I every find myself in Italy I know where to get the best ice cream. Barrie, het was altijd prettig om met iemand over zowel baby's als Playstation spellen te kunnen praten.

Surya, ik weet zeker dat de Spar twee keer zoveel geitenkaas inkoopst sinds jij op de Uithof werkt en ik kom je ongetwijfeld nog wel tegen in "jouw" stad. Jim, ik hoop dat we onze schaakpartijen nog lange tijd kunnen voortzetten, misschien iets minder Siciliaans.

De afdeling Experimentele Psychologie in Utrecht is een geweldige plek om te promoveren. Eveline & Ria, jullie zorgen ervoor dat een afdeling vol met verstrooide onderzoekers soepel functioneert in de steeds bureaucratischere universiteit. Het is mooi om te zien dat een hele groep mensen zo enthousiast kan worden over details als de beeldverversing van verschillende monitoren, dank daarvoor Hinze, en het belang van een goed model voor je experiment (Casper & Ignace). Siarhei, bedankt voor alle hulp bij het bouwen van proefopstellingen ondanks mijn soms extreem specifieke eisen.

Jackie, I really enjoyed all the conversations we had on the many, many trips to get coffee and/or tea just to get out of the lab. Brian & Andrew, thanks for all the scientific, and sometimes not-so scientific, discussions. Shawn, thank you for spending a lot of time in the lab participating in my experiments in spite of the weird diagnoses that would sometimes result from that.

Acknowledgements

Elizabeth, Bill & Oscar, it was great to stay with you guys on my visits to Madison. You were a home away from home and I've learned a lot from you about American culture (although I still don't like cilantro).

Omdat het prettig is om ook af en toe het lab uit te komen ben ik ook Marco dankbaar voor de muzikale afleiding en onze eindeloze pogingen daar iets serieus van te maken. Michael, bedankt voor de discussies over websites, Macs en mijn Doubling Season trauma.

Uiteraard wil ik ook mijn familie bedanken voor alle steun. Pa, ma, Marc-Paul, Karin, Jan & Cora, heel erg bedankt dat jullie er altijd zijn geweest wanneer het nodig was.

Bianca, jij bent een anker in mijn soms ietwat chaotische leven en ik kijk heel erg uit naar de nieuwe avonturen die we samen gaan beleven. *Always and forever.*

Appendix

LIST OF PUBLICATIONS

List of publications

Barendregt M, Rokers B & Dumoulin SO (*In preparation*). The neural correlates of seen and unseen motion in depth.

Barendregt M, Dumoulin SO & Rokers B (*Accepted*). Impaired velocity processing reveals an agnosia for motion in depth. *Psychological Science*

Barendregt M, Harvey BM, Rokers B & Dumoulin SO (2015). Transformation from a retinal to a cyclopean representation in human visual cortex. *Current Biology*, 25 (15), 1982-1987

Barendregt M, Dumoulin SO & Rokers B (2014). Stereomotion scotomas occur after binocular combination. *Vision Research*, 105, 92-99

Dumoulin SO, Hess RF, May KA, Harvey BM, Rokers B & Barendregt M (2014). Contour extracting networks in early extrastriate cortex. *Journal of vision*, 14 (5), 18-18

Appendix

CURRICULUM VITAE

Curriculum Vitae

Martijn Barendregt was born in Rotterdam, The Netherlands on March 1st, 1987. He graduated from the Willem van Oranje high school in Oud-Beijerland in 2005. Initially he studied Economics & Computer Science at the Erasmus University in Rotterdam but after one year switched to Utrecht University to study Cognitive Artificial Intelligence (BSc). After obtaining his degree he completed the research master programme Neuroscience & Cognition in Utrecht. In 2012 he started as a PhD student at Utrecht University's Experimental Psychology group, supervised by Prof Serge Dumoulin. A large part of his PhD program consisted of a collaboration with Dr Bas Rokers at the University of Wisconsin-Madison and therefore he spend a couple of months every year in Madison (USA). He is currently a post doctoral associate with Dr Tomas Knapen, Dr Steven Scholte and Dr Heleen Slagter at the Vrije Universiteit Amsterdam and the University of Amsterdam.

Martijn Barendregt is geboren op 1 maart 1987 in Rotterdam. Hij behaalde in 2005 zijn vwo-diploma aan de Willem van Oranje in Oud-Beijerland. Hierna begon hij aan een studie Informatica & Economie aan de Erasmus Universiteit Rotterdam, maar stapte na een jaar over naar Cognitieve Kunstmatige Intelligentie in Utrecht. In 2011 voltooide hij de research master Neuroscience & Cognition aan de Universiteit Utrecht. Hij begon in 2012 als aio op de afdeling Psychonomie onder begeleiding van Prof Serge Dumoulin. Een groot deel van zijn aio-project besloeg een samenwerking met Dr Bas Rokers aan de University of Wisconsin-Madison en hij spendeerde hiervoor ieder jaar een aantal maanden in Madison (USA). Momenteel is hij werkzaam als post doc in het lab van Dr Tomas Knapen, Dr Steven Scholte en Dr Heleen Slagter aan de Vrije Universiteit Amsterdam en de Universiteit van Amsterdam.

